

Appendix B
Groundwater Modeling

Pacific Gas & Electric

**Appendix B: Development of a
Groundwater Flow and Solute
Transport Model**

Pacific Gas & Electric
Topock Compressor Station, Needles, California
October 2011

1. Introduction and Objectives	1
1.1 Introduction	1
1.2 Study Objectives and Scope	1
2. Conceptual Site Model	1
2.1 Regional Geologic Framework	2
2.2 Site Hydrogeology and Groundwater Occurrence	3
3. Groundwater Flow Model Development	3
3.1 Groundwater Flow Submodel Code Selection and Description	4
3.2 Submodel Domain	5
3.3 Submodel Discretization	5
3.4 Boundary Conditions	5
3.5 Hydraulic Conductivity	6
4. Solute Transport Model Development	6
4.1 Code Selection	6
4.2 Solute Transport Parameters	7
4.2.1 Porosity	7
4.2.2 Mass Transfer Coefficient	8
4.2.3 Chromium Adsorption	8
4.2.4 Chromium Reduction	9
4.2.5 Initial Hexavalent Chromium Distribution	9
4.2.6 Byproduct Generation	9
4.2.7 Byproduct Adsorption and Precipitation	11
4.2.8 Naturally Occurring Manganese and Arsenic	15
4.3 Parameter Assessment	16
4.4 Remediation Design	17
4.4.1 National Trails Highway IRZ	17

4.4.2	Riverbank Extraction	19
4.4.3	Uplands Injection	20
4.4.4	Extraction Wells northeast of the Compressor Station	20
4.4.5	East Ravine Extraction	20
4.4.6	Topock Compressor Station Injection	21
4.5	Flow Conditions	21
5.	Solute Transport Results	22
5.1	Hexavalent Chromium	22
5.2	Manganese	22
5.3	Arsenic	23
6.	Sensitivity Analysis	23
6.1	NTH IRZ Well Spacing	23
6.2	Injected TOC Concentrations	24
6.3	Riverbank Extraction Rates	25
6.4	Manganese Sorption and Generation	26
6.5	Arsenic Precipitation and Generation	26
6.6	Chromium Sorption	27
7.	Conclusions	27
8.	References	27

Tables

Table B-1	Byproduct generation terms used in fate and transport model
Table B-2	Byproduct attenuation terms used in fate and transport model

Figures

Figure B-1	Regional and Submodel Domain Extents
Figure B-2	Submodel Domain and Finite Difference Grid
Figure B-3	Thickness Model Layer 1
Figure B-4	Thickness Model Layer 2

Figure B-5 Thickness Model Layer 3

Figure B-6 Thickness Model Layer 4

Figure B-7 Thickness Model Layer 5

Figure B-8 Hydraulic Conductivity Model Layer 1

Figure B-9 Hydraulic Conductivity Model Layer 2

Figure B-10 Hydraulic Conductivity Model Layer 3

Figure B-11 Hydraulic Conductivity Model Layer 4

Figure B-12 Hydraulic Conductivity Model Layer 5

Figure B-13 Initial Hexavalent Chromium Concentration Distribution Model Layer 1

Figure B-14 Initial Hexavalent Chromium Concentration Distribution Model Layer 2

Figure B-15 Initial Hexavalent Chromium Concentration Distribution Model Layer 3

Figure B-16 Initial Hexavalent Chromium Concentration Distribution Model Layer 4

Figure B-17 Remediation Design Well Locations

Figure B-18 Conceptual Remedy Cross-Section Locations

Figure B-19 Conceptual Remedy Cross-Section A-A'

Figure B-20 Conceptual Remedy Cross-Section B-B'

Figure B-21 Conceptual Remedy Cross-Section C-C'

Figure B-22 Conceptual Remedy Cross-Section D-D'

Figure B-23 Conceptual Remedy Cross-Section E-E'

Figure B-24 Conceptual Remedy Cross-Section F-F'

Figure B-25 Simulated Groundwater Contours Under Ambient Flow Conditions

Figure B-26 Simulated Groundwater Contours Under Active Remedy Flow Conditions

Figure B-27 Simulated Hexavalent Chromium Transport Results in Model Layer 1

Figure B-28 Simulated Hexavalent Chromium Transport Results in Model Layer 2

Figure B-29	Simulated Hexavalent Chromium Transport Results in Model Layer 3
Figure B-30	Simulated Hexavalent Chromium Transport Results in Model Layer 4
Figure B-31	Simulated Manganese Transport Results in Model Layer 1
Figure B-32	Simulated Manganese Transport Results in Model Layer 2
Figure B-33	Simulated Manganese Transport Results in Model Layer 3
Figure B-34	Simulated Manganese Transport Results in Model Layer 4
Figure B-35	Simulated Arsenic Transport Results in Model Layer 1
Figure B-36	Simulated Arsenic Transport Results in Model Layer 2
Figure B-37	Simulated Arsenic Transport Results in Model Layer 3
Figure B-38	Simulated Arsenic Transport Results in Model Layer 4
Figure B-39	NTH IRZ Well Spacing Sensitivity: Initial 150ft and 75ft Spacing with Simulated Hexavalent Chromium Transport Results in Model Layer 4
Figure B-40	NTH IRZ Well Spacing Sensitivity: Revised 150ft and 75ft Spacing with Simulated Hexavalent Chromium Transport Results in Model Layer 4
Figure B-41	NTH IRZ Well Spacing Sensitivity: Revised 150ft and 75ft Spacing with Simulated Hexavalent Chromium Transport Results in Model Layer 2
Figure B-42	NTH IRZ Well Spacing Sensitivity: Revised 150ft and 75ft Spacing with Simulated Manganese Transport Results in Model Layer 2
Figure B-43	TOC Concentration Sensitivity: Simulated Hexavalent Chromium Transport Results in Model Layer 2
Figure B-44	TOC Concentration Sensitivity: Simulated Hexavalent Chromium Transport Results in Model Layer 4
Figure B-45	TOC Concentration Sensitivity: Simulated Manganese Transport Results in Model Layer 2
Figure B-46	Riverbank Extraction Rate Sensitivity: Simulated Hexavalent Chromium Transport Results in Model Layer 2
Figure B-47	Riverbank Extraction Rate Sensitivity: Simulated Manganese Transport Results in Model Layer 2
Figure B-48	Sensitivity of Manganese Generation and Sorption After 10 Years of Simulated Transport

- Figure B-49 Sensitivity of Arsenic Generation and Precipitation After 10 Years of Simulated Transport
- Figure B-50 Sorption Sensitivity: Simulated Hexavalent Chromium Transport Results in Model Layer 2

1. Introduction and Objectives

1.1 Introduction

Pacific Gas and Electric Company (PG&E) is actively pursuing a strategy to remediate the hexavalent chromium in groundwater resulting from historical operations at the Topock Compressor Station (TCS) and immediate surrounding area (herein referred to as the Site) located in eastern San Bernardino County about 12 miles southeast of the City of Needles, California. The compressor station is approximately 1,500 feet west of the Colorado River, and one-half mile west of Topock, Arizona. This appendix documents the groundwater flow and solute transport model that was generated for the Site.

1.2 Study Objectives and Scope

The objectives of this modeling study were to develop a groundwater flow and solute transport model for use as follows:

- Evaluate subsurface flow conditions
- Evaluate the fate and transport of hexavalent chromium
- Evaluate fate and transport of manganese and arsenic
- Evaluate potential remedial systems

This report describes the results of four major components of the modeling study at the Site:

- Updates to the groundwater flow model
- Development of a groundwater flow submodel
- Solute transport model development
- Remediation system analysis

2. Conceptual Site Model

A conceptual groundwater flow model is a narrative description of the principal components of a groundwater flow system developed from regional, local, and site-specific data. The primary components of a groundwater flow system include: (1) areal extent, configuration, and types of aquifers and aquitards; (2) hydraulic properties of aquifers and aquitards; (3) natural groundwater recharge and discharge zones; (4) anthropogenic influence on groundwater (sources and sinks); and, (5) areal and

vertical distribution of groundwater hydraulic head potential. These aquifer system components serve as the framework for the construction of a numerical groundwater flow model. The following sections describe the regional and Site hydrogeology and are taken from earlier investigation reports.

2.1 Regional Geologic Framework

The Topock site is situated in a basin-and-range geologic environment in the Mohave Valley. The Colorado River is the main source of water to this groundwater basin, but at the southern end where the site is located, groundwater is fed by a modest amount of local recharge from mountain runoff. The most prominent geologic structural feature in the study area is a Miocene-age, low-angle normal fault (referred to as a detachment fault) that forms the northern boundary of the Chemehuevi Mountains found to the southeast of the study area. The surface expression of the Chemehuevi detachment fault is evident as a pronounced northeast-southwest lineament that can be traced along the northern boundary of the Chemehuevi Mountains, terminating at the abrupt bend in the Colorado River east of the Compressor Station. The exposed Chemehuevi Mountains are Precambrian and Mesozoic metamorphic and igneous rocks formed by tectonic uplift along a Miocene-age low-angle normal fault. Sedimentary deposits in the area are made up of Pliocene lacustrine deposits and Tertiary and Quaternary-to recent alluvial fan deposits and fluvial deposits of the Colorado River. Younger Colorado River fluvial deposits occur within the saturated zone underlying the floodplain, the present river channel, and the marsh area (Metzger and Loeltz 1973; Howard et al. 1997).

The site is located at the southern (downstream) end of the Mohave Valley groundwater basin. On a regional scale, groundwater in the northern and central area of the valley is recharged primarily by the Colorado River, while under natural conditions net groundwater discharges occurs in the southern area, above where the alluvial aquifer thins near the entrance to Topock Gorge. The groundwater directly beneath the Topock site is derived mostly from the relatively small recharge from the nearby mountains. Under natural conditions, groundwater flows from west/southwest to east/northeast across the site.

2.2 Site Hydrogeology and Groundwater Occurrence

The Colorado River is 1,500 feet east of the Topock Compressor Station with a mean elevation of approximately 450 feet msl. The TCS is at an elevation of approximately 600 feet msl on an incised alluvial terrace. Bat Cave Wash, a large north-south incision adjacent to the compressor station, only has flows after large precipitation events. The stretch of the Colorado River east of the site is 600-700 feet wide. Flows in the river fluctuate daily and seasonally due to upstream regulated water releases by the Bureau of Reclamation at Davis Dam on Lake Mohave. Flows range from 4,000 to 25,000 cubic feet per second, and river levels fluctuate between 2 and 3 feet in a day, depending on the time of year.

Groundwater occurs within the alluvial fan and fluvial sediments referred to as the Alluvial Aquifer. The water table in the alluvial aquifer is very flat throughout the site and generally within 1 to 3 feet of the river level. The saturated thickness in the Alluvial Aquifer varies greatly, pinching to the south due to the surface proximity of the underlying bedrock. Groundwater flow directions at the site are to the east and northeast.

3. Groundwater Flow Model Development

The groundwater flow model used in the CMS/FS was calibrated in 2005. The details of the model design and calibration have been described in a previous report (CH2M HILL 2005b). Some modifications were made to the 2005 model prior to the CMS to incorporate basic properties in the East Ravine area (CH2M HILL 2009, Appendix E). The model was developed using MicroFEM (Hemker 2006), a finite element flow model code, and the domain extends several miles from the site in all directions (Figure B-1; CH2M HILL 2005b). Groundwater budget was developed from regional river gradient and estimates of precipitation recharge, subsurface inflow beneath major and minor washes, evapotranspiration, and subsurface outflow. The Colorado River acts as both a source and sink for groundwater flow, as does Topock Marsh. This water budget, along with aquifer parameters estimated from pumping tests and regional literature, form the basis of the hydrogeological understanding of the Site and its environs, and provide the framework for the solute transport model.

From the finite element flow model, a submodel was extracted and converted to MODFLOW to improve the resolution for solute transport modeling using MT3DMS.

The submodel domain was selected to be able to model the full extent of the hexavalent chromium plume as well as the proposed remedial elements. The relative model domains are depicted in Figure B-1. . As discussed in Section 3.1 of the main report, a series of updates to the groundwater flow model were performed for this study prior to development of the solute transport model. Those updates are summarized in Section 3.1 of the main body of this report.

The updated flow model was then used to develop the solute transport submodel. The domain of the solute transport submodel was focused on the plume area to design the in situ remediation zone (IRZ) and to estimate concentrations of selected constituents over the duration of the remedy. The boundary conditions of the solute transport model were assigned using groundwater fluxes exported from the flow model. The hydraulic properties in the solute transport model are consistent with the flow model.

3.1 Groundwater Flow Submodel Code Selection and Description

The simulation program MODFLOW was selected for the construction of the numerical groundwater flow submodel at the Site. MODFLOW is, a publicly available groundwater flow simulation program developed by the U.S. Geological Survey (USGS) (McDonald and Harbaugh 1988). MODFLOW is thoroughly documented; widely used by consultants, government agencies, and researchers; and is consistently accepted in regulatory and litigation proceedings.

MODFLOW simulates transient or steady-state, saturated groundwater flow in three dimensions. The program is designed to simplify the specification of boundary conditions by designing the data input to align with common field variables. The boundary conditions supported by MODFLOW include specified head, precipitation recharge, injection or extraction wells, evapotranspiration, horizontal flow barriers (HFBs), drains, and rivers or streams. Aquifers simulated by MODFLOW can be confined or unconfined, or convertible between conditions. For the Site, which consists of a heterogeneous geologic system with variable unit thicknesses and boundary conditions, MODFLOW's three-dimensional capability and boundary condition versatility are essential for the proper simulation of groundwater flow conditions.

MODFLOW uses the method of finite differences to solve the equations of groundwater flow. Using a block-centered finite-difference approach, MODFLOW replaces the continuous system represented by the equations of flow, by a system of discrete blocks in space. The solution of the finite-difference equations produces time-varying values of head at each of the discrete points representing the real aquifer system.

3.2 Submodel Domain

The submodel was designed to represent groundwater conditions over approximately 1.3 square miles of the original groundwater flow model. The submodel domain is shown in Figures B-1 and B-2. The submodel extents were designed to incorporate the extent of the hexavalent chromium distribution, the Colorado River adjacent to the Site, and the extent of the proposed remediation system.

3.3 Submodel Discretization

The model contains 232 rows, 256 columns, and 5 layers for a total of 296,960 active cells (Figure B-2). The uniform cell size is 25 ft by 25 ft occurs throughout the entire submodel domain. The model grid was not rotated, and the majority of grid cells are aligned with the direction of groundwater flow. The boundaries of the model grid are defined as constant head cells that reflect the flux of the original groundwater flow model under the same flow conditions.

Consistent with the original flow model, the submodel layers have variable thickness. Figures B-3 through B-7 depict how the thickness of the model layers vary in the solute transport submodel. In general, the aquifer decreases in thickness from North to South as the southern bedrock outcrop is approached. South of the bedrock contact, the upper four layers represent the shallow bedrock in this area and no longer are consistent with the alluvial portions of these layers to the north.

3.4 Boundary Conditions

The boundary conditions included in the submodel include the perimeter constant flux boundaries based on the fluxes computed from the original groundwater flow model. The Colorado River and portion of the marshland located on the east side of the Colorado River is represented by river cells with stage and conductance values consistent with the original groundwater flow model. The final boundary conditions simulated in the submodel domain are the well cells which represent the proposed extraction and injection locations for the various remedial scenarios.

3.5 Hydraulic Conductivity

Model layers 1 through 4 represent the alluvial aquifer throughout the majority of the submodel, with the exception of the southern portion of the model where all layers represent the bedrock. Model layer 5 represents the bedrock throughout the full model domain. The hydraulic conductivity distribution of the upper four layers representing the alluvial aquifer were simulated as highly heterogeneous layers as depicted in Figures B-8 to B-12. All hydraulic conductivity values in the submodel were assigned on the basis of the groundwater flow model properties.

4. Solute Transport Model Development

Solute transport modeling was performed to evaluate the migration and fate of hexavalent chromium detected in the groundwater, as well as the fate and transport of potential IRZ byproducts manganese and arsenic. The solute transport model used the results from the calibrated groundwater flow model to simulate solute transport constituent under average flow conditions. The solute transport model was used to evaluate the fate and transport of hexavalent chromium, as well as the select byproducts manganese, and arsenic, to evaluate various potential remedial systems.

4.1 Code Selection

The solute transport was performed using the modular three-dimensional transport model referred to as MT3D. MT3D was originally developed by Zheng (1990) at S.S. Papadopoulos & Associates, Inc. for the Robert S. Kerr Environmental Research Laboratory of the U.S. Environmental Protection Agency. The MT3D code uses the flows computed by MODFLOW in its transport calculations. MT3D also uses the same finite-difference grid structure and boundary conditions as MODFLOW, simplifying the effort to construct the solute transport model. MT3D is regularly updated (Zheng and Wang 1999), and the most recent version is referred to in the literature as MT3DMS, where MS denotes the Multi-Species structure for accommodating add-on reaction packages. MT3DMS has a comprehensive set of options and capabilities for simulating advection, dispersion/diffusion, and chemical reactions of contaminants in groundwater flow systems under a range of hydrogeologic conditions. Recent updates to MT3DMS have included the dual-domain formulation and the ability to incorporate site specific processes.

The major inputs to MT3DMS for the modeling assessment are as follows:

- Mobile and Immobile Porosity: affecting the groundwater velocity and dissolved storage;
- Mass Transfer Coefficient: affecting the exchange of mass between mobile and immobile portions of the aquifer;
- Partition Coefficient: affecting the adsorption on hexavalent chromium and byproducts to soil particles;
- Carbon Degradation Rate: affecting the rate of hexavalent chromium reduction/precipitation.
- Byproduct Generation Rate: affecting the rate of generation of manganese and arsenic from the introduction of carbon to aquifer.

4.2 Solute Transport Parameters

4.2.1 Porosity

The first phase of calibration was to accurately represent the groundwater velocity in the impacted portion of the aquifer. The groundwater velocity is computed within MT3DMS by dividing the groundwater flux term from MODFLOW by the mobile porosity. The mobile porosity is that fraction of the aquifer through which the majority of groundwater is moving. While often conceptualized as solely a pore scale concept, it also represents aquifer-scale behavior driven by hydraulic conductivity contrasts in different portions of the aquifer matrix. The immobile porosity is the remaining portion of the void space, where groundwater flows much slower or not at all, and the void space is primarily a storage reservoir for dissolved mass. Mass is exchanged between mobile and immobile portions of the aquifer by diffusion. This conceptualization of solute transport is the dual-domain formulation, and is often referred to as *advection-diffusion*. There is extensive literature on the dual-domain model (Gillham et al. 1984; Molz et al. 2006; Flach et al. 2004; Harvey and Gorelick 2000; Feehley et al. 2000; Julian et al. 2001; Zheng and Bennet 2002), and it is generally considered the most accurate approach for simulating solute transport.

The total (combination of mobile and immobile) porosity of the aquifer is controlled by grain sizes and sorting. The mechanics of deposition and consolidation of unconsolidated materials result in aquifer soils at the Site exhibiting a total porosity of approximately 35%. Local variability will not have an impact on overall results, and 35% is a reliable estimate for the total porosity of modeled Layers 1 through 4. This is the reference value that was used to divide the aquifer between mobile and immobile regions.

The estimated mobile porosity of the aquifer is 10% of the total volume, with the immobile porosity to be 25% of the total volume. These values are typical of porosity values obtained at other sites (Payne et al. 2008).

4.2.2 Mass Transfer Coefficient

An estimated mass transfer coefficient (MTC) value of 1.0×10^{-3} was utilized for all model layers in the solute transport model. The solute transport model was run with initialized current plumes to determine if the selected MTC produced reasonable results with the constituent distribution currently observed. It was recognized that variations in historic plume interpretations were not just a function of plume movement, but also improved delineation of the plume that developed over time as the monitoring well network density evolved. The current plume interpretation is based on a much more advanced monitoring well network, which improved the resolution of the plume delineation. The MTC value for the solute transport model was systematically adjusted between 1.0×10^{-05} [1/day] and 1.0 [1/day], until the solute transport model produced reasonable plume movement.

4.2.3 Chromium Adsorption

The retardation factor (R_f) is used by the solute transport model to represent the amount of adsorption of a constituent between the dissolved or solute phase and adsorbed to the aquifer. The retardation factor used for hexavalent chromium is based on the linear sorption isotherm and is calculated in MT3D using the bulk density (ρ_b), the porosity (n) of the aquifer material, and a distribution coefficient (K_d), according to the following equation:

$$R_f = 1 + \frac{\rho_b K_d}{n} \quad (4-1)$$

The presence of background hexavalent chromium concentrations associated with the naturally occurring mineralogy suggests nominal adsorption (low K_d value) is representative of the aquifer. This assessment is consistent with the literature, which identifies a wide range of K_d values (USEPA 1999) for naturally occurring hexavalent chromium in aquifer soils with a normal pH range. The model includes a small amount of adsorption for hexavalent chromium, incorporating a distribution coefficient (K_d) of 0.05 liter per kilogram (L/kg). A K_d value of 0.05 L/kg results in a retardation factor of approximately 1.25 for the hexavalent chromium plume in the solute transport model. This indicates the plume will migrate about 25% slower than the ambient groundwater flow velocity. Given the limits of the current plume and the understanding of

groundwater flow through the region, the K_d value of 0.05 L/kg is a reasonable estimate of natural chromium adsorption rates at the Site. Site core samples were analyzed for Cr(VI) in liquid and solid phases in a previous study (CH2M HILL 2005a) and showed a range of K_d values from zero to 0.09 L/kg, the assigned value of 0.05 L/kg is therefore consistent with these measured values.

4.2.4 Chromium Reduction

The reduction and precipitation of hexavalent chromium in the aquifer was simulated by accounting for the reduction/precipitation of chromium in the presence of injected carbon (as part of an *in situ* remediation approach). To account for this, the model assumed hexavalent chromium reduction/precipitation whenever the injected carbon exceeds a concentration of 0.1 parts per million (ppm). At the same time, a carbon half-life of 20 days was assigned to account for the degradation of the injected carbon over time. By simulating both hexavalent chromium and carbon simultaneously, the interactions between the plume and the active IRZ were accounted for in the solute transport model.

4.2.5 Initial Hexavalent Chromium Distribution

The initial chromium plume concentration distribution was based on second quarter 2011 and historical data. In the upper four model layers, the plume delineation varied to reflect the differing hexavalent chromium concentrations encountered with depth. The initialized chromium distribution in the immobile portions of the aquifer, hexavalent chromium concentrations were assumed to be equal to concentrations in the mobile portions. The distribution of the hexavalent chromium initialized in the model for model layers 1 through 4 is shown in Figures B-13 through B-16.

4.2.6 Byproduct Generation

The introduction of dissolved organic carbon into the aquifer will facilitate treatment of Cr(VI) in groundwater through precipitation of stable, low solubility Cr(III) minerals. This precipitation reaction results from the formation of geochemical conditions that are similar to those currently present in the fluvial aquifer that comprises the rind adjacent to the river. Naturally occurring minerals in the rind are currently dissolved due to the presence of natural organic carbon, at the same time Cr(VI) is undergoing precipitation in this rind. The goals of the *in situ* groundwater treatment are to promote these geochemical conditions in the deeper aquifer where the majority of the Cr(VI) is present in order to facilitate treatment. Once geochemical conditions form in the

alluvial aquifer that are similar to the fluvial aquifer, there will be natural minerals that dissolve (specifically natural iron minerals) and naturally-occurring manganese and arsenic associated with these natural minerals may become soluble. These byproducts of the introduction of organic carbon will be generated only in the presence of organic carbon, and their migration will be limited in distance outside of the reactive zone where Cr(VI) is treated. These secondary water quality effects are discussed in detail in Appendix G of the Corrective Measures/Feasibility Study Report for Chromium in Groundwater (CMS/FS; CH2M Hill, 2009). Byproducts will be generated due to dissolution of naturally-occurring iron minerals in the aquifer and the distance over which they travel will be controlled by attenuation mechanisms, principally sorption. The groundwater model was used to evaluate the generation of byproducts and their fate and transport.

Byproduct generation is simulated in the fate and transport model by linking the concentration of organic carbon to a corresponding concentration of dissolved manganese and arsenic. The basis for this relationship is the floodplain and upland in situ pilot test (ISPT) results (ARCADIS 2008, 2009). At the maximum concentration of organic carbon planned for use (100 mg/L), manganese generation will be limited as was observed in the pilot tests. The relationship between organic carbon and manganese concentration is shown in Figure G13 of Appendix G of the CMS/FS (CH2M Hill, 2009). Similarly, Figure G14 of Appendix G of the CMS/FS provides a summary of the relationship of organic carbon concentration to the concentration of arsenic. In both cases, a range of concentrations of manganese and arsenic may be generated at 100 mg/L of organic carbon. The generation rate for manganese was determined based upon the average concentration of manganese generated at concentrations greater than 10 mg/L organic carbon but less than 100 mg/L for both the upland and floodplain ISPT data set (0.016 mg of Mn per mg of organic carbon). The generation rate for arsenic was determined based upon an evaluation of the upland and floodplain ISPT data set (0.000108 mg of As per mg of organic carbon). A range of generation rates for Mn and As were selected based upon this base case, as detailed in Table 1.

Table 1. Byproduct generation terms used in fate and transport model.

Byproduct	Generation Term (mg of Byproduct per mg Organic Carbon per Liter)		
	Low (0.5x base)	Base Case	High (2x base)

	case)		case)
Manganese	0.008	0.016	0.032
Arsenic	0.0005	0.00108	0.0017

The generation of Mn and As occurs in the presence of organic carbon, when concentrations of organic carbon decline to be 0.1 mg/L then sorption and precipitation of Mn and As can occur. However, at concentrations of organic carbon above 0.1 mg/L, Mn and As sorption does not occur in the model and the sorption parameters are turned off. This convention in the model is consistent with the upland and floodplain ISPT data where Mn and As persisted in the presence of organic carbon, and this is also consistent with the natural conditions in the fluvial rind (dissolved Mn and As is present due to the natural organic matter in the fluvial aquifer). Organic carbon affects iron minerals by causing these to dissolve; iron minerals are the predominant sorbing mineral phases for Mn and As and they do not function as effectively when organic carbon is present. Outside of the carbon footprint, Mn and As will sorb and these reactions are described in the following section.

4.2.7 Byproduct Adsorption and Precipitation

As discussed in Appendix G of the CMS/FS (CH2M Hill, 2009), the dissolution of iron, manganese and arsenic in the IRZs is temporary (dissolution will stop as organic carbon concentrations decrease to below 0.1 mg/L) and then these elements will return to baseline concentrations. Iron, manganese and arsenic that have dissolved and move out of the reactive zone under the influence of groundwater flow will undergo reactions that will transition these dissolved, naturally occurring elements to sorbed or precipitated forms, thereby removing these from groundwater. Dissolved iron will react by sorbing to solid-phase iron minerals outside of the reactive zone, and it will also precipitate through reaction with dissolved oxygen in the aquifer. Manganese and arsenic will sorb to iron minerals present naturally in the aquifer outside of the reactive zone, across the floodplain, and to these newly-formed iron minerals. The byproducts manganese and arsenic have been shown to sorb to aquifer minerals in a variety of environments (Fuller and Harvey, 2000; Smedley and Kinniburgh, 2002); the floodplain and upland pilot test demonstrated that Mn and As were not detected outside of the footprint of organic carbon in downgradient monitoring wells (ARCADIS 2008, 2009). An evaluation of the concentration of natural manganese, under IM-3 pumping conditions (pumping results in a gradient reversal on the floodplain) shows that the natural byproducts from the rind attenuate across the floodplain. The manganese

concentration shows a maximum at approximately 300 feet away from the river (due to the influence of IM-3 pumping) and then the concentration declines significantly from there. The decline in concentration is due to reaction of manganese with the aquifer in the location of the aquifer where the oxidation-reduction potential transitions from reducing conditions (negative redox potential) to less reducing conditions (positive redox potential). The field data demonstrates that natural byproduct Mn will attenuate across the aquifer outside of the natural fluvial rind. The field data provides a validation of the conceptual model used as the basis for attenuation in the byproduct fate and transport model.

Manganese and arsenic attenuate predominantly through sorption to aquifer soil outside of the footprint of dissolved organic carbon. Other reactions are possible, such as oxidation (manganese can react with dissolved oxygen resulting in dissolved manganese (Mn^{2+}) transitioning to solid manganese (hydr)oxide minerals ($MnOOH$). However, this reaction can be slow at circumneutral pH and is therefore ignored in the byproduct model. Manganese can also precipitate in the presence of dissolved bicarbonate (alkalinity); this reaction can serve to limit the concentration of manganese generated within the reactive zone where alkalinity can be highest. This reaction was also ignored in the model and is captured in the generation rate of manganese; generation rate is based upon observations of the concentration of manganese generated in the floodplain and upland ISPT. The predominant attenuation mechanism is therefore sorption of dissolved manganese and arsenic to soil minerals. Sorption of dissolved cations (e.g. Mn^{2+}) and arsenic by iron (hydr)oxide minerals is well documented in the technical literature. Sorption parameters were developed in the groundwater model as follows:

- a) The concentration of iron in the soil was determined through soil sampling. Fine grained (silt/clay) soil was recovered from the alluvial aquifer (upland) during installation of the ISPT wells (ARCADIS, 2009b) and analyzed for the concentration of iron as well as the form of iron through sequential selective extraction (Gleyzes et al., 2002).
- b) Based upon selective extraction results of the silt and clay, the concentration of poorly-crystalline (amorphous) iron (iron (hydr)oxides that possess relatively “strong-binding” sorption sites for manganese and arsenic) was determined to be 3.5 g/L of aquifer soil, and crystalline iron (iron (hydr)oxides that possess “weaker” sorption sites for manganese and arsenic) was determined to be 5.6 g/L.

- c) The concentration of sorptive forms of iron were scaled back by three orders of magnitude (to 0.1% of their measured values in silt/clay) to account for the fact that the predominant flow path for groundwater will be through coarse-grained aquifer materials (sands).
- d) The concentrations of sorptive iron (0.1% of the measured concentrations, or 3.5 mg/L strong site iron and 5.6 mg/L of weak site iron) were compared to the analysis of coarse grained material completed during a separate study of alluvial aquifer material in the floodplain (CH2M Hill, 2005a). This study showed that strong site iron in the coarse grained soil was 1 – 2 mg/L, and weak site iron was greater (3.6 g/L). These results confirm selection of the strong and weak site iron concentrations as best representations of the iron concentration and form in the aquifer soil.
- e) Sorption “isotherms” were constructed by preparing a geochemical model using PHREEQC (version 2.18 (USGS, 1999)) and a surface complexation model using manganese and arsenic thermodynamic sorption parameters for binding to strong and weak site iron (Dzombak and Morel, 1990). The concentration of iron in coarse grained soil was entered into the model as well as groundwater chemical parameters determined in the floodplain (ARCADIS 2009b). Manganese and arsenic were added to the model at low (ppb) concentrations to high (ppm) concentrations, spanning the expected concentrations in the floodplain and higher, in order to simulate concentrations associated with the soil and in the dissolved phase, according to a procedure described in EPA, 2005.
- f) The sorption isotherms were linearized on a log-log scale and Freundlich parameters were obtained from an analysis of the isotherms (Essington, 2004). The Freundlich equation is as follows:

$$q_e = K_f C_e^N$$

Where q_e is the concentration of manganese sorbed to the soil, K_f is the Freundlich partition coefficient, C_e is the concentration of manganese in the dissolved phase, and N is an exponent used to fit the curve. The exponent is also a measure of surface site heterogeneity; as N approaches 1, surface sites are more homogenous in their

chemical identity. The Freundlich partition coefficient (K_F) is similar to the linear solid-solution partition coefficient (K_d) except that K_F accommodates non-linear sorption behavior, where sorption is greatest at lower concentrations of dissolved manganese and as concentrations increase, surface sorption sites become filled and the magnitude of partitioning to the solid phase decreases. Based upon the shape of the sorption isotherms generated from the PHREEQC model, which invokes surface complexation, sorption site saturation occurs at highest manganese concentrations and the Freundlich parameters are appropriate.

- g) Sorption isotherms were generated at various concentrations of iron and were evaluated against field data obtained during installation of the upland ISPT wells. Manganese concentrations in soil were also determined during the analysis of soil iron minerals and manganese associated with the strong and weak site iron (as determined by selective extraction) was used to generate a field isotherm by evaluation of this data against measured groundwater concentrations at these locations (ARCADIS 2009b). Field isotherms matched the model isotherms when sorptive iron was scaled back by 10% - field and model isotherms were for silt/clay soil. Comparison of the model output to the field isotherms provides a measure of the representativeness of the model data with field observations.
- h) The Freundlich parameters for manganese were used in the fate and transport model in the MT3DMS solute transport component of the model. Arsenic sorption by the soil, as predicted by the sorption isotherms, was orders of magnitude greater than for manganese. An arsenic half-life was therefore used and this was based upon the measurement of arsenic in the floodplain ISPT as arsenic moved from within the carbon footprint to outside the footprint. The arsenic concentration in groundwater attenuated rapidly once it was outside of the influence of carbon, consistent with the sorption model. The use of a kinetic parameter provides a more conservative evaluation of arsenic in groundwater (whereas the use of a sorption parameter provides for extremely strong sorption and little ability to evaluate concentrations outside of the reduced zone).

A summary of the byproduct attenuation parameters used in the model is provided in Table 2.

Table 2. Byproduct attenuation terms used in fate and transport model.

Byproduct	Attenuation Terms (Freundlich Parameters (Mn) and Half Life (As))		
	Low	Base Case	High
Manganese	$K_F=0.64, N=0.54$	$K_F=1.28, N=0.57$	$K_F= 2.56, N=0.51$
Arsenic	15 days	30 days	60 days

As discussed above, manganese concentrations in groundwater have been monitored across the floodplain under IM-3 pumping conditions. An evaluation of the concentration trends for manganese across a transect of wells from the east (along the river) to the west (toward National Trails Highway) shows that as groundwater moves through less reducing geochemical conditions (away from the river), the concentration of manganese attenuates. The attenuation profile is simulated in the model by an analysis of manganese concentrations along a similar transect, moving from west (along the IRZ at National Trails Highway) to the east (toward the river). The attenuation profile predicted by the model output matches the field data and is further confirmation that the geochemical parameters used to simulate byproduct attenuation are reasonable. In addition, the parameter ranges shown in Tables 1 and 2 provide for an evaluation of the sensitivity of the model to the generation and attenuation factors. In summary the geochemical parameters were selected based upon an analysis of field analytical data, literature values and accepted geochemical modeling approaches; these parameters result in model output that simulates byproduct generation and attenuation consistent with observation made relative to natural conditions at the Topock site.

4.2.8 Naturally Occurring Manganese and Arsenic

In addition to the manganese and arsenic concentrations generated as byproducts as a result of the IRZ remediation strategy, there is naturally occurring manganese and arsenic that is accounted for in the solute transport model. With respect to manganese, there is a naturally occurring reducing rind that surrounds the Colorado River. This naturally occurring manganese in groundwater is the result of the decay of organic debris located in the Colorado River floodplain. Observed reducing rind manganese concentrations range in concentration from less than 1 ppm to as high as 9 ppm. To simulate a naturally occurring conservative manganese concentration

distribution in the rind, an additional simulation was performed under ambient (non-pumping) conditions. This assumed the rind was present in model layers 1 and 2, and extends approximately 250 ft on either side of the surface water features, as well as under the surface water features and marshland. Because this manganese distribution was established under ambient conditions, the impact of active remediation flow was also evaluated. This naturally occurring rind was then simulated in conjunction with the manganese generated as IRZ byproduct to determine the cumulative manganese distribution throughout the solute transport submodel domain.

With respect to arsenic, the primary naturally occurring arsenic that was simulated was associated with the proposed freshwater injection. Groundwater extracted from HNWR-1 located in Arizona was assumed to have a naturally occurring arsenic concentration of 17 ppb. This concentration was continuously applied to all of the simulated freshwater injection wells to evaluate the potential impact of the naturally occurring arsenic.

4.3 Parameter Assessment

A sensitivity analysis quantifies the impact that variations on model parameter values have on differences between Site observations and model predictions. This approach is extremely challenging for this study because of the various complexities of the area. However, various aspects of the hexavalent chromium plume and behavior of manganese and arsenic were analyzed in detail with the solute transport model to determine an appropriate range of solute transport parameters to use for the predictive modeling.

By adjusting parameters such as chromium partition coefficient, manganese freundlich constants, arsenic precipitation rate, manganese liberation rate, arsenic liberation rate, a reasonable qualitative and quantitative fit to the observed data and flow conditions was obtained.

In addition to varying the parameters for the constituents of concern, additional analyses were conducted to evaluate additional parameter impacts on the solute transport model. These parameters include the TOC injection concentration, the riverbank extraction well rate, and the NTH IRZ well spacing.

4.4 Remediation Design

There are seven different components of the proposed remediation design that are simulated concurrently with the solute transport model to effectively remediate the hexavalent chromium plume while reducing the impact of potential byproducts. Figure B-17 shows the locations of each of the proposed wells. Conceptual remedy cross-sections were developed based on the model structure and the locations of these cross-sections are shown in Figure B-18. Figures B-19 through B-24 show the individual cross-sections that depict the intercepted remedial wells in cross-section relative to the submodel structure. Each of these components is described in detail in the following sections:

4.4.1 National Trails Highway IRZ

The National Trails Highway IRZ (NTH IRZ) consists of a line of IRZ wells located along National Trails Highway running north-south for a distance of approximately 3,000 ft. These wells are designed to creating a reducing zone along the downgradient axis of the hexavalent chromium plume that is simulated in the upper 4 model layers. This system component is designed to be a recirculating system where all the water extracted along the NTH IRZ will be amended with carbon and injected into the IRZ NTH line resulting in a net flow of 0 gpm along the NTH IRZ line. Numerous elements of the NTH IRZ were evaluated with the solute transport model to determine the optimum treatment pattern. These elements include:

- Extraction / Injection well locations
- Well spacing
- Well cycling pattern (active operation / full shut down)
- Carbon loading concentration
- Extraction / Injection well rates

The first system design that produced reasonable effects was a NTH IRZ layout that consisted of a 20 well system and is shown in Figure B-17. The total extraction and injection rate for this layout was 300 gpm. The 300 gpm was extracted from four of the IRZ wells, 3 located at the northern end of the NTH IRZ operating at 66.7 gpm each, and one located toward the middle of the NTH IRZ operating at 100 gpm. By extracting at these locations the natural west to east flow gradient is generally preserved to encourage flow through the reduced groundwater. The spacing between each the northern NTH IRZ extraction wells is approximately 300 ft. In this area,

initialized hexavalent chromium concentrations are at relatively low levels with respect to the rest of the hexavalent chromium plume. In addition to the 4 NTH IRZ extraction wells, 16 injection wells were simulated in all four model layers. The injection rates were varied along the NTH IRZ based on the aquifer thickness. The aquifer thickness varies from over 300 ft thick at the northern end of the NTH IRZ to approximately 10 ft thick at the southern end of the NTH IRZ. The majority of the injection wells were spaced 150 ft apart, except in 2 locations towards the northern end of the NTH IRZ where spacing was reduced to 75 ft to prevent breakthrough of the hexavalent chromium plume. The simulated carbon concentration injected was 100 ppm. Higher TOC concentrations result in a more comprehensive reducing zone, however it also produces increased levels of byproducts. A carbon inject concentration of 100 ppm in the 150 ft well spacing layout limits the potential for gaps in treated groundwater while managing byproducts generated. A pattern of 6 months on, followed by 18 months off allowed for completed coverage of the hexavalent chromium passing through the reduced groundwater. Turning the system off allows for the established anaerobic conditions to continue without adding additional carbon that would increase the potential of byproduct generation.

While this simulated layout was effective in the solute transport model simulations and minimizes the number of wells necessary, additional wells should be considered as a conservative approach to establish a comprehensive treatment zone across the NTH IRZ. A second layout that was considered consisted of a well spacing of 75 ft along the NTH IRZ. Figure B-20 shows the 75 ft well spacing NTH IRZ in cross-section. Despite increasing the number of injection wells in this scenario, the total extraction and injection rates were still maintained at 300 gpm. However, because the spacing of the NTH IRZ wells is decreased, the carbon injection concentrations can potentially be lowered as well to reduce generated byproducts. The design tries to minimize the total number of NTH IRZ wells necessary while maintaining effective remediation. The goal is to limit the number of NTH IRZ well locations, therefore the 20 NTH IRZ well layout depicted in Figure B-17 provides the desired remedial impact with less infrastructure. However, contingency well locations are being considered in the event that additional infrastructure is deemed necessary. While the model suggests that either of these NTH IRZ layouts are viable options, the design should still be flexible enough to adapt to observed field conditions and system performance during operation. Freshwater Injection

To accelerate the remedial process, a series of freshwater injection wells were simulated upgradient of the plume extent in all 4 upper model layers. The naturally occurring hydraulic gradient toward the Colorado River is relatively low, which extends

4.4.3 Uplands Injection

The water extracted from the riverbank extraction wells is recirculated to 2 upland injection wells. These wells inject into model layers 1 through 4 at rates of 75 gpm each. Special consideration was taken in the solute transport model to allow any potential byproduct concentrations extracted at the riverbank extraction wells to be accounted for in the injected upland wells. The upland well locations that receive the riverbank extraction wells are depicted in Figure B-17. Figure B-22 shows the upland injection wells in cross-section.

4.4.4 Extraction Wells northeast of the Compressor Station

Four extraction wells were simulated between the TCS and the NTH IRZ in the aquifer area northeast of the TCS. The purpose of these extraction wells is to accelerate the capture and treatment of the hexavalent chromium plume immediately downgradient of the TCS. These wells are simulated in model layers 1 through 4 and operate at a total rate of 19 gpm. The rate at each of the individual wells is varied based on the thickness of the screened aquifer, with the highest rate in the thicker northwest portion of the aquifer and the lowest rate in the thinner southeast portion of the aquifer. This extracted water is assumed to be treated and injected into 2 TCS injection wells. The locations and rates of the 4 extraction wells is shown in Figure B-17. Figure B-21 shows the extraction wells northeast of the compressor station in cross-section.

4.4.5 East Ravine Extraction

Located in the southeast portion of the plume that exists in the bedrock, 4 extraction wells were simulated and are referred to as the East Ravine Extraction wells. The purpose of these wells is to extract the hexavalent chromium impacted groundwater located in the bedrock. These wells are screened in the upper four layers of the model. In this portion of the model, the upper four layers represent the shallow bedrock and the hydraulic conductivities are considerably lower than the hydraulic conductivities of the alluvial aquifer. Because of the tighter material in this vicinity, sustainable extraction rates are limited. In the solute transport model, the East Ravine Extraction wells extract at a total rate of only 2 gpm, with the rate divided evenly over all four wells. The extracted water will be injected along with water extracted from the Wells northeast of the Compressor Station into the two TCS wells. The location of the East Ravine Extraction wells is shown in Figure B-17. Figure B-20 shows the East Ravine extraction wells in cross-section.

4.4.6 Topock Compressor Station Injection

Water from the extraction wells northeast of the Compressor Station and the East Ravine Extraction wells is treated and injected into two wells located in the immediate vicinity of the TCS. These two wells are screened in model layers 1 through 4 and inject at rates of 10.5 gpm each. They are located within the footprint of the plume and serve to treat hexavalent chromium impacted water in the immediate vicinity and accelerate groundwater flow towards the extraction wells northeast of the Compressor Station and the NTH IRZ. Similar to the NTH IRZ, these injection wells are carbon amended. They are proposed to operate constantly although carbon loading was varied over time to reduce the impact of byproducts. During the 6 month period where the NTH IRZ is active, TCS injection well carbon concentrations are 100 ppm, and during the 18 month NTH IRZ off period, carbon concentrations are reduced to 5 ppm. An additional element considered for the TCS injection wells is that because they are located within the footprint of the plume, stagnation points may develop upgradient of these wells. To compensate for these potential stagnation areas, it is recommended that the southern freshwater injection well located upgradient of the TCS should inject at a higher rate than the TCS injection wells. In these solute transport runs the southern freshwater injection rate is maintained at 50 gpm to continue the eastward push of groundwater despite the 21 gpm injected at the TCS. The locations of the two TCS injection wells are shown in Figure B-17. Figure B-23 shows the TCS injection wells in cross-section.

4.5 Flow Conditions

The simulated groundwater contours for the solute transport model under ambient conditions is shown in Figure B-25. This figure indicates the dominant flow direction under ambient conditions in the vicinity of the area of concern is from west to east in the direction of the Colorado River. The impact of the proposed remediation design on the submodel groundwater flow is shown in Figure B-26. Figure B-26 depicts the two potential groundwater conditions that exist with the proposed remedy design. One condition shows conditions with the NTH IRZ under operating conditions for a 6 month period, while the second image shows conditions with the NTH IRZ turned off for an 18 month period. In both the active remediation scenarios, flow direction of the groundwater within the footprint of the plume remains from east to west towards the Colorado River, however gradients are steeper than the original ambient conditions indicating an improved potential period of performance.

5. Solute Transport Results

5.1 Hexavalent Chromium

The solute transport model was run for a period of 30 years utilizing the transport parameters and flow conditions described in the previous report section for the simulated hexavalent chromium. The results are shown for years 0.5, 1.5, 5, 10, 20, and 30 years for each of the four model layers in Figures B-27 through B-30. These figures show the impact the injected carbon concentrations and remediation design flow conditions have on the chromium distribution over time. Carbon is actively injected into the NTH IRZ during the first 6 months of the simulation, followed by an 18 month period where the NTH IRZ is turned off. This 6 month on / 18 month off NTH IRZ cycle period is repeated for the full duration of the 30 year transport run. This solute transport run indicates the NTH IRZ successfully creates a remediation barrier along the majority of the NTH IRZ line in all four model layers. The sections of the plume that are initialized on the east side of the NTH IRZ and the low hexavalent chromium concentrations in the vicinity of the NTH IRZ wells that are not treated by the NTH IRZ, are hydraulically controlled by the riverbank extraction wells. By year 30 of the simulated transport run, the majority of the hexavalent chromium plume in all four model layers has been remediated. The only exception by year 30 is the portion of the hexavalent chromium that is initialized in the bedrock in the vicinity of the East Ravine extraction wells. This is due to the tight hydraulic conductivity values simulated in the bedrock the limit flow velocities and remediation timeframes. This is a limitation of the groundwater flow model and solute transport model because potential fractured bedrock or high conductivity channels that potentially exist in the bedrock cannot be accounted for in this analysis. The effectiveness of the East Ravine extraction wells located in the bedrock need to be closely monitored during the remediation design implementation.

5.2 Manganese

The results for the simulated manganese are presented for the same 30 year period and 4 model layers as the hexavalent chromium results in Figures B-31 through B-34. The manganese runs take into account both the simulated naturally occurring manganese as well as potential manganese generated as a byproduct from carbon amended injection wells. These figures indicate generated byproduct manganese concentrations are significantly lower than the naturally occurring manganese. The manganese transport run indicates that portions of the naturally occurring manganese rind and generated manganese byproduct will be extracted by the riverbank extraction

5. Solute Transport Results

5.1 Hexavalent Chromium

The solute transport model was run for a period of 30 years utilizing the transport parameters and flow conditions described in the previous report section for the simulated hexavalent chromium. The results are shown for years 0.5, 1.5, 5, 10, 20, and 30 years for each of the four model layers in Figures B-27 through B-30. These figures show the impact the injected carbon concentrations and remediation design flow conditions have on the chromium distribution over time. Carbon is actively injected into the NTH IRZ during the first 6 months of the simulation, followed by an 18 month period where the NTH IRZ is turned off. This 6 month on / 18 month off NTH IRZ cycle period is repeated for the full duration of the 30 year transport run. This solute transport run indicates the NTH IRZ successfully creates a remediation barrier along the majority of the NTH IRZ line in all four model layers. The sections of the plume that are initialized on the east side of the NTH IRZ and the low hexavalent chromium concentrations in the vicinity of the NTH IRZ wells that are not treated by the NTH IRZ, are hydraulically controlled by the riverbank extraction wells. By year 30 of the simulated transport run, the majority of the hexavalent chromium plume in all four model layers has been remediated. The only exception by year 30 is the portion of the hexavalent chromium that is initialized in the bedrock in the vicinity of the East Ravine extraction wells. This is due to the tight hydraulic conductivity values simulated in the bedrock the limit flow velocities and remediation timeframes. This is a limitation of the groundwater flow model and solute transport model because potential fractured bedrock or high conductivity channels that potentially exist in the bedrock cannot be accounted for in this analysis. The effectiveness of the East Ravine extraction wells located in the bedrock need to be closing monitored during the remediation design implementation.

5.2 Manganese

The results for the simulated manganese are presented for the same 30 year period and 4 model layers as the hexavalent chromium results in Figures B-31 through B-34. The manganese runs take into account both the simulated naturally occurring manganese as well as potential manganese generated as a byproduct from carbon amended injection wells. These figures indicate generated byproduct manganese concentrations are significantly lower than the naturally occurring manganese. The manganese transport run indicates that portions of the naturally occurring manganese rind and generated manganese byproduct will be extracted by the riverbank extraction

wells and injected into the two upland injection wells. This potential manganese impact in the uplands needs to be monitored over time to avoid elevated manganese concentrations. A potential method to mitigate this upland manganese impact would be to blend the riverbank extracted water with the freshwater injection.

5.3 Arsenic

The results for the simulated arsenic are presented for the same 30 year period and 4 model layers as the hexavalent chromium and manganese results in Figures B-35 through B-38. The arsenic runs take into account both the simulated naturally occurring arsenic associated with the freshwater injection as well as potential arsenic generated as a byproduct from carbon amended injection wells. The solute transport run indicates that arsenic concentrations associated with carbon amended injection never exceed 10 ppb. The only arsenic concentrations that exceed 10 ppb is associated with the naturally occurring arsenic concentrations that are injected into the 5 freshwater injection wells at a conservative concentration of 17 ppb. Despite constant injection rates and arsenic concentrations at these locations, steady state conditions develop within 5 years where the arsenic footprint appears static. This is due to the fact that the simulated arsenic precipitates so rapidly in these areas, the arsenic footprint is unable to expand further.

6. Sensitivity Analysis

A sensitivity analysis was conducted to evaluate the relative impact various components of the groundwater flow and solute transport models have on the solute transport model results. The sensitivity analyses presented in this appendix include NTH IRZ well spacing, injected TOC concentrations, riverbank extraction rates, manganese sorption and generation, arsenic precipitation and generation, and hexavalent chromium sorption.

6.1 NTH IRZ Well Spacing

The NTH IRZ remedial wells are designed to create a reducing zone along the downgradient axis of the hexavalent chromium plume that is simulated in the upper 4 model layers. The primary two NTH IRZ layouts evaluated consisted of 150 ft spacing and 75 ft spacing between NTH IRZ injection wells. In both scenarios, the total extraction and injection rates of the entire NTH IRZ are maintained at 300 gpm each, for a net flow difference of 0 gpm. The 150 ft spacing layout was evaluated with a TOC concentration of 100 ppm, while the 75 ft spacing layout had a reduced TOC

concentration of 75 ppm. The impact of these two layouts with respect to the hexavalent chromium, after 10 years of simulated transport in model layer 4, are displayed in Figure B-39. It is clear that the original 150 ft spacing layout allows some hexavalent chromium groundwater concentrations to pass through the NTH IRZ remedial system towards the northern end of the system, while the 75 ft spacing layout provides an effective reducing zone. To address the breakthrough occurring with the original 150 ft spacing layout, two injection wells were added to reduce the spacing to 75 ft in the area of concern. Figure B-40 displays the revised 150 ft spacing layout in comparison to the 75 ft spacing layout with respect to the hexavalent chromium after 10 years of simulated transport in model layer 4. This figure indicates the two NTH IRZ injection wells added to the 150 ft well spacing layout design successfully create a full reducing zone to prevent hexavalent chromium from migrating through the NTH IRZ remedial system. Figure B-41 depicts the revised 150 ft spacing layout in comparison to the 75 ft spacing layout with respect to the hexavalent chromium after 10 years of simulated transport for model layer 2. A small portion of the hexavalent chromium flows downgradient from the central portion of the NTH IRZ in the 75 ft spacing version at the end of an 18 month off cycle (year 10), however when the system is turned back on for a 6 month period, the downgradient hexavalent chromium is reduced.

The NTH IRZ well spacing was also evaluated with respect to manganese concentrations. Figure B-42 depicts the simulated manganese distribution after 10 years in model layer 2 for both the revised 150 ft well spacing and 75 ft well spacing layouts. This figure clearly indicates that the 75 ft well spacing produces a lower manganese byproduct concentration distribution, while the revised 150 ft well spacing produces a relatively higher concentration with slightly further downgradient eastward expansion. This is a result of the higher rates per individual injection well in the 150 ft NTH IRZ spacing and a slightly higher injected TOC concentration. Arsenic was also evaluated with the various NTH IRZ well spacing scenarios, but all results were negligible due to the low arsenic byproduct generation.

6.2 Injected TOC Concentrations

The next parameter evaluated with respect to hexavalent chromium reduction and byproduct generation was the injected TOC concentration. The revised 150 ft NTH IRZ well spacing layout was utilized to evaluate a range of injected TOC concentrations from 50 ppm to 150 ppm. The impact of the injected TOC concentration on simulated hexavalent chromium transport after 10 years for model layers 2 and 4 is depicted in Figures B-43 and B-44, respectively. Slight hexavalent chromium breakthrough occurs in model layer 2 at an injected TOC concentration of 50 ppm, but there are only minor

differences in the solute transport results for hexavalent chromium at the 50 ppm, 100 ppm, and 150 ppm TOC injection concentrations.

Figure B-45 displays the sensitivity of manganese to the various injected TOC concentrations after 10 years of simulated transport. This figure indicates a direct relationship between TOC concentrations and manganese byproduct generation. Compared to the base injected TOC concentration of 100 ppm, an injected TOC concentration of 50 ppm results in approximately 50% less manganese generation, and an injected TOC concentration of 150 ppm results in approximately 50% more manganese generation. A similar trend occurs for arsenic, but all results for arsenic were still negligible due to the low arsenic byproduct generation.

During implementation of the NTH IRZ remedial design, hexavalent chromium and byproduct concentrations will be monitored to evaluate the effectiveness of the system. Injected TOC concentration will be adjusted to minimize byproducts while still generating an effective reducing zone to treat the hexavalent chromium.

6.3 Riverbank Extraction Rates

The riverbank extraction wells in the remedial system design serve a dual purpose: to capture low level hexavalent chromium impacts downgradient of the NTH IRZ system and to accelerate the groundwater velocity through the NTH IRZ induced reducing zone to minimize the remedial timeframe of the hexavalent chromium plume. A range of riverbank extraction rates were evaluated from 0 gpm to 300 gpm. Figure B-46 depicts the impact of riverbank extraction rates of 0 gpm, 150 gpm, and 300 gpm on simulated hexavalent chromium transport after 10 years for model layer 2. This sensitivity analysis indicates that the footprint of the >1,000 ppb hexavalent chromium plume when pumping 300 gpm is approximately 50% smaller when compared to the footprint at the 0 gpm extraction rate.

Figure B-47 depicts the impact of the range of riverbank extraction rates on simulated manganese in model layer 2 after 10 years of transport. In the vicinity of the NTH IRZ and the riverbank extraction wells, the difference between the manganese byproduct distribution is minimal, with higher riverbank extraction rates resulting in a more spread out manganese byproduct distribution. However, there is a significant difference in the uplands where the riverbank extracted water is injected. Under no riverbank extraction, there is no upland manganese injection. The 150 gpm river bank extracted water is injected into 2 upland wells (75 gpm each), while the 300 gpm river bank extracted water is injected into 3 upland wells (100 gpm each). The resulting

manganese concentration distribution at year 10 indicates double the uplands footprint with 300 gpm riverbank extraction as compared to the 150 gpm riverbank extraction.

6.4 Manganese Sorption and Generation

To evaluate the sensitivity of the solute transport model to the manganese geochemical parameters, an analysis was performed varying the sorption and generation terms for manganese in the solute transport model within a reasonable range (see sections 4.2.6 and 4.2.7). To visualize the impact the variations of the manganese parameters has on the solute transport modeling results, the change in dissolved manganese mass after 10 years relative to the base scenario were computed and are depicted in a bar chart in Figure B-48. Both the sorption and generation parameters were reduced by half and doubled to determine the relative impact on the dissolved manganese mass after 10 years of simulated transport. Doubling the sorption parameters resulted in a 36% decrease in dissolved manganese mass at year 10, and halving the sorption parameters resulted in a 20% increase in dissolved manganese at year 10. Doubling the generation parameters resulted in a 33% increase in dissolved manganese mass at year 10, and halving the generation parameters resulted in a 11% decrease in dissolved mass at year 10.

6.5 Arsenic Precipitation and Generation

To evaluate the sensitivity of the solute transport model to the arsenic geochemical parameters, an analysis was performed varying the precipitation and generation terms for arsenic in the solute transport model within a reasonable range (see sections 4.2.6 and 4.2.7). To visualize the impact the variations of the arsenic parameters has on the solute transport modeling results, the change in dissolved arsenic mass after 10 years relative to the base scenario were computed and are depicted in a bar chart in Figure B-49. Both the precipitation and generation parameters were reduced by half and doubled to determine the relative impact on the dissolved manganese mass after 10 years of simulated transport. Doubling the precipitation parameter resulted in a 50% decrease in dissolved manganese mass at year 10, and halving the precipitation parameter resulted in a 91% increase in dissolved arsenic at year 10. Doubling the generation parameters resulted in an 11% increase in dissolved arsenic mass at year 10, and halving the generation parameters resulted in a 6% decrease in dissolved mass at year 10.

6.6 Chromium Sorption

To evaluate the sensitivity of the solute transport model results to the hexavalent chromium sorption parameter, the distribution coefficient (K_d) of hexavalent chromium was doubled. The base K_d of 0.05 L/kg was increased to a K_d of 0.10 L/kg. The resulting impact on the hexavalent chromium transport after 10 years of transport in model layer 2 is depicted in Figure B-50. Doubling the hexavalent chromium K_d results in an approximate 20% increase in remediation time as the retardation factor increases with higher K_d values.

7. Conclusions

Based on the various sensitivity analyses and solute transport runs, the solute transport model indicates that the proposed remedial design is effective in remediating the current hexavalent chromium plume distribution while minimizing the potential adverse impacts from byproduct generation. This solute transport model can be utilized as a tool to evaluate potential remedial options, but the implemented remedial system will still be closely monitored to determine the effectiveness of this proposed approach. During installation and implementation of the remedial design, the additional hydrogeologic data and groundwater concentration collected can be utilized to update the groundwater flow and transport models to improve their effectiveness as evaluation tools.

8. References

- Anderson, M. P. and W. W. Woessner, 1992. *Applied Groundwater Modeling: Simulation of Flow and Advective Transport*, Academic Press, Inc., New York, 381 p.
- Andrews, C.B. and C.J. Neville, 2003. Groundwater Flow in a Desert Basin: Challenges of Simulating Transport of Dissolved Chromium. *Ground Water* 41(2):219-226.
- ARCADIS, 2008. Floodplain Reductive Zone In-Situ Pilot Test Final Completion Report. March 5, 2008.

ARCADIS, 2009. Upland Reductive Zone In-Situ Pilot Test Final Completion Report. March 3, 2009.

ARCADIS, 2009b. Third Quarter 2009 Monitoring Report for the Upland Reductive Zone In-Situ Pilot Test. December 15, 2009.

CH2M HILL, 2011. IM-3 monitoring report.

CH2M HILL, 2009. Corrective Measures/Feasibility Study Report for Chromium in Groundwater.

CH2M HILL, 2005a. Summary of Results—Aerobic Zone Hexavalent Chromium Core Testing, PG&E Topock Compressor Station, Needles, California. May 20, 2005.

CH2M HILL, 2005b. Groundwater Model Update Report, PG&E Topock Compressor Station, Needles, California. July 29, 2005.

Dribblee, T.W. Jr. 1967. Areal geology of the western Mojave Desert, California. Professional Paper 522. Washington, D.C.: USGS.

Dzombak, D.A., and Morel, F.M. 1990. Surface Complexation Modeling: Hydrous Ferric Oxide. New York: Wiley-Interscience. 393pp.

EPA, 2005. Allison, J.D., and Allison, T.L. Partition coefficients for metals in surface water, soil, and waste. U.S. Environmental Protection Agency EPA/600/R-05/074.

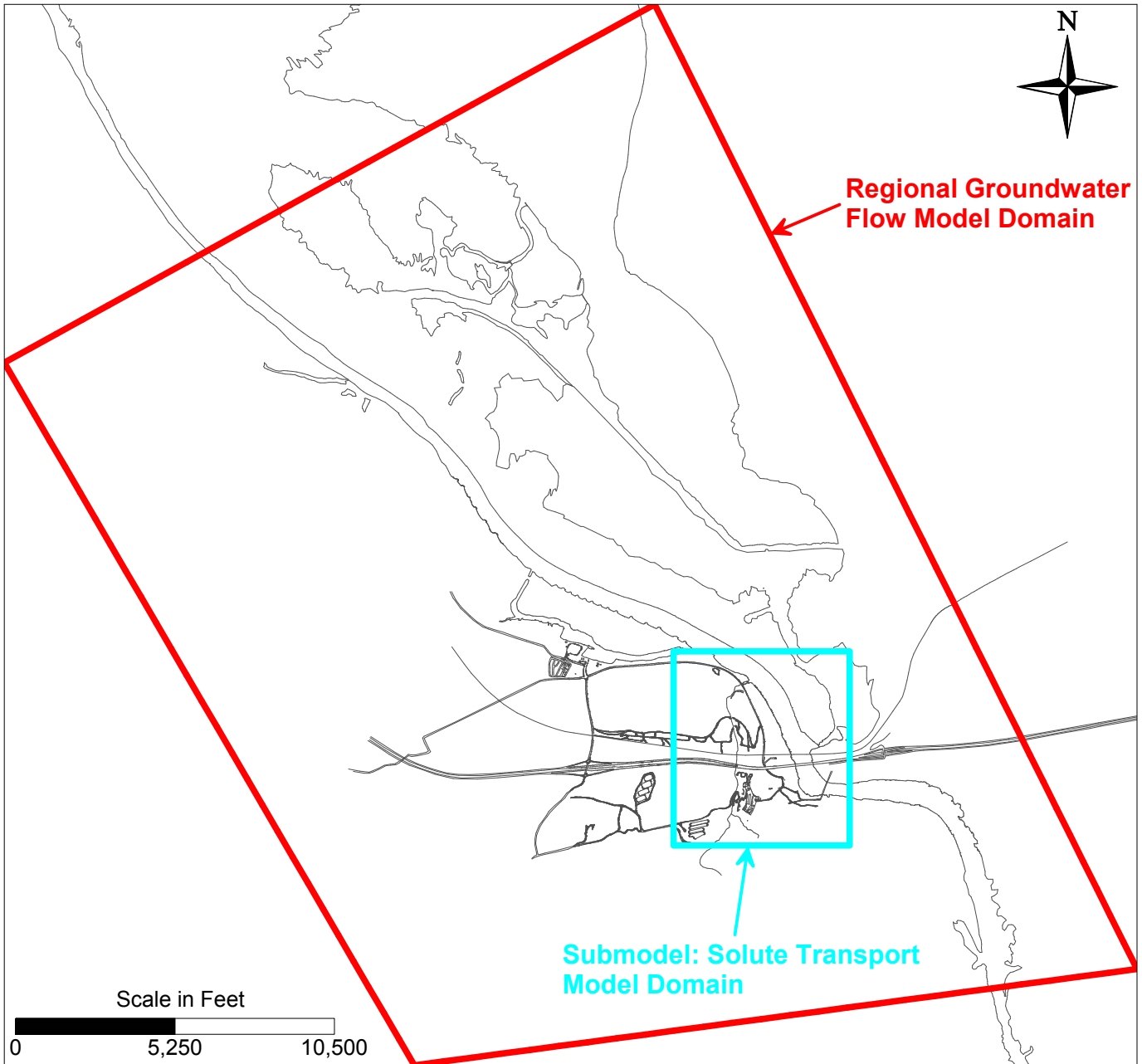
Essington, M.E. Soil and Water Chemistry, An Integrative Approach. New York: CRC Press. 534pp.

Feehley, C.E., C. Zheng, and F.J. Molz. 2000. *A dual-domain mass transfer approach for modeling solute transport in heterogeneous aquifers: Application to the macrodispersion experiment (MADE) site*. Water Resources Research 36, no. 9: 2501–2515.

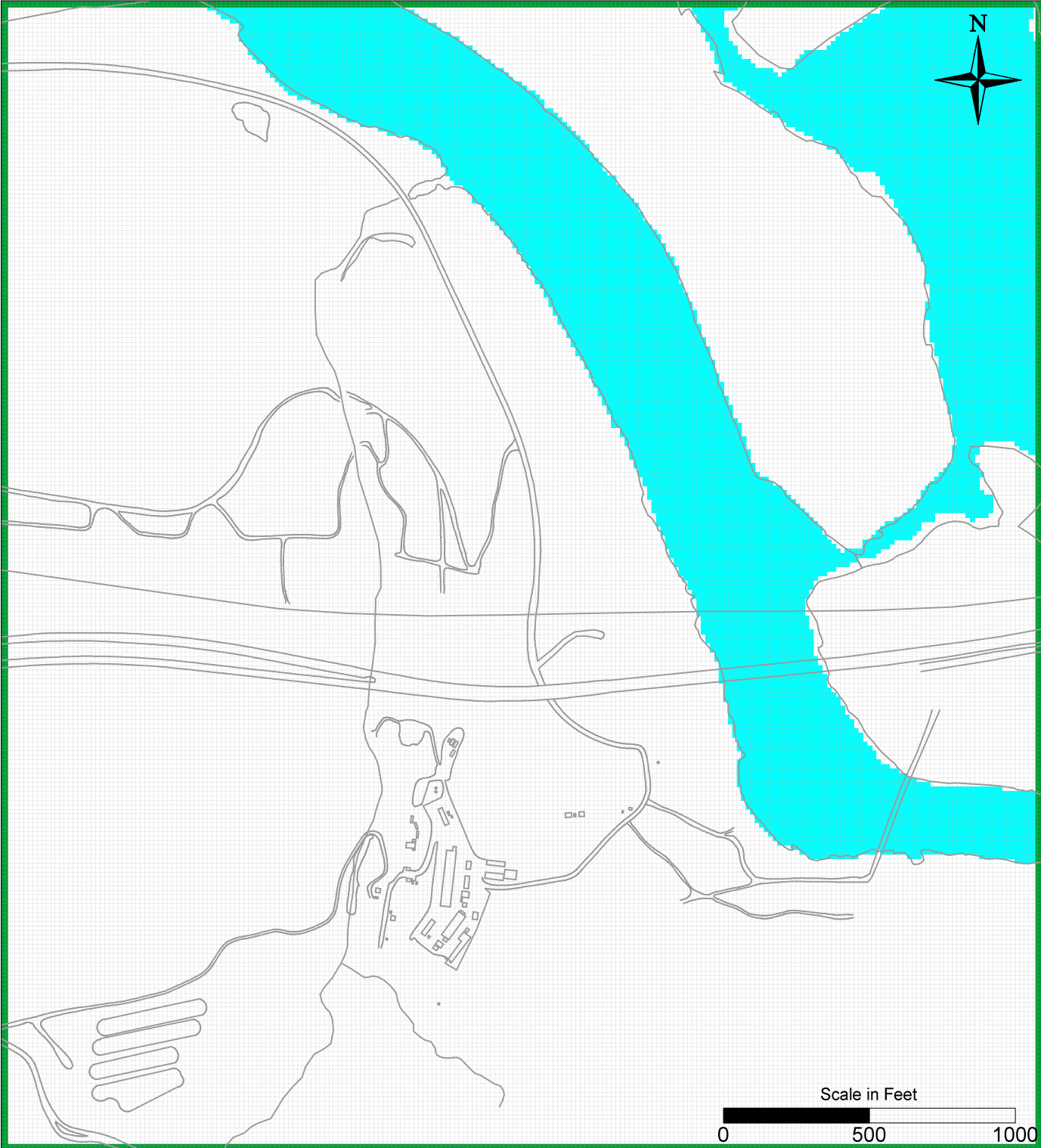
Flach, G.P., S.A. Crisman, and F.J. Molz III, 2004. Comparison of Single-Domain and Dual-Domain Subsurface Transport Models. *Ground Water* 42, no. 6: 815-828.

- Fuller, C.C. and Harvery, J.W., 2000. *Reactive Uptake of Trace Metals in the Hyporheic Zone of a Mining-Contaminated Stream, Pinal Creek, Arizona*. *Environmental Science and Technology* 34(7): 1150-1155.
- Gillham, R.W., E.A. Sudicky, J.A. Cherry, and E.O. Frind. 1984. *An advection-diffusion concept for solute transport in heterogeneous unconsolidated geological deposits*. *Water Resources Research* 20, no.3: 369-378
- Gleyzes, C., Teller, S., Astruc, M., 2002. *Fractionation studies of trace elements in contaminated soils and sediments: a review of sequential extraction procedures*. *Trends in Analytical Chemistry* 21(6-7), 451-467.
- Harvey, C.F., and S.M. Gorelick. 2000. *Rate-limited mass transfer or macrodispersion: Which dominates plume evolution at the macrodispersion experiment (MADE) site?* *Water Resources Research* 36, no. 3: 637–650.
- Hemker, C.J. 2006. MicroFEM, version 3.60. Groundwater flow modeling software, available at <http://www.microfem.com>.
- Howard, K. A., B.E. John, and J.E. Nielson. 1997. *Preliminary Geological Map of Eastern and Northern Parts of the Topock 7.5-minute Quadrangle, Arizona and California*, United States Geological Survey Open-File report 95-534
- Julian, H.E., M.J. Boggs, C. Zheng, and C.E. Feehley. 2001. *Numerical simulation of a natural gradient tracer experiment for the natural attenuation study: Flow and physical transport*. *Ground Water* 39, no. 4: 534–545.
- Konikow, L., 1978. *Calibration of Groundwater Models, in Proceedings of the Specialty Conferences on Verification of Mathematical and Physical Models in Hydraulic Engineering*, College Park, Maryland, August 9-11, 1978.
- McDonald, M. G., and A. W. Harbaugh, 1988. *A Modular Three-Dimensional Finite-Difference Ground-Water Flow Model, Techniques of Water-Resources Investigations, Book 6, Chapter A1*. U. S. Geological Survey. Reston, Virginia.
- Metzger, D.G., Loeltz, O.J. 1973. *Geohydrology of the Needles Area, Arizona, California, and Nevada*. U.S. Geological Professional Paper 486-J

- Molz, F.J., C. Zheng, S.M. Gorelick, and C.F. Harvey. 2006. *Comment on "Investigating the Macrodistribution Experiment (MADE) site in Columbus, Mississippi, using a three-dimensional inverse flow and transport model" by Heidi Christiansen Barlebo, Mary C. Hill, and Dan Rosbjerg*. Water Resources Research. 42 no. 6 W06603
- Payne, F.C., J.A. Quinnan, and S.T. Potter. 2008. Remediation Hydraulics. CRC Press, Boca Raton, Florida.
- PG&E, 2011. March 18, 2011 response to the February 11, 2011 Water Board's request that PG&E provide additional details Information on the input parameters used in modeling in support of the Feasibility Study
- Smedley, P.L., and Kinniburgh, D.G. 2002. A review of the source, behaviour and distribution of arsenic in natural waters. Applied Geochemistry 17: 517–568
- U.S. Environmental Protection Agency (USEPA). 1999. Understanding Variation in Partition Coefficient, K_d, Values, Volume II: Review of Geochemistry and Available K_d Values for Cadmium, Cesium, Chromium, Lead, Plutonium, Radon, Strontium, Thorium, Tritium, and Uranium. Appendix E.
- USGS, 1999. Parkhurst, D.L. and Appelo, C.A.J. User's Guide to PHREEQC (Version 2) – A Computer Program for Speciation, Batch-Reaction, One-Dimensional Transport, and Inverse Geochemical Calculations. United States Geological Survey Water-Resources Investigations Report 99-4259.
- Zheng, C., 1990. *MT3D: A Modular Three-Dimensional Transport Model for Simulation of Advection, Dispersion, and Chemical Reactions of Contaminants in Groundwater Systems*. Prepared for the U.S. Environmental Protection Agency. Robert S. Kerr Environmental Research Laboratory, Ada, Oklahoma. Developed by S.S. Papadopoulos & Associates, Inc., Rockville, Maryland.
- Zheng, C., and G. D. Bennett, 2002, *Applied Contaminant Transport Modeling Second Edition*, John Wiley & Sons, New York, 621 pp.
- Zheng, C., and P. Wang, 1999. *MT3DMS: A Modular Three-Dimensional Multispecies Transport Model for Simulation of Advection, Dispersion, and Chemical Reactions of Contaminants in Groundwater Systems*. Prepared for the U.S. Army Corps of Engineers, Washington, DC. University of Alabama, Tuscaloosa,.



PG&E TOPOCK COMPRESSOR STATION NEEDLES, CALIFORNIA MODELING APPENDIX	
REGIONAL MODEL AND SUBMODEL DOMAIN EXTENTS	
	FIGURE B-1



LEGEND

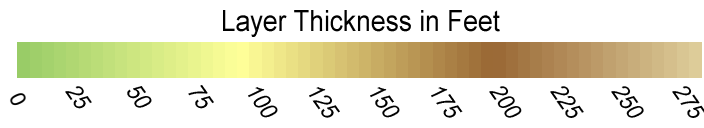
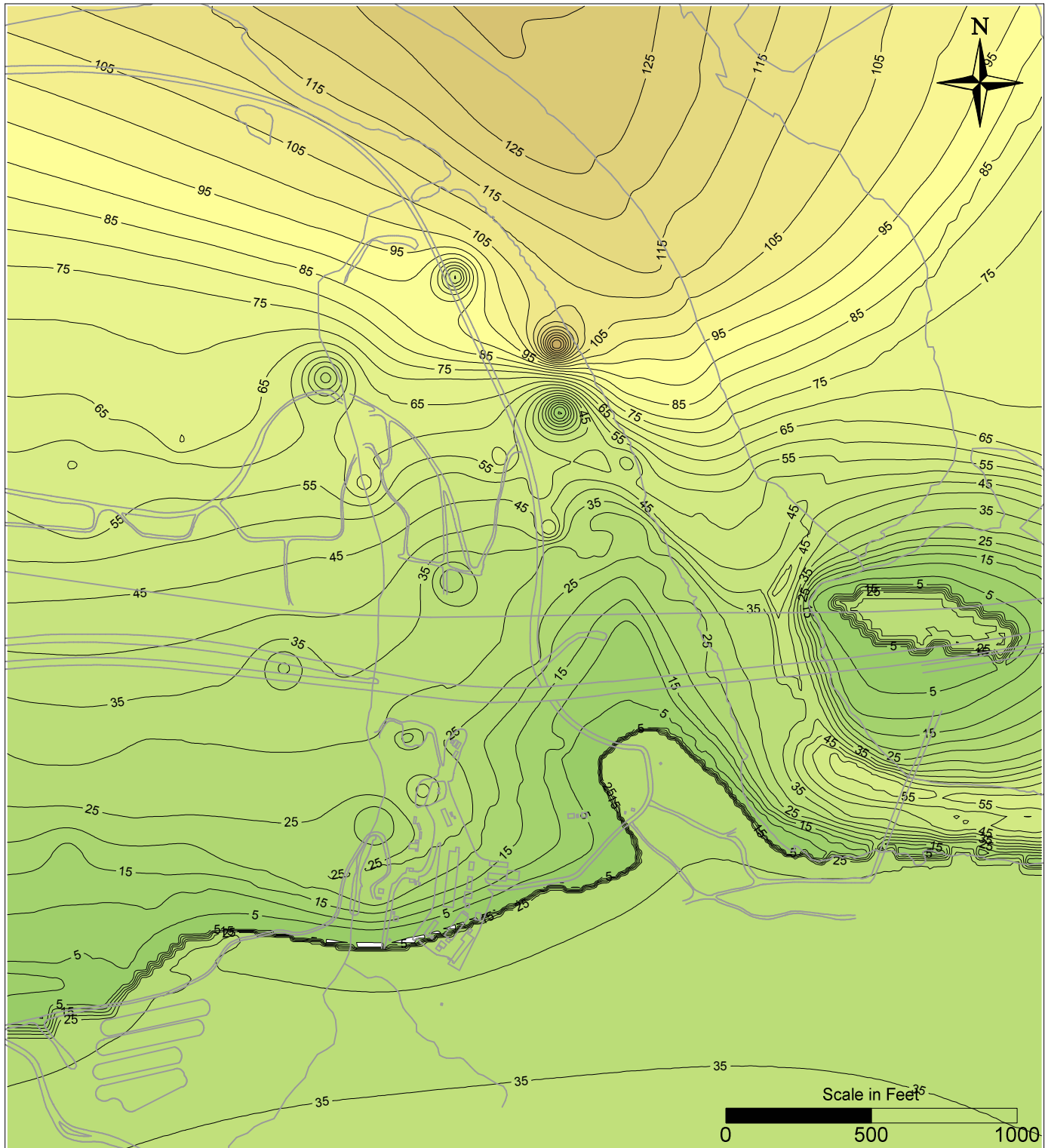
-  Finite Difference Grid Cell
-  Constant Flux Boundary Cell
-  River Boundary Cell

PG&E
 TOPOCK COMPRESSOR STATION
 NEEDLES, CALIFORNIA
 MODELING APPENDIX

SUBMODEL DOMAIN AND
 FINITE DIFFERENCE GRID



FIGURE
 B-2

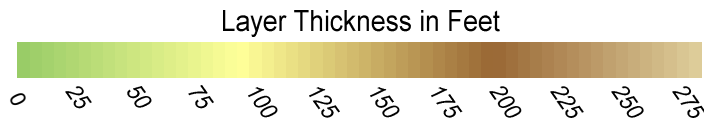
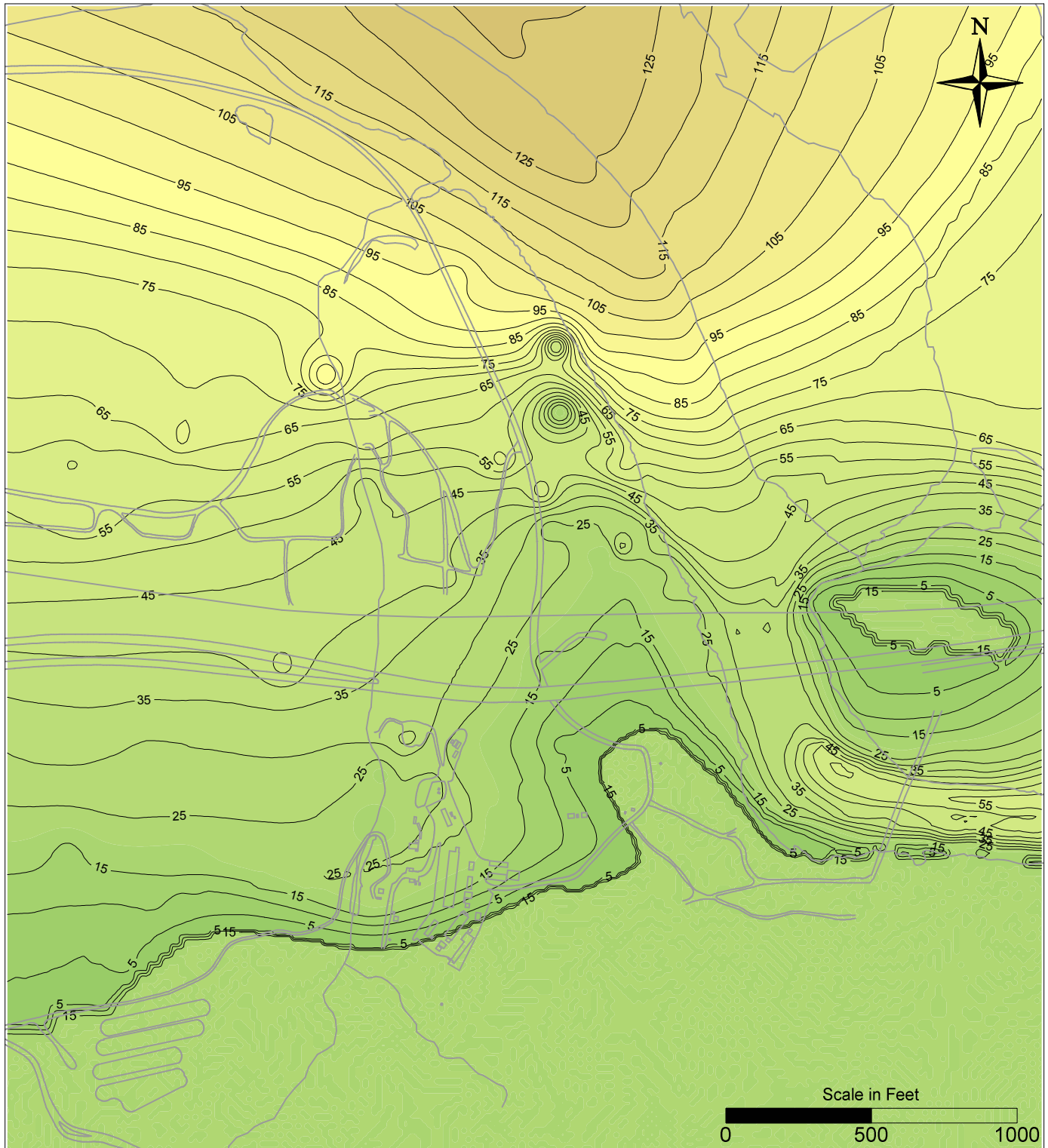


PG&E
 TOPOCK COMPRESSOR STATION
 NEEDLES, CALIFORNIA
 MODELING APPENDIX

THICKNESS MODEL LAYER 1



FIGURE
 B-3

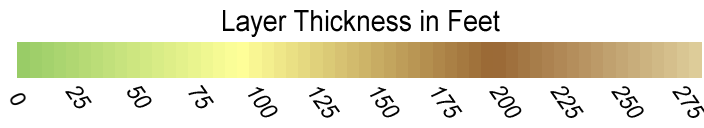
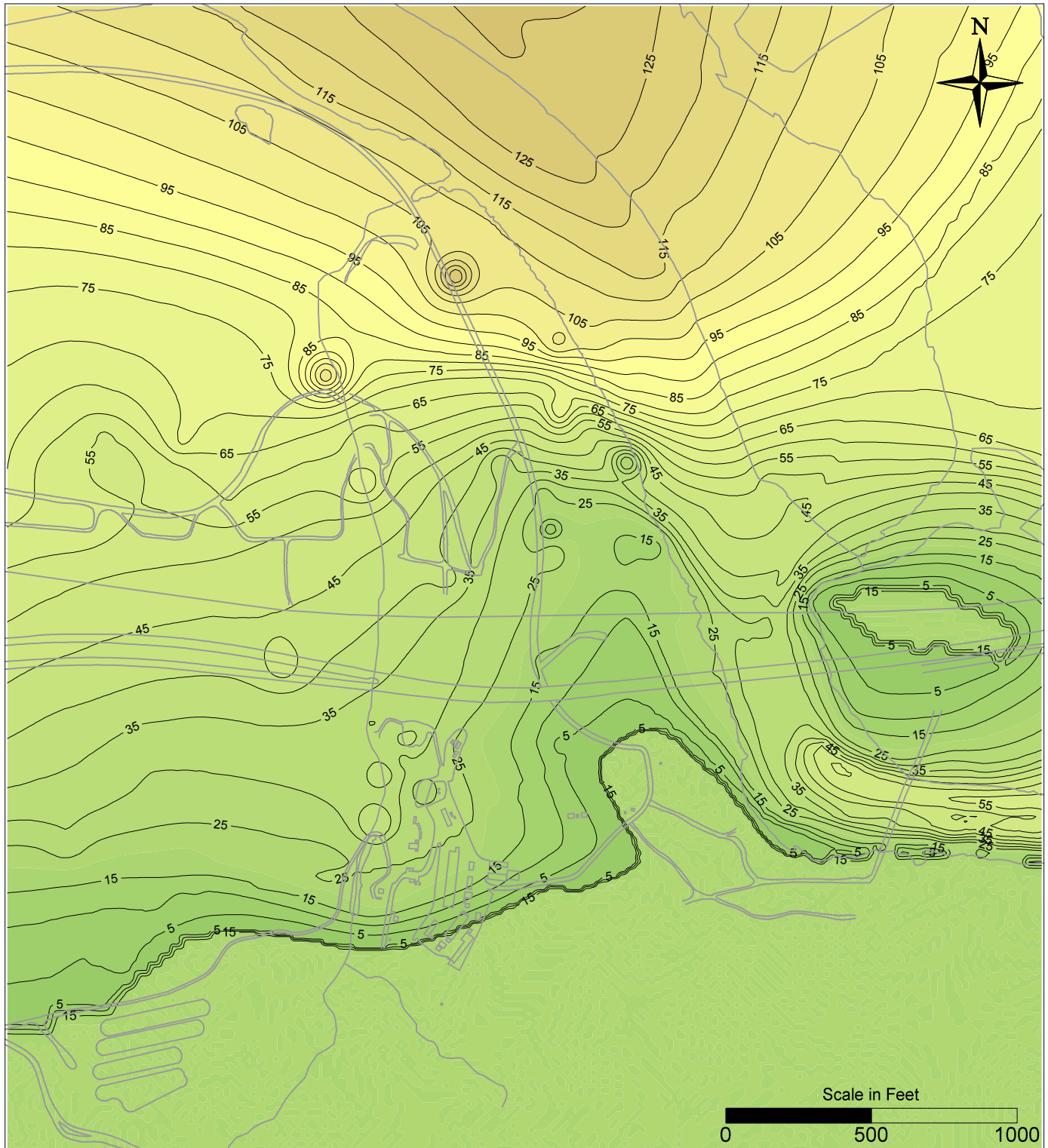


PG&E
 TOPOCK COMPRESSOR STATION
 NEEDLES, CALIFORNIA
 MODELING APPENDIX

THICKNESS MODEL LAYER 2



FIGURE
 B-4

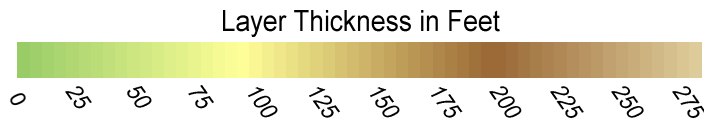
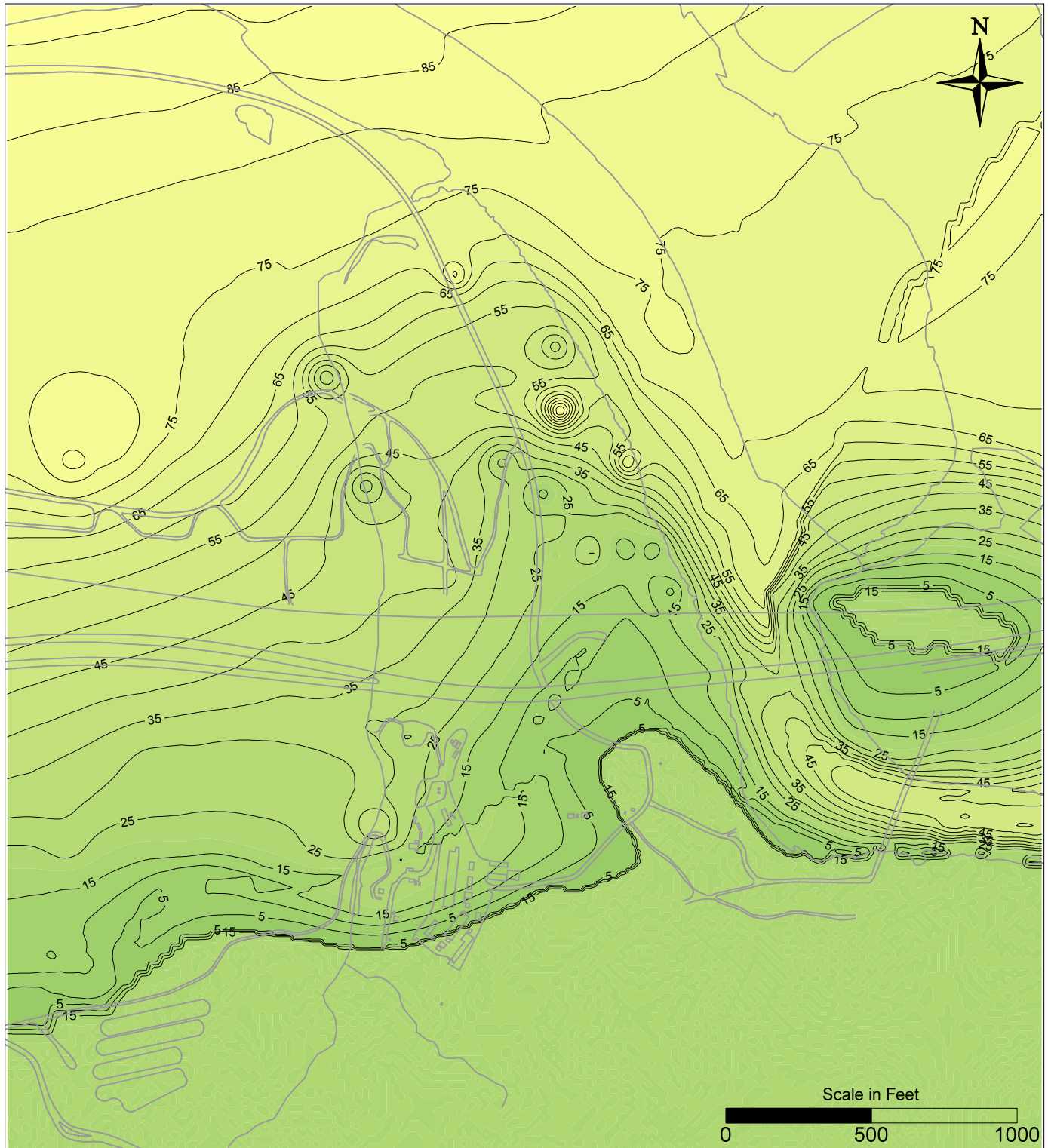


PG&E
 TOPOCK COMPRESSOR STATION
 NEEDLES, CALIFORNIA
 MODELING APPENDIX

THICKNESS MODEL LAYER 3



FIGURE
 B-5

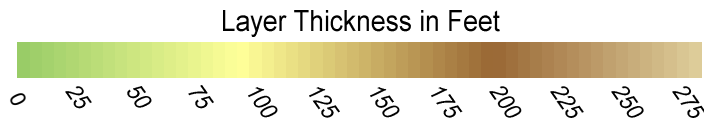
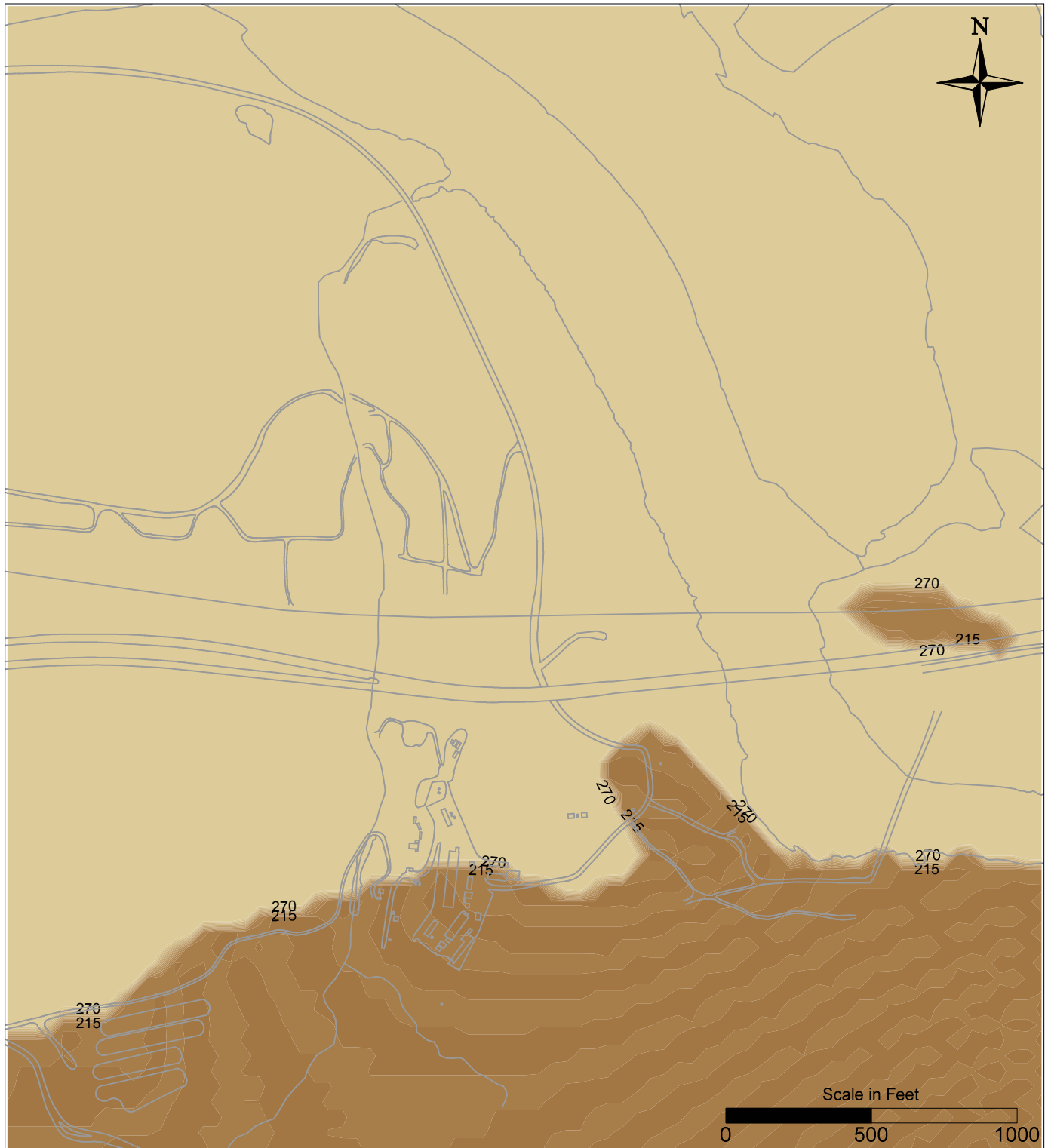


PG&E
 TOPOCK COMPRESSOR STATION
 NEEDLES, CALIFORNIA
 MODELING APPENDIX

THICKNESS MODEL LAYER 4



FIGURE
 B-6

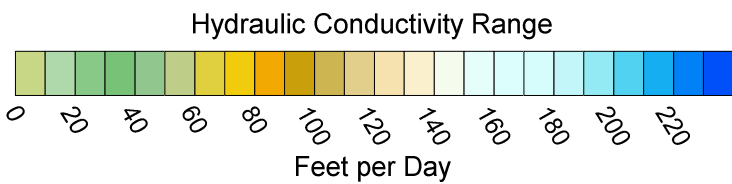
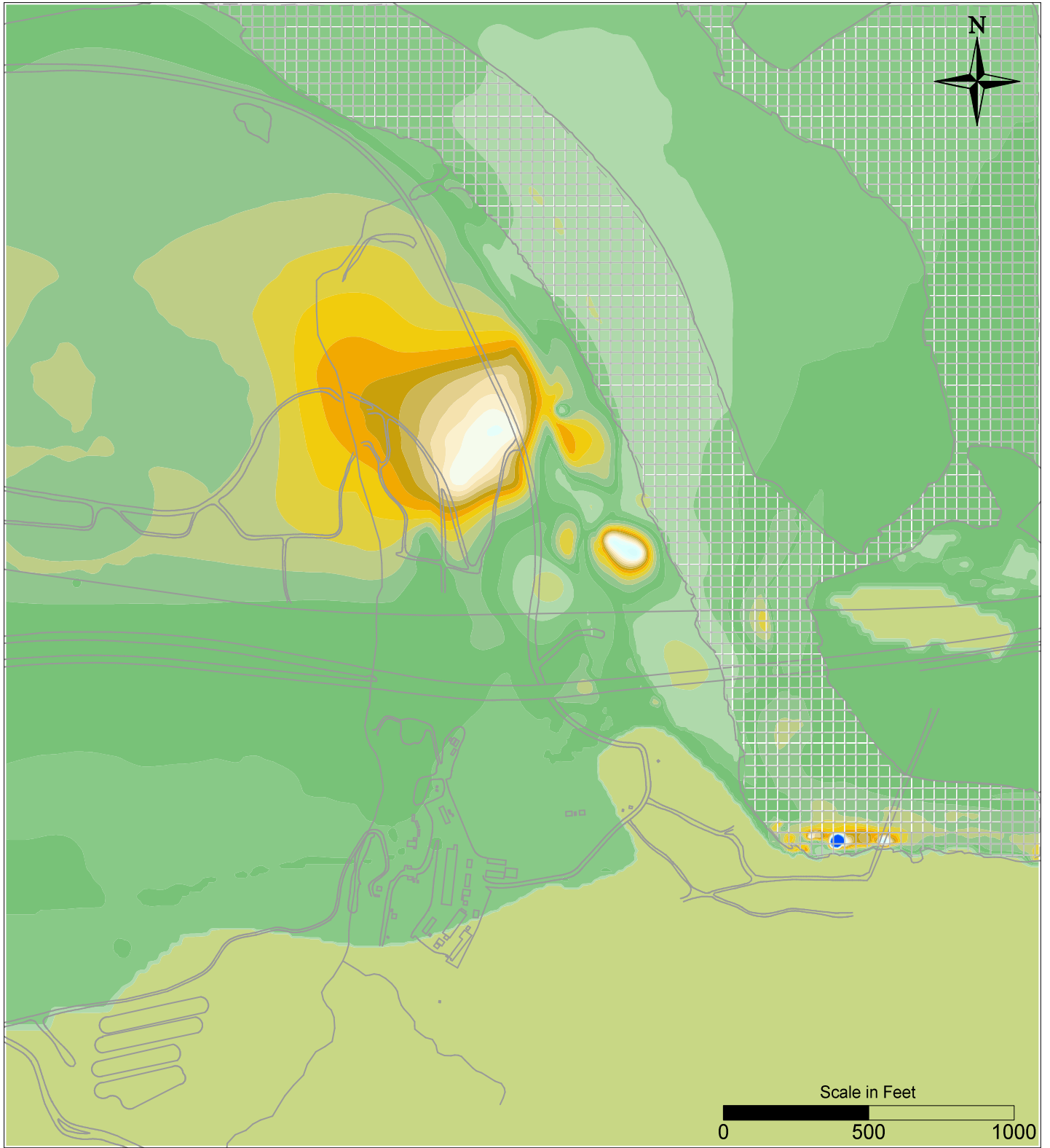


PG&E
 TOPOCK COMPRESSOR STATION
 NEEDLES, CALIFORNIA
 MODELING APPENDIX

THICKNESS MODEL LAYER 5



FIGURE
B-7

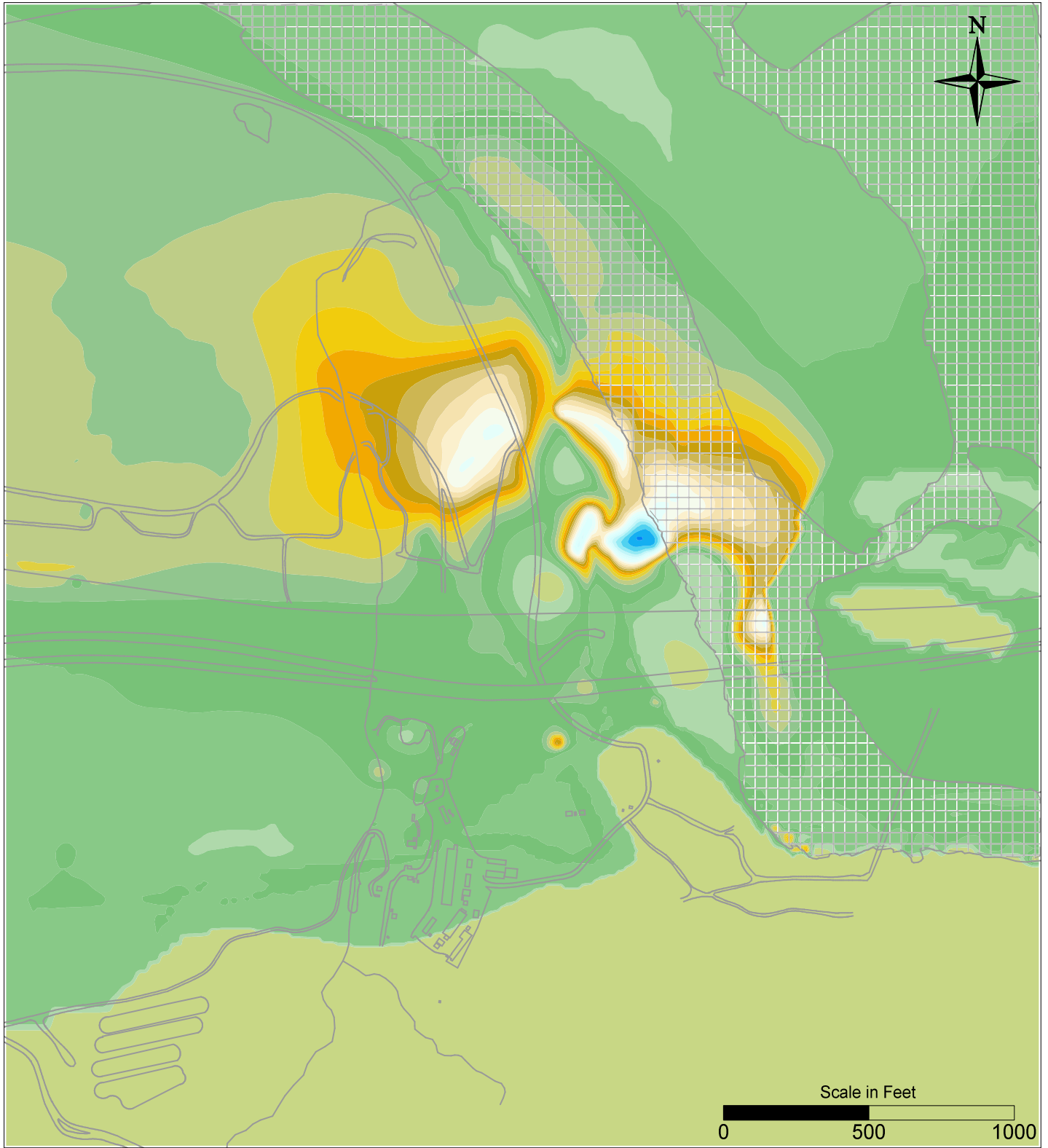


PG&E
 TOPOCK COMPRESSOR STATION
 NEEDLES, CALIFORNIA
 MODELING APPENDIX

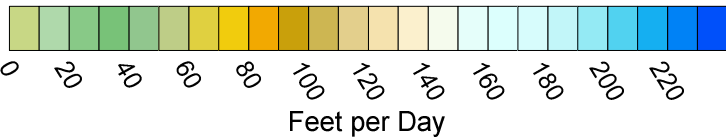
HYDRAULIC CONDUCTIVITY MODEL LAYER 1



FIGURE
 B-8



Hydraulic Conductivity Range

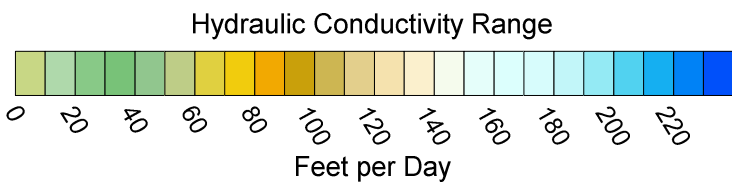
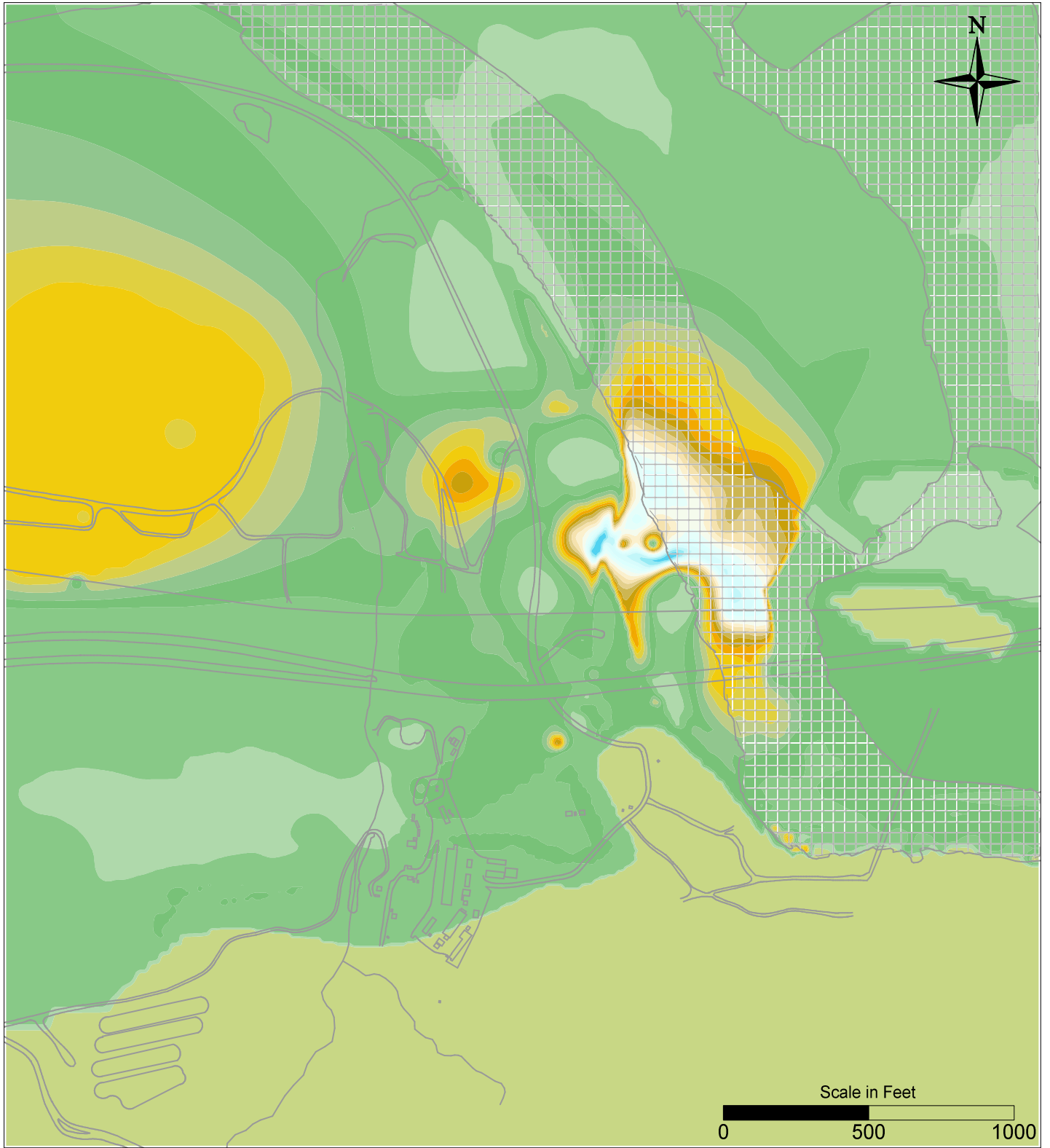


PG&E
 TOPOCK COMPRESSOR STATION
 NEEDLES, CALIFORNIA
 MODELING APPENDIX

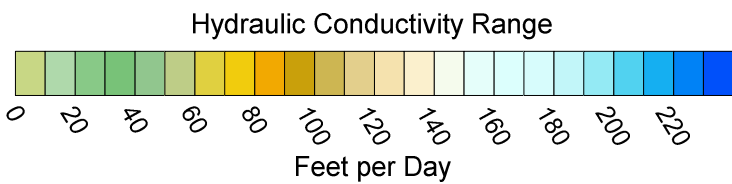
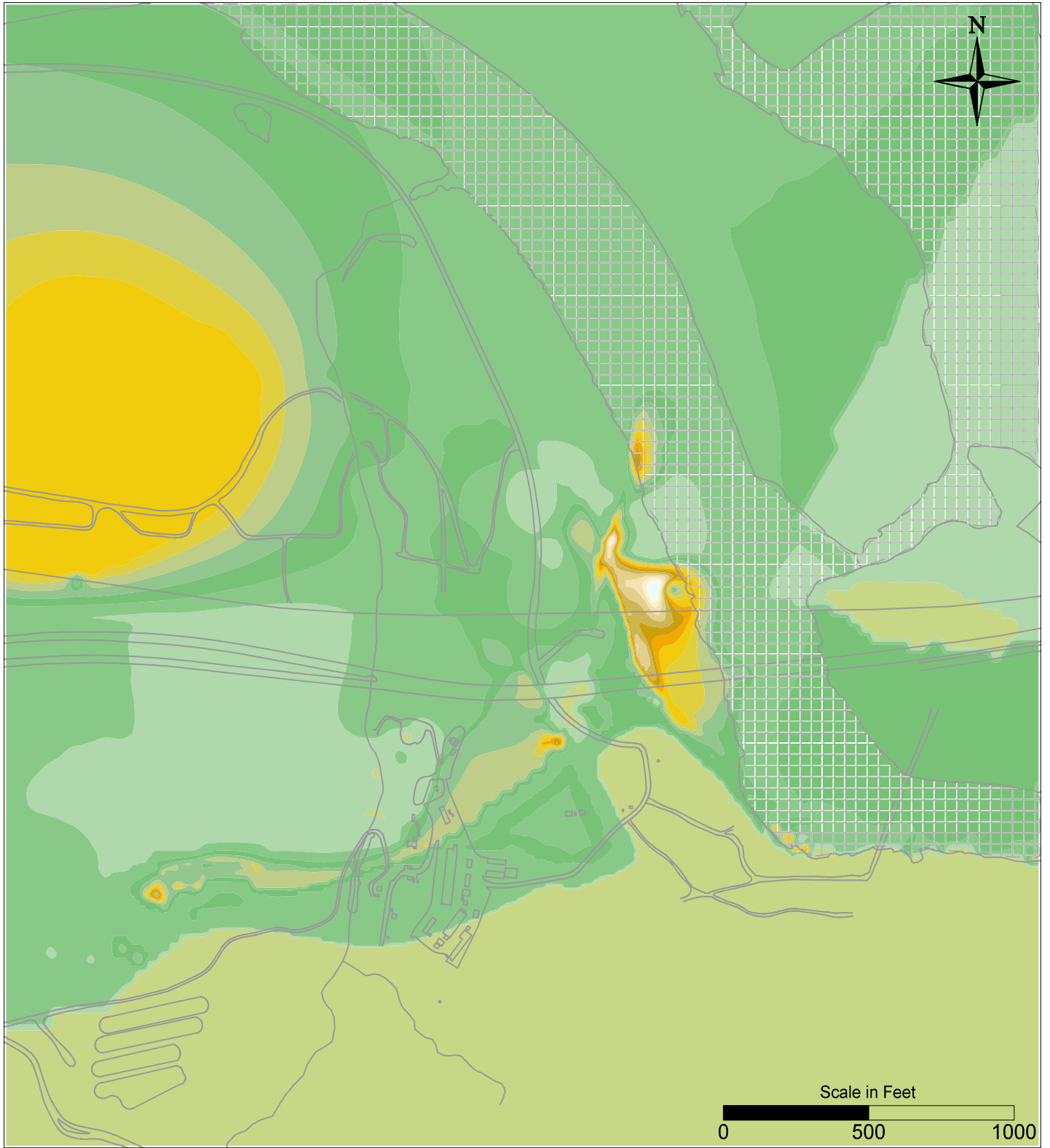
HYDRAULIC CONDUCTIVITY MODEL LAYER 2



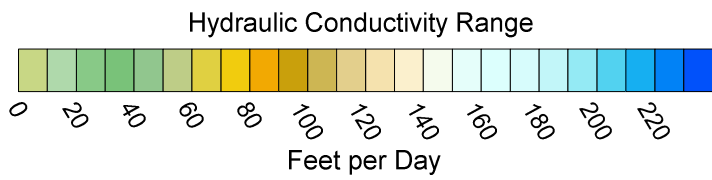
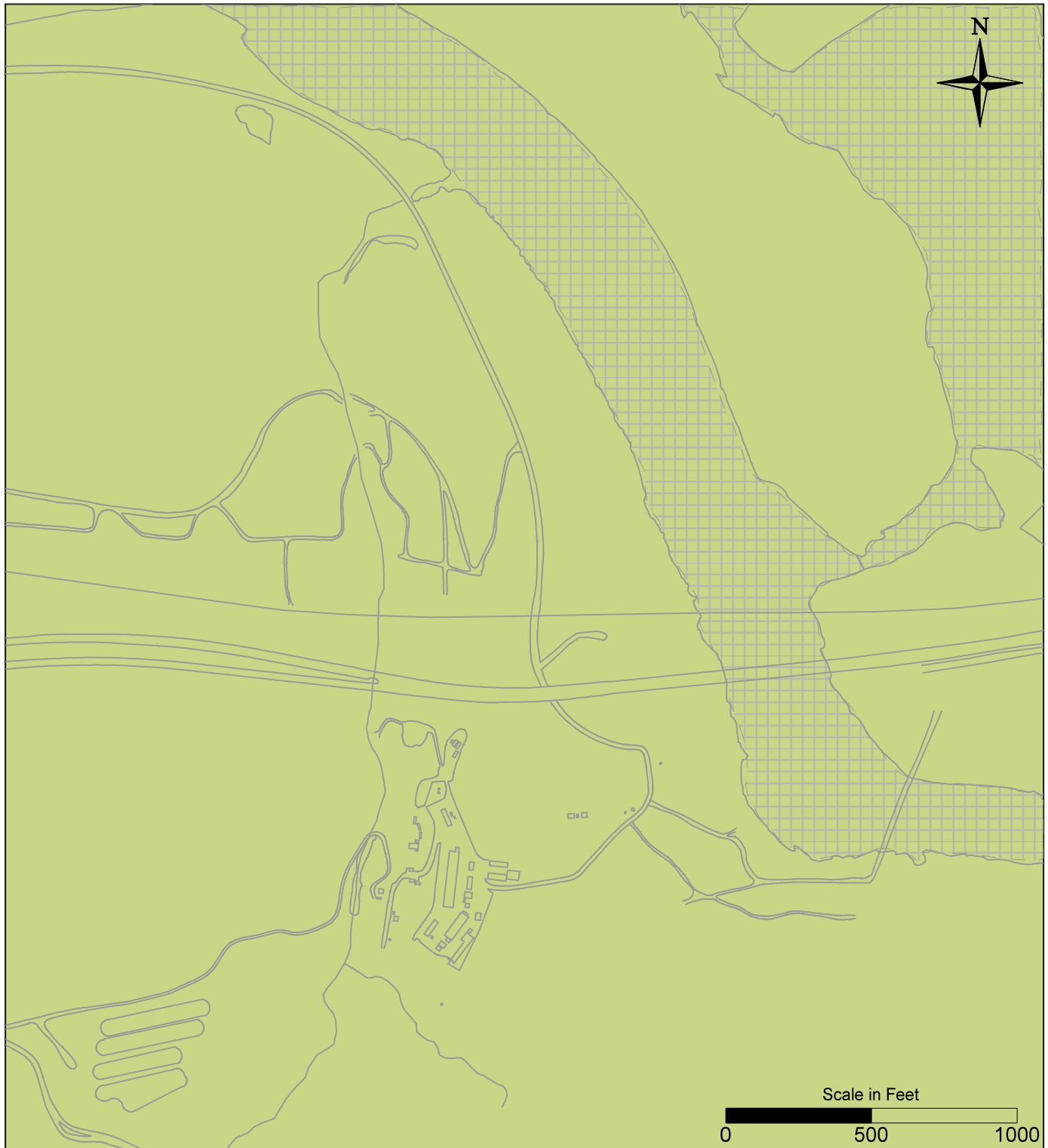
FIGURE
 B-9



PG&E TOPOCK COMPRESSOR STATION NEEDLES, CALIFORNIA MODELING APPENDIX	
HYDRAULIC CONDUCTIVITY MODEL LAYER 3	
	FIGURE B-10



PG&E TOPOCK COMPRESSOR STATION NEEDLES, CALIFORNIA MODELING APPENDIX	
HYDRAULIC CONDUCTIVITY MODEL LAYER 4	
	FIGURE B-11

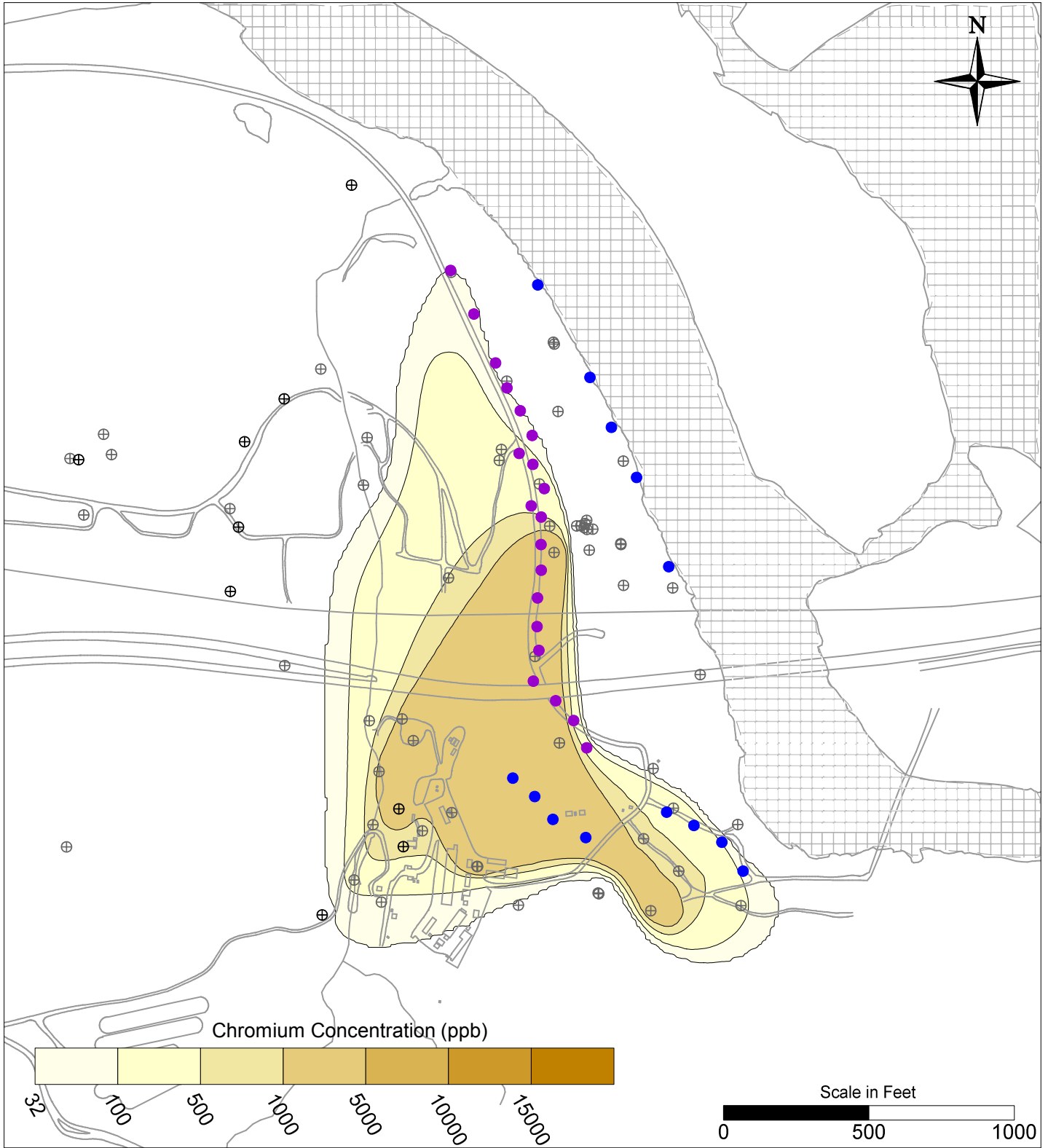


PG&E
 TOPOCK COMPRESSOR STATION
 NEEDLES, CALIFORNIA
 MODELING APPENDIX

HYDRAULIC CONDUCTIVITY MODEL LAYER 5



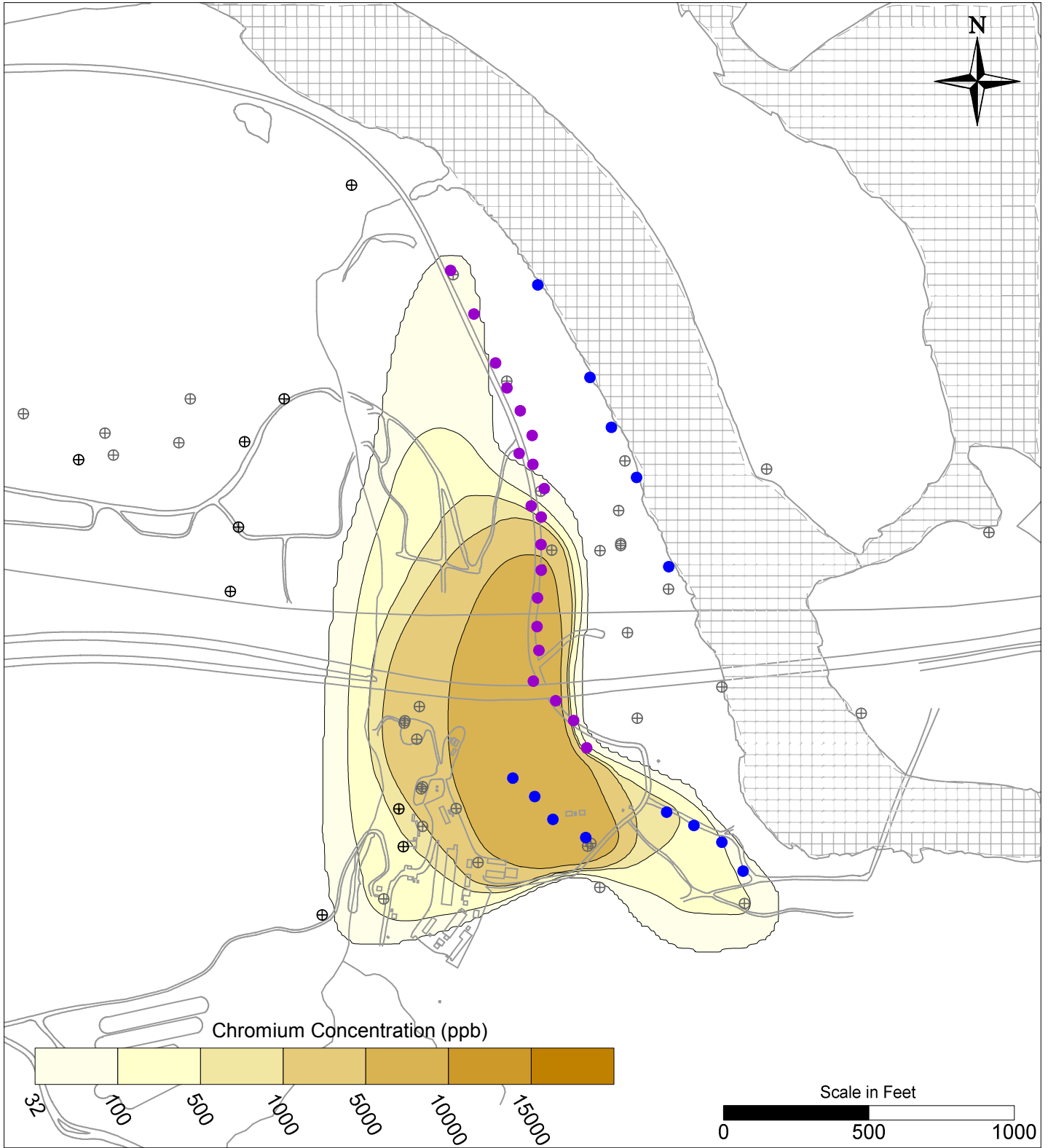
FIGURE
B-12



LEGEND

- IRZ WELLS
- ⊕ UPGRADIENT INJECTION WELLS
- EXTRACTION WELLS
- ⊕ MONITORING WELLS

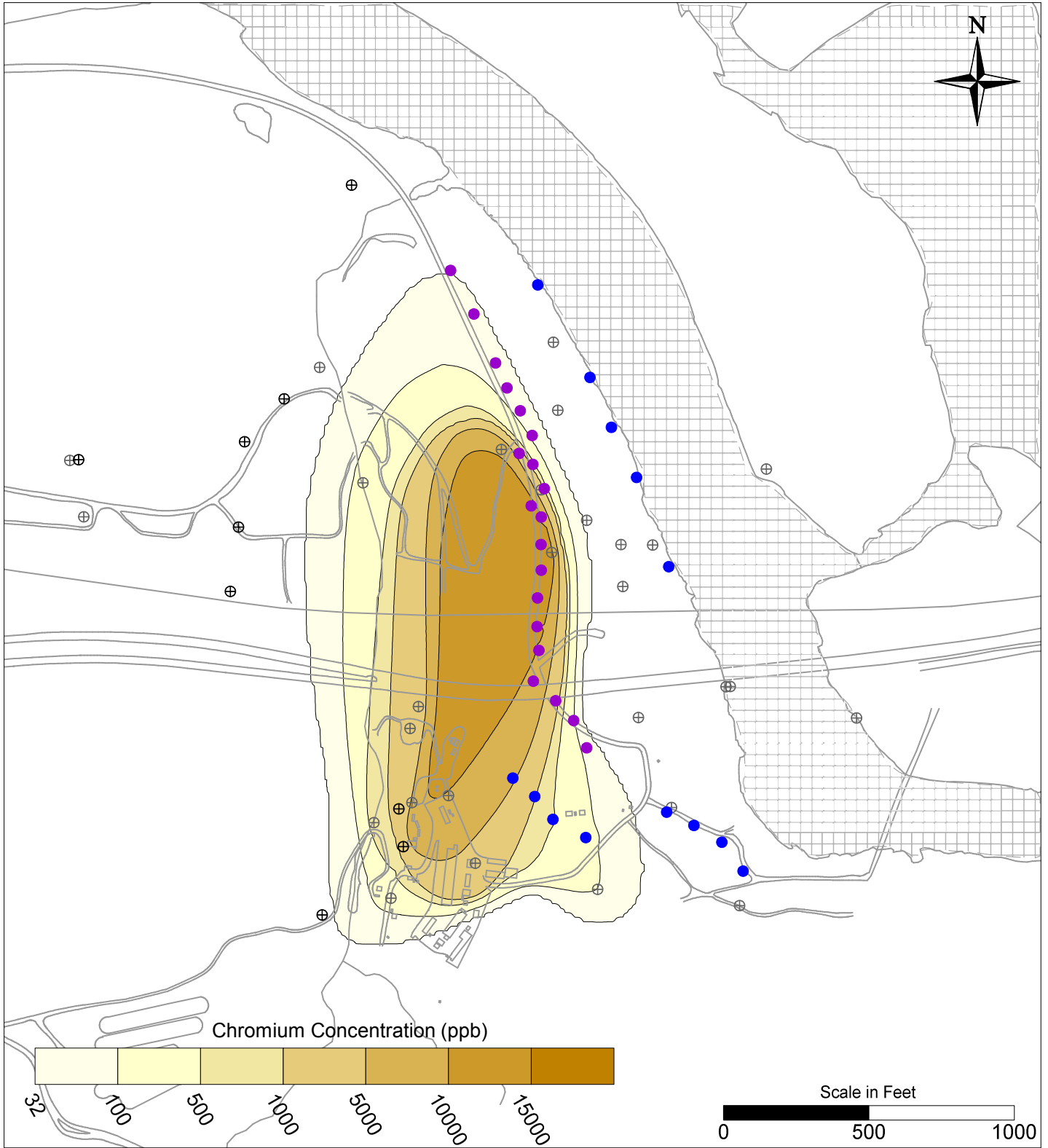
PG&E TOPOCK COMPRESSOR STATION NEEDLES, CALIFORNIA MODELING APPENDIX	
INITIAL HEXAVALENT CHROMIUM CONCENTRATION DISTRIBUTION MODEL LAYER 1	
	FIGURE B-13



LEGEND

- IRZ WELLS
- ⊕ UPGRADIENT INJECTION WELLS
- EXTRACTION WELLS
- ⊕ MONITORING WELLS

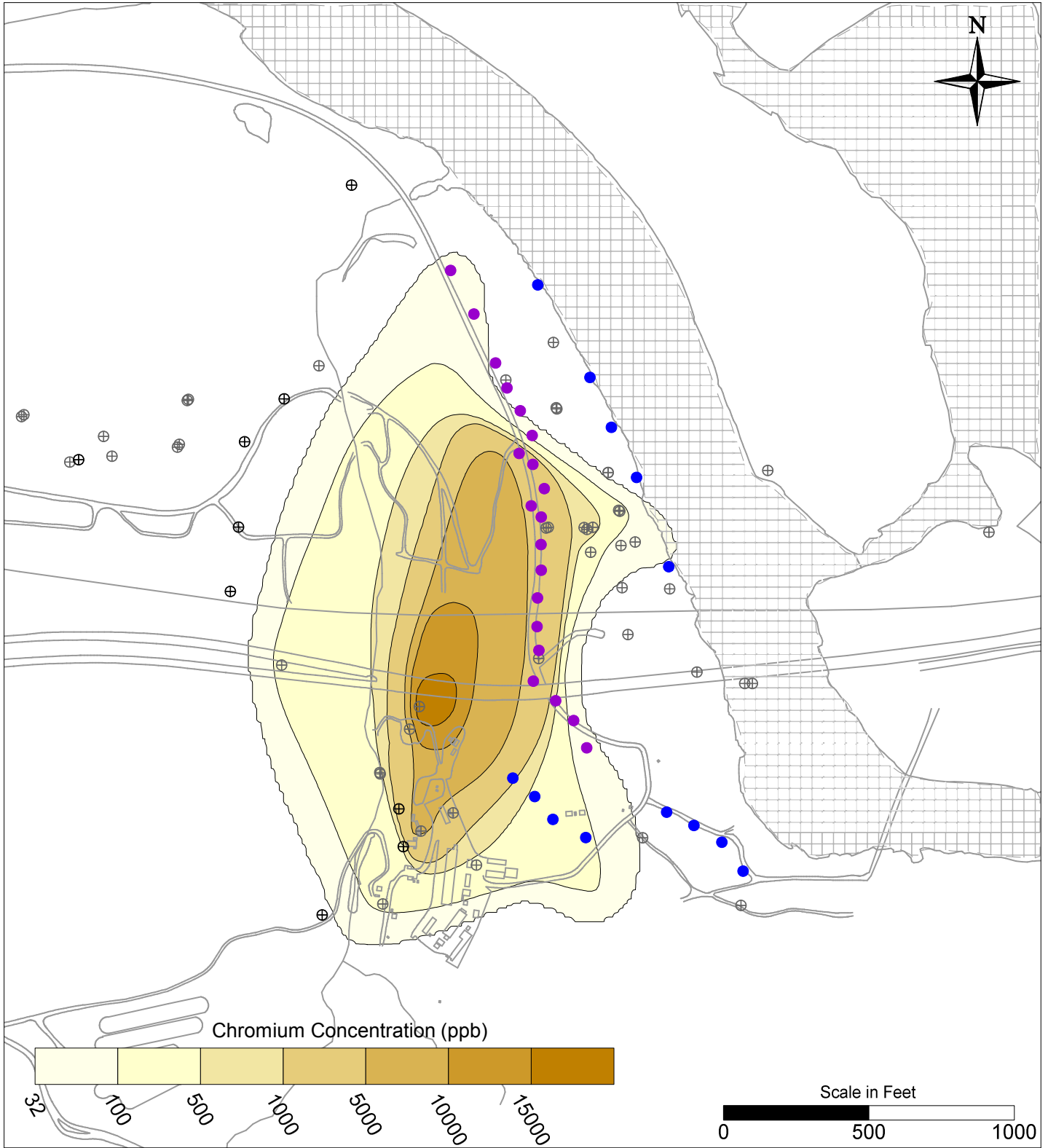
PG&E TOPOCK COMPRESSOR STATION NEEDLES, CALIFORNIA MODELING APPENDIX	
INITIAL HEXAVALENT CHROMIUM CONCENTRATION DISTRIBUTION MODEL LAYER 2	
	FIGURE B-14



LEGEND

- IRZ WELLS
- ⊕ UPGRADIENT INJECTION WELLS
- EXTRACTION WELLS
- ⊕ MONITORING WELLS

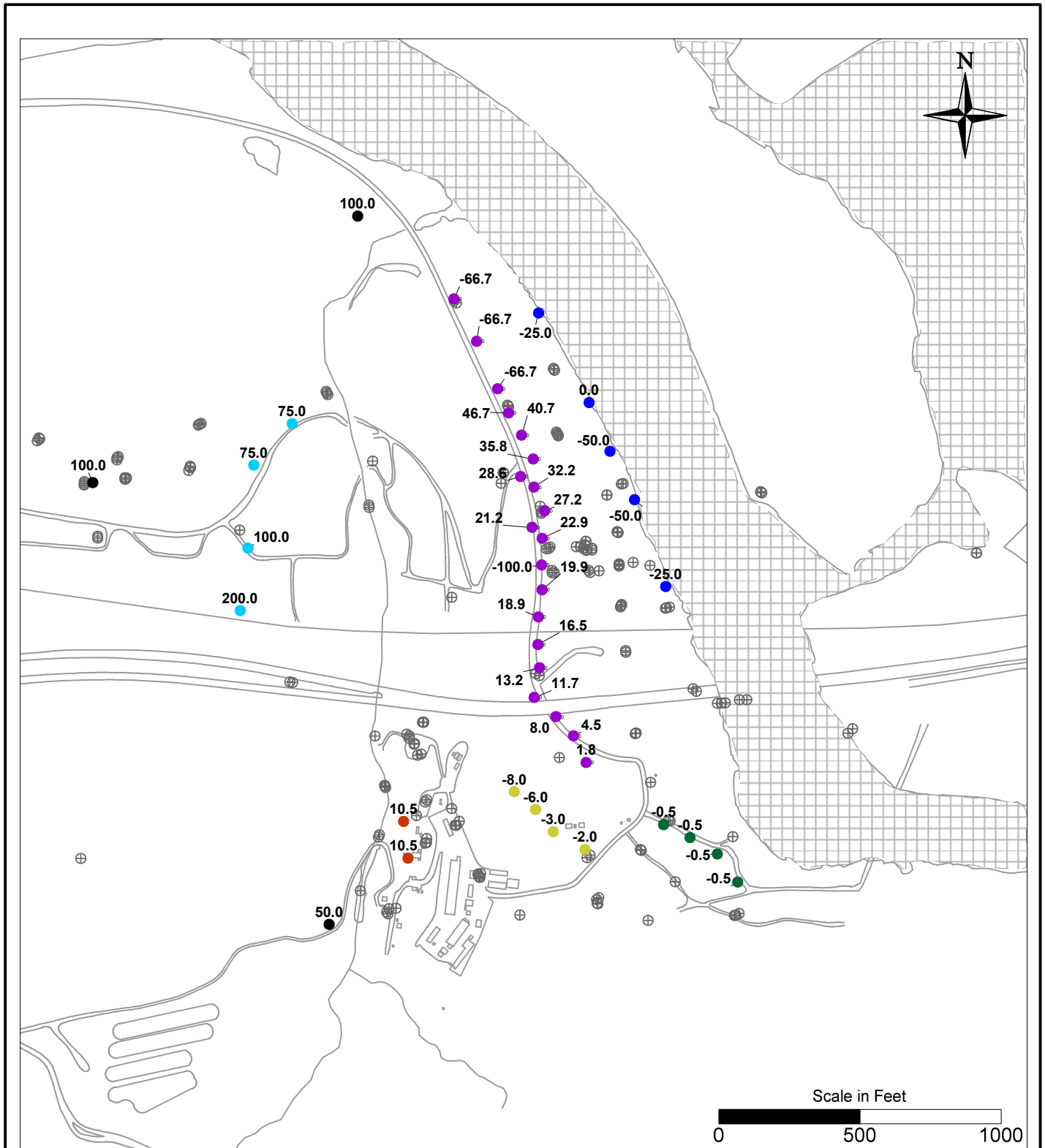
PG&E TOPOCK COMPRESSOR STATION NEEDLES, CALIFORNIA MODELING APPENDIX	
INITIAL HEXAVALENT CHROMIUM CONCENTRATION DISTRIBUTION MODEL LAYER 3	
	FIGURE B-15



LEGEND

- IRZ WELLS
- ⊕ UPGRADIENT INJECTION WELLS
- EXTRACTION WELLS
- ⊕ MONITORING WELLS

PG&E TOPOCK COMPRESSOR STATION NEEDLES, CALIFORNIA MODELING APPENDIX	
INITIAL HEXAVALENT CHROMIUM CONCENTRATION DISTRIBUTION MODEL LAYER 4	
	FIGURE B-16



LEGEND

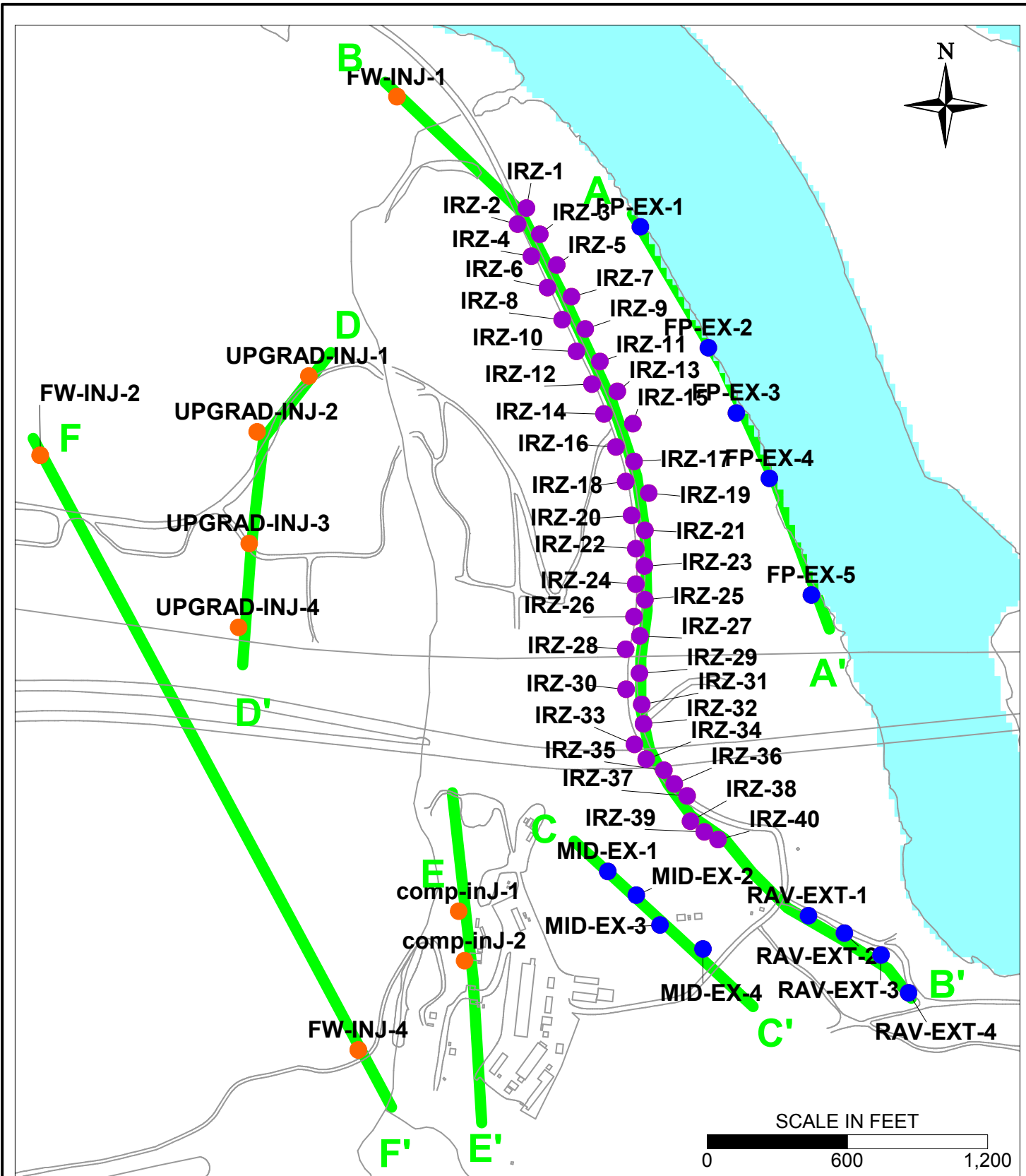
- IRZ WELLS
 - COMPRESSOR STATION INJECTION
 - UPGRADIENT INJECTION WELLS
 - FRESHWATER INJECTION
 - RAVINE EXTRACTION WELLS
 - RIVERBANK EXTRACTION WELLS
 - MIDWAY EXTRACTION WELLS
 - ⊕ MONITORING WELLS
- Active Rates in GPM

PG&E
TOPECO COMPRESSOR STATION
NEEDLES, CALIFORNIA
MODELING APPENDIX

REMEDIATION DESIGN WELL LOCATIONS



FIGURE
B-17



LEGEND

- IRZ WELLS
- UPGRADIENT INJECTION WELLS
- EXTRACTION WELLS
- CROSS SECTION LOCATIONS

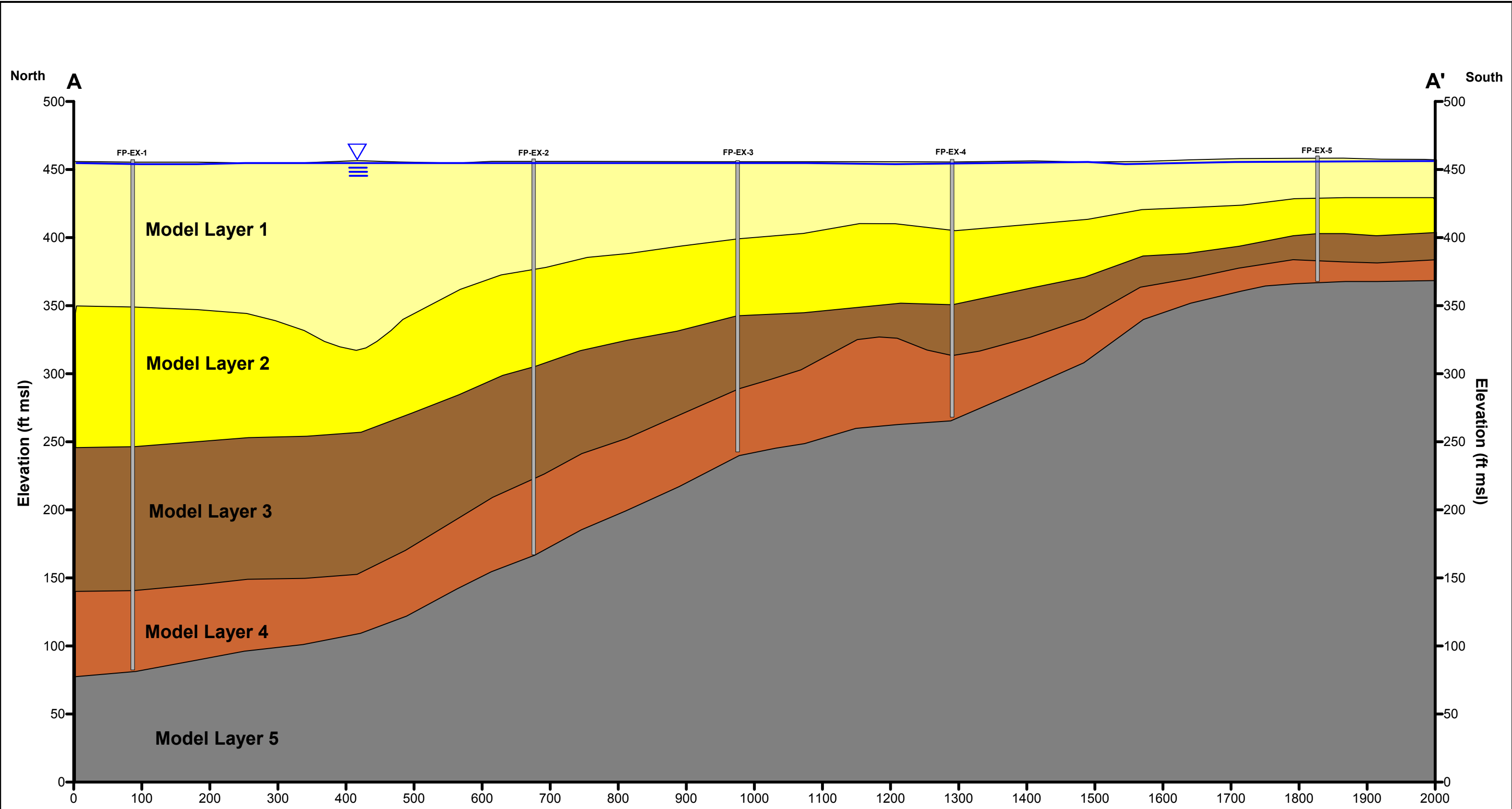
PG&E
TOPOCK, CALIFORNIA

CONCEPTUAL REMEDY
CROSS-SECTION LOCATIONS

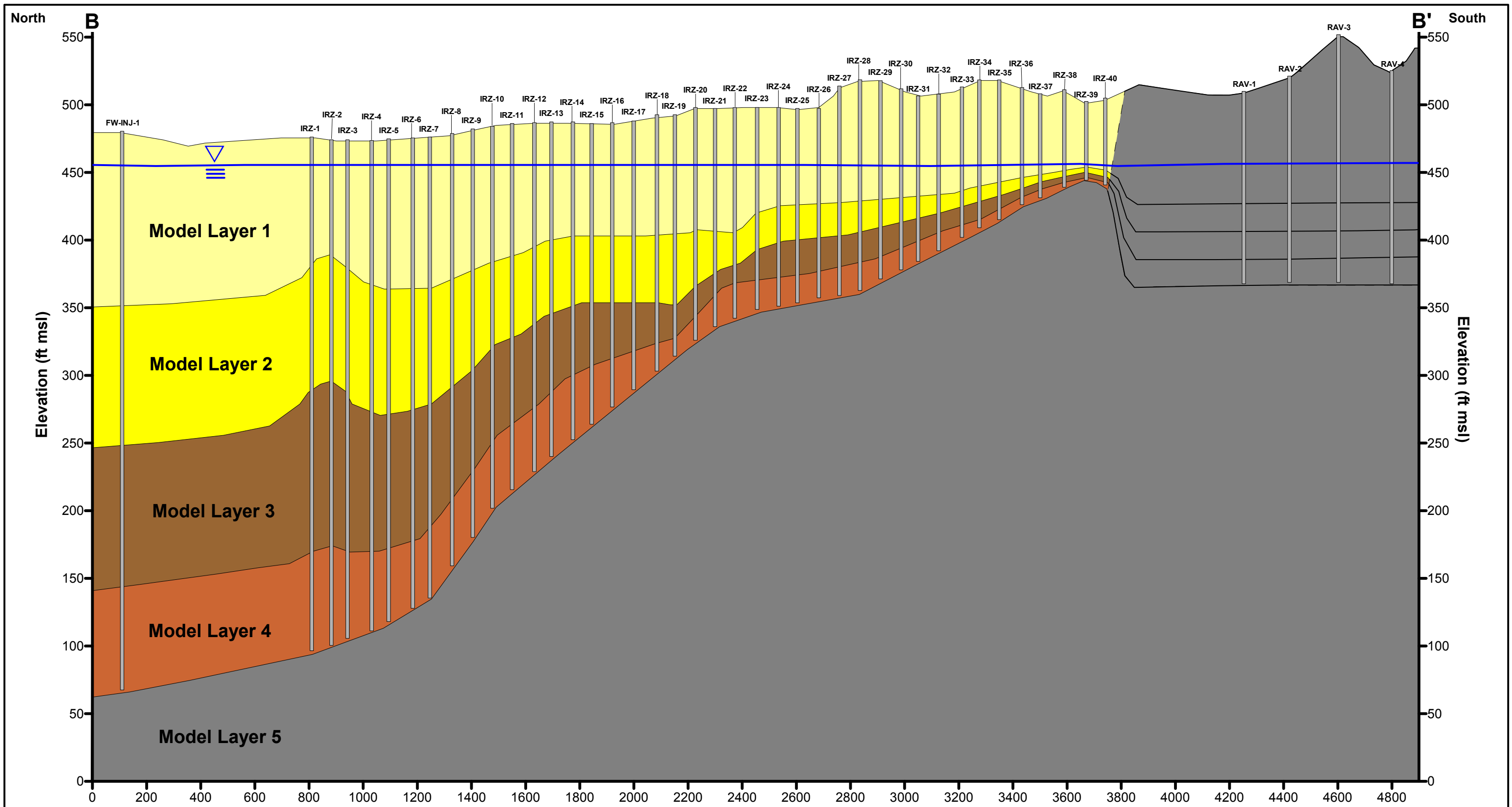


FIGURE

B-18



PG&E TOPOCK COMPRESSOR STATION NEEDLES, CALIFORNIA	
CONCEPTUAL REMEDY CROSS-SECTION A-A'	
	FIGURE B-19

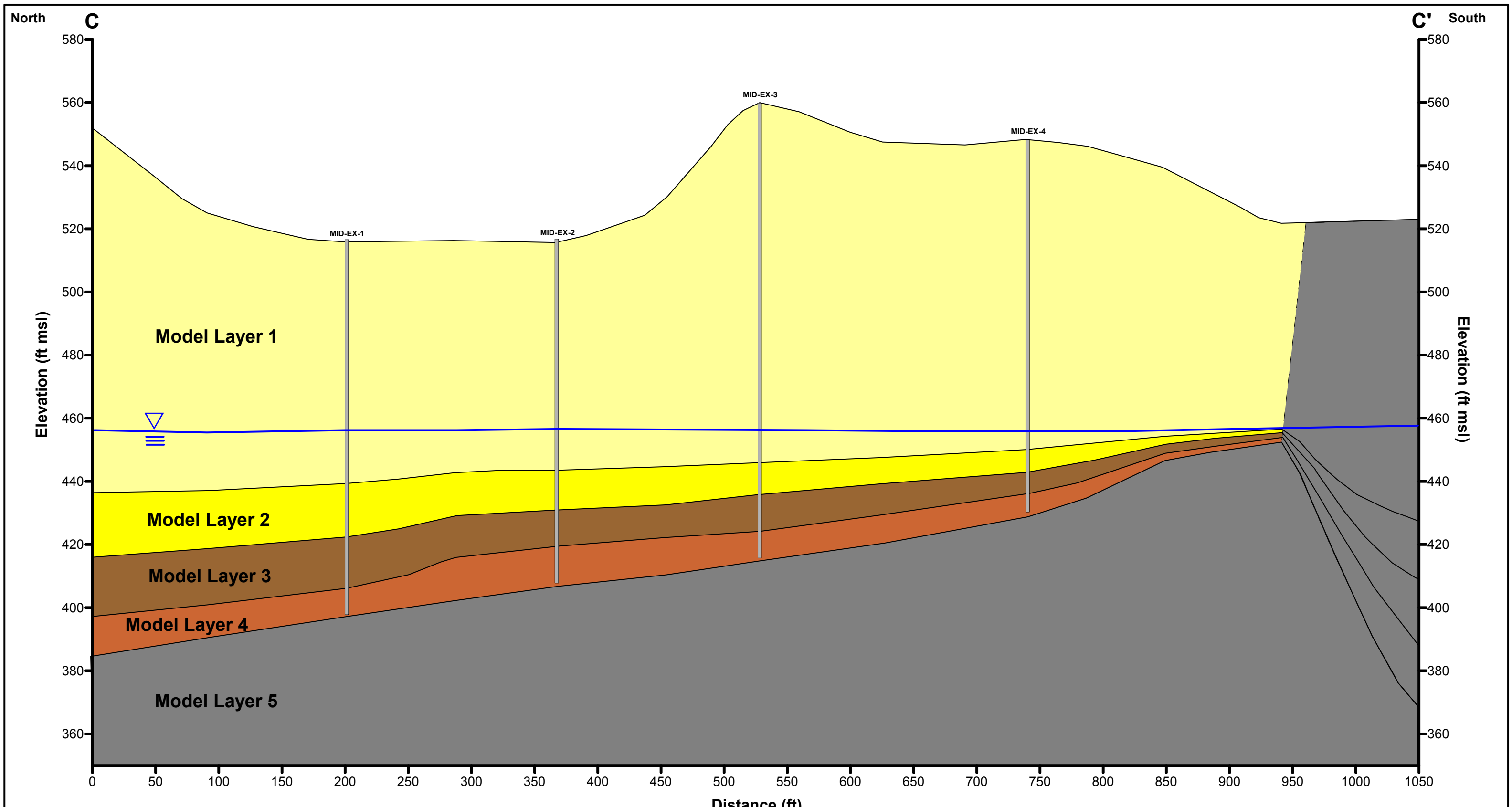


PG&E TOPOCK COMPRESSOR STATION
NEEDLES, CALIFORNIA

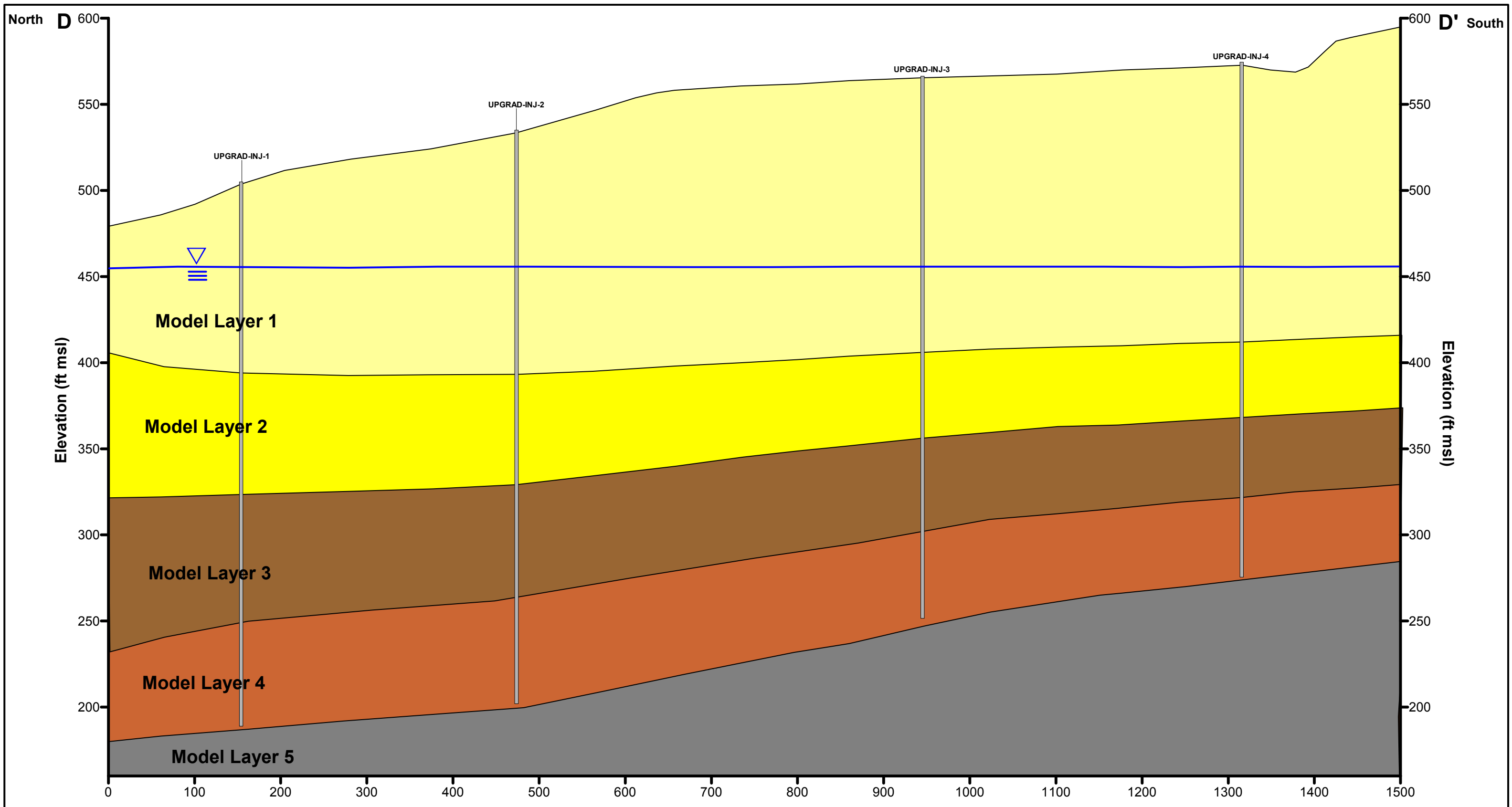
CONCEPTUAL REMEDY
CROSS-SECTION B-B'

 **ARCADIS**

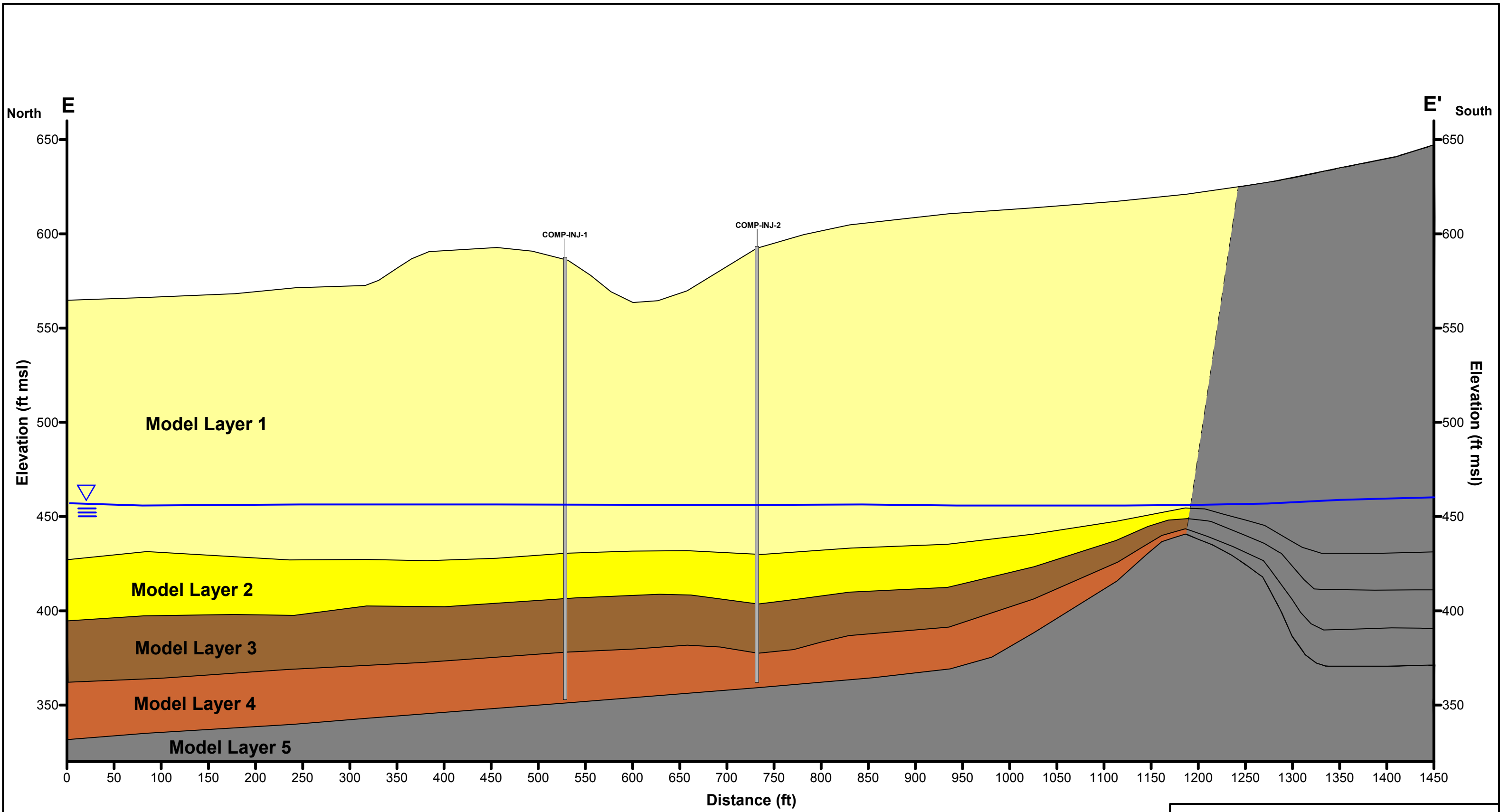
FIGURE
B-20



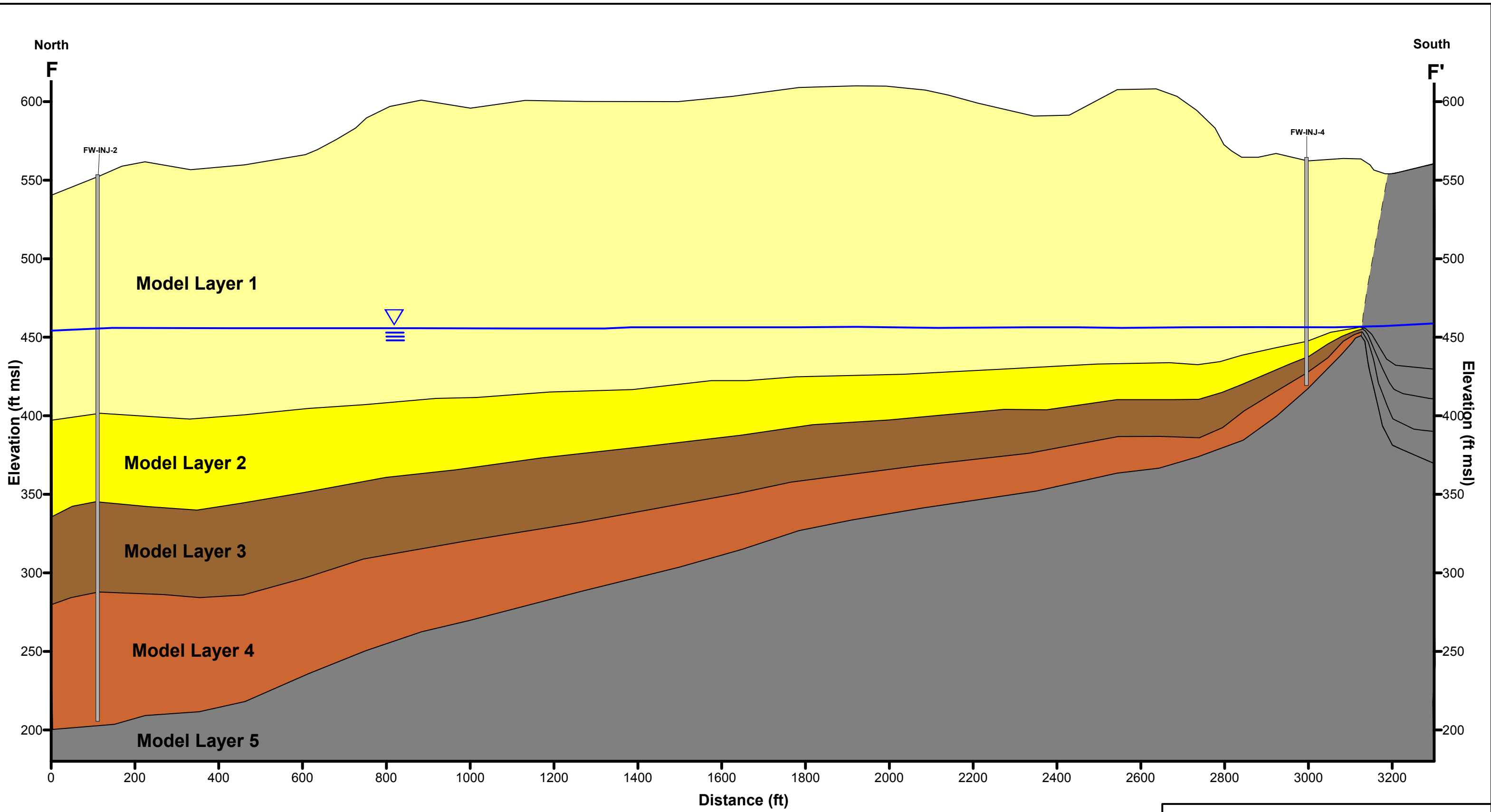
PG&E TOPOCK COMPRESSOR STATION NEEDLES, CALIFORNIA	
CONCEPTUAL REMEDY CROSS-SECTION C-C'	
	FIGURE B-21



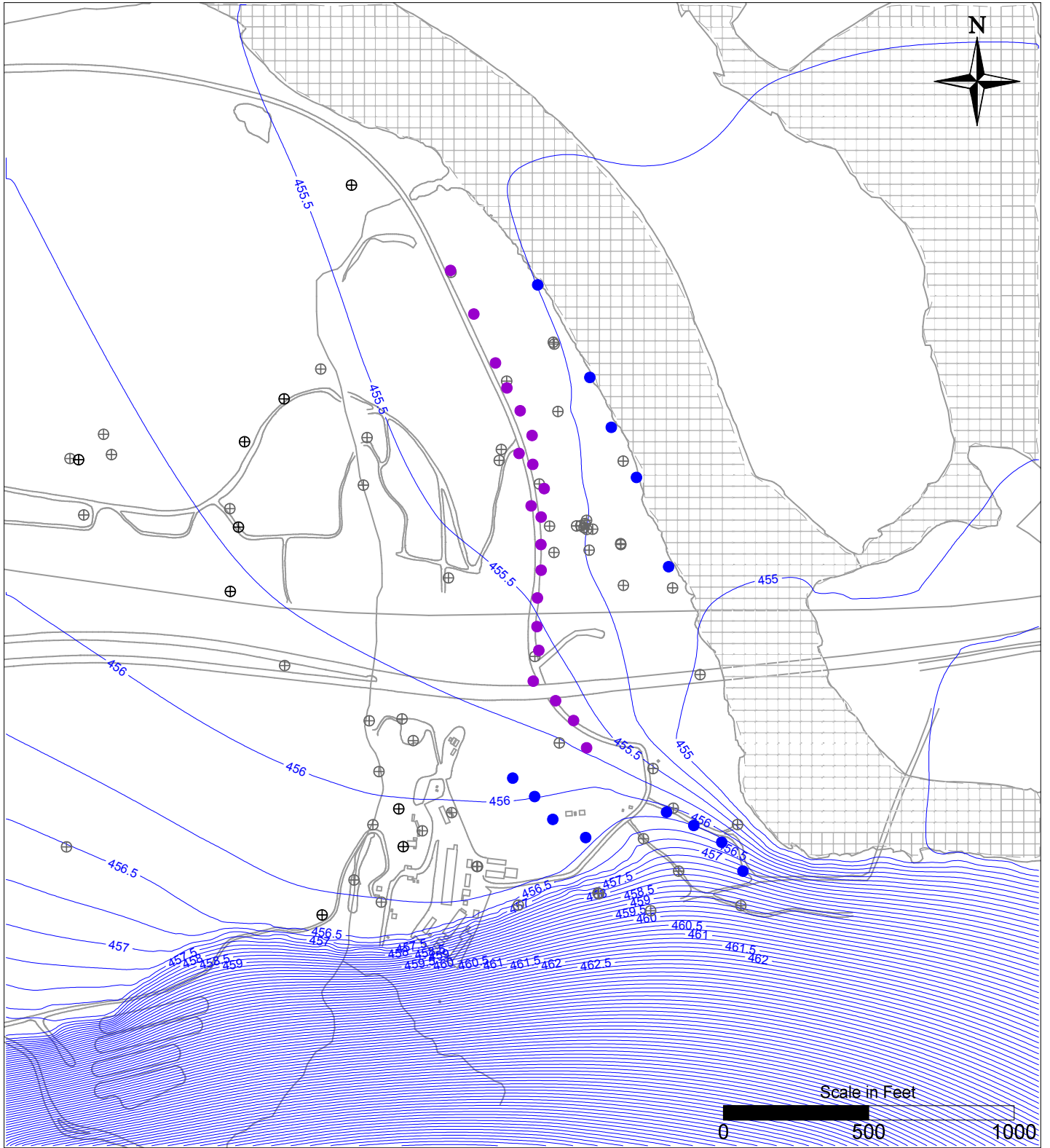
PG&E TOPOCK COMPRESSOR STATION NEEDLES, CALIFORNIA	
CONCEPTUAL REMEDY CROSS-SECTION D-D'	
	FIGURE B-22



PG&E TOPOCK COMPRESSOR STATION NEEDLES, CALIFORNIA	
CONCEPTUAL REMEDY CROSS-SECTION E-E'	
	FIGURE B-23



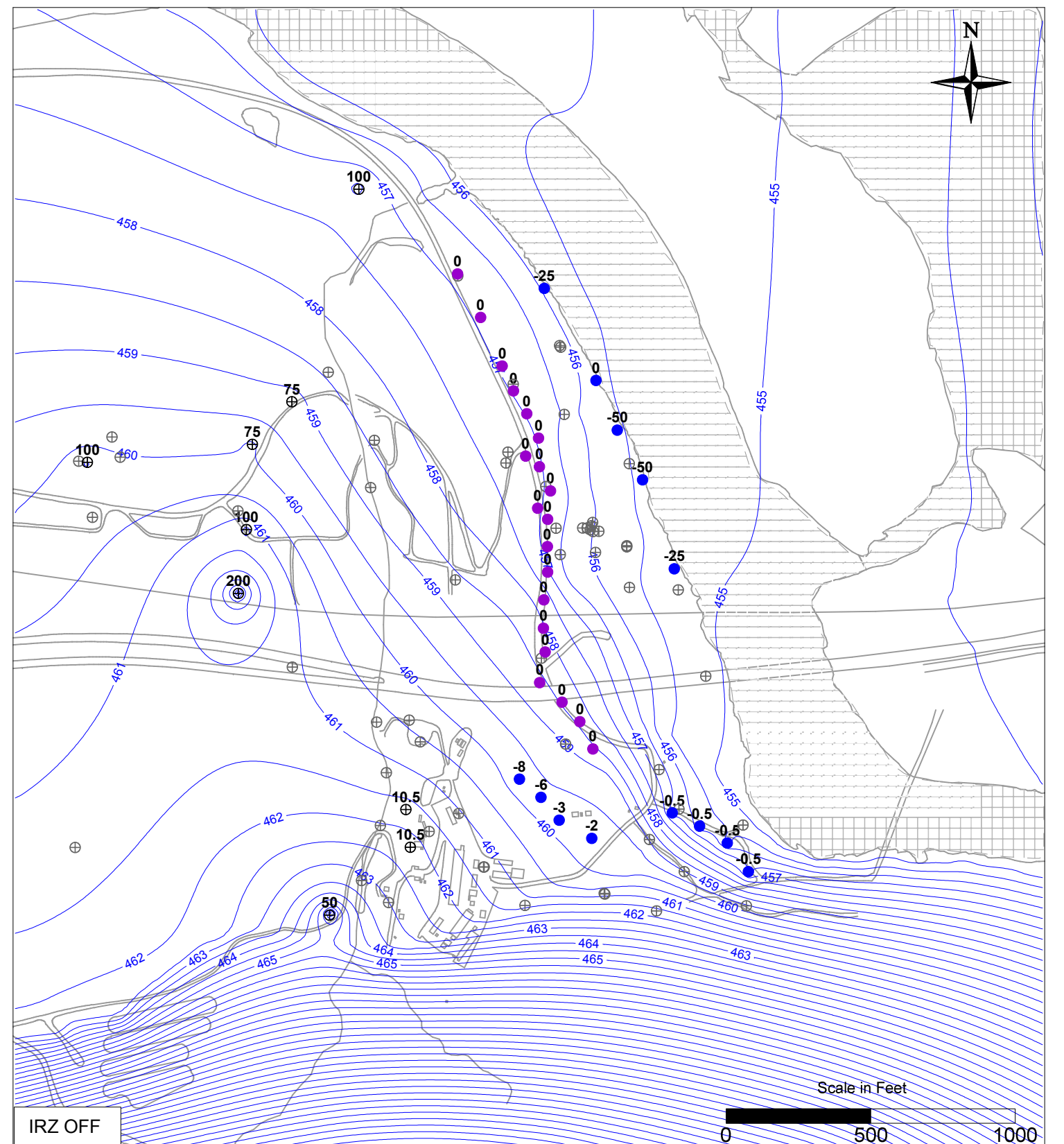
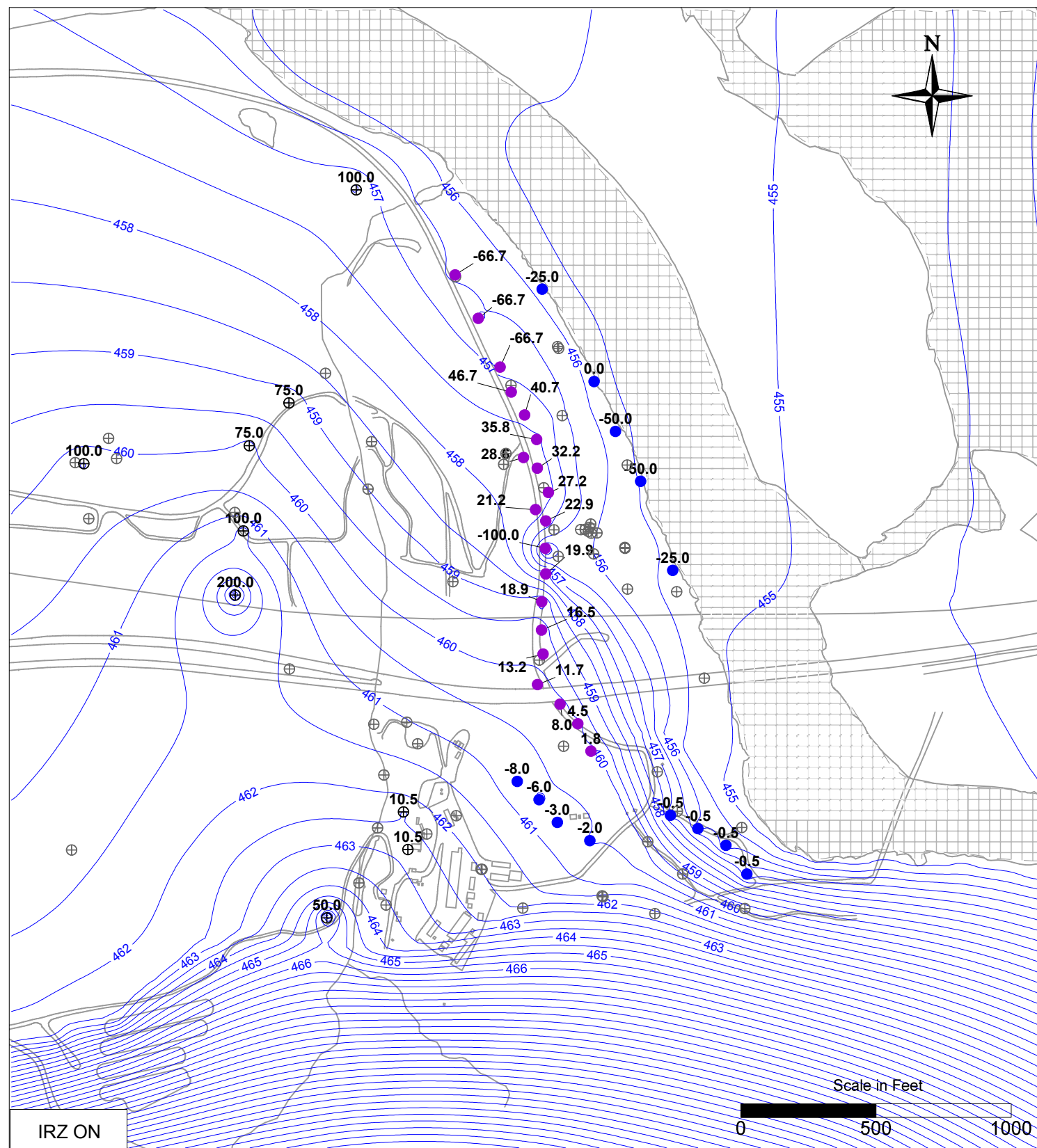
PG&E TOPOCK COMPRESSOR STATION NEEDLES, CALIFORNIA	
CONCEPTUAL REMEDY CROSS-SECTION F-F'	
	FIGURE B-24



LEGEND

- IRZ WELLS
- ⊕ UPGRADIENT INJECTION WELLS
- EXTRACTION WELLS
- ⊕ MONITORING WELLS
- 460— SIMULATED GROUNDWATER LEVELS (FT MSL)

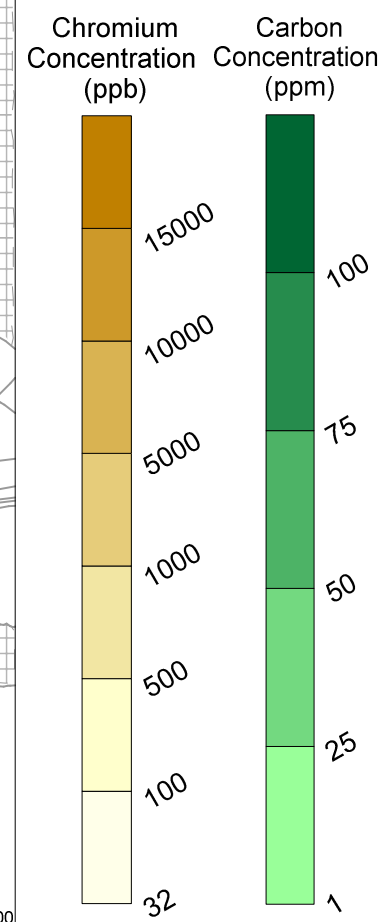
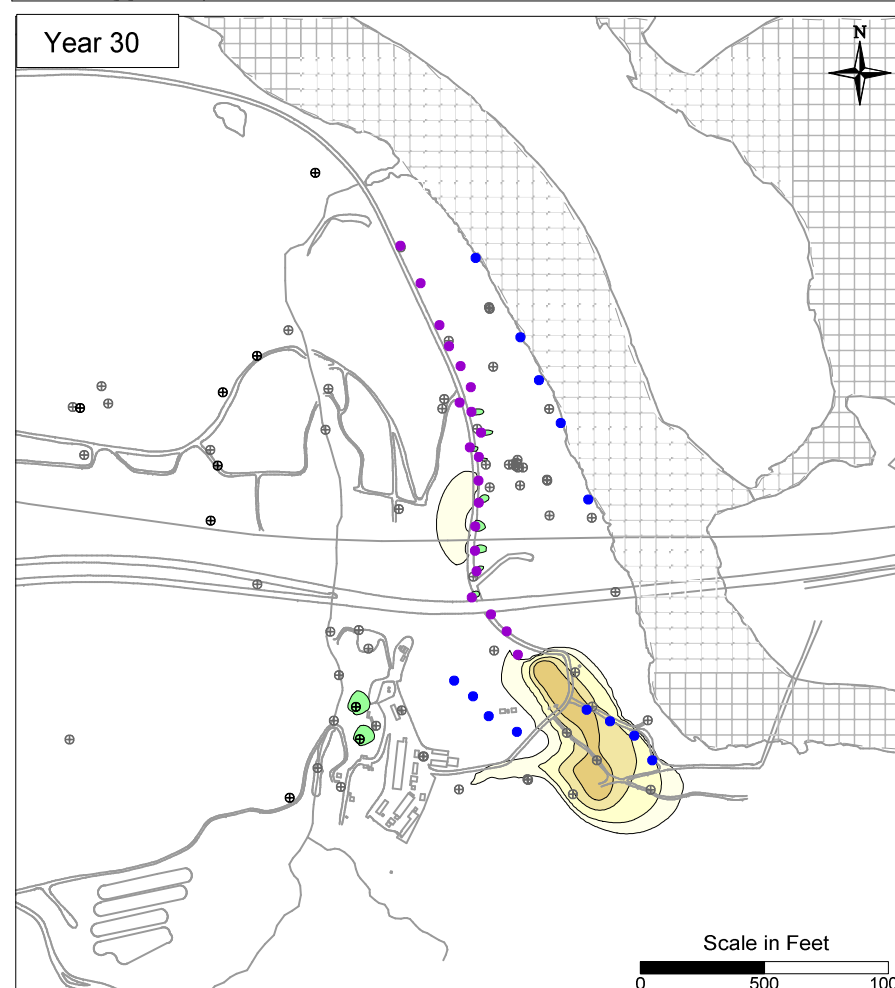
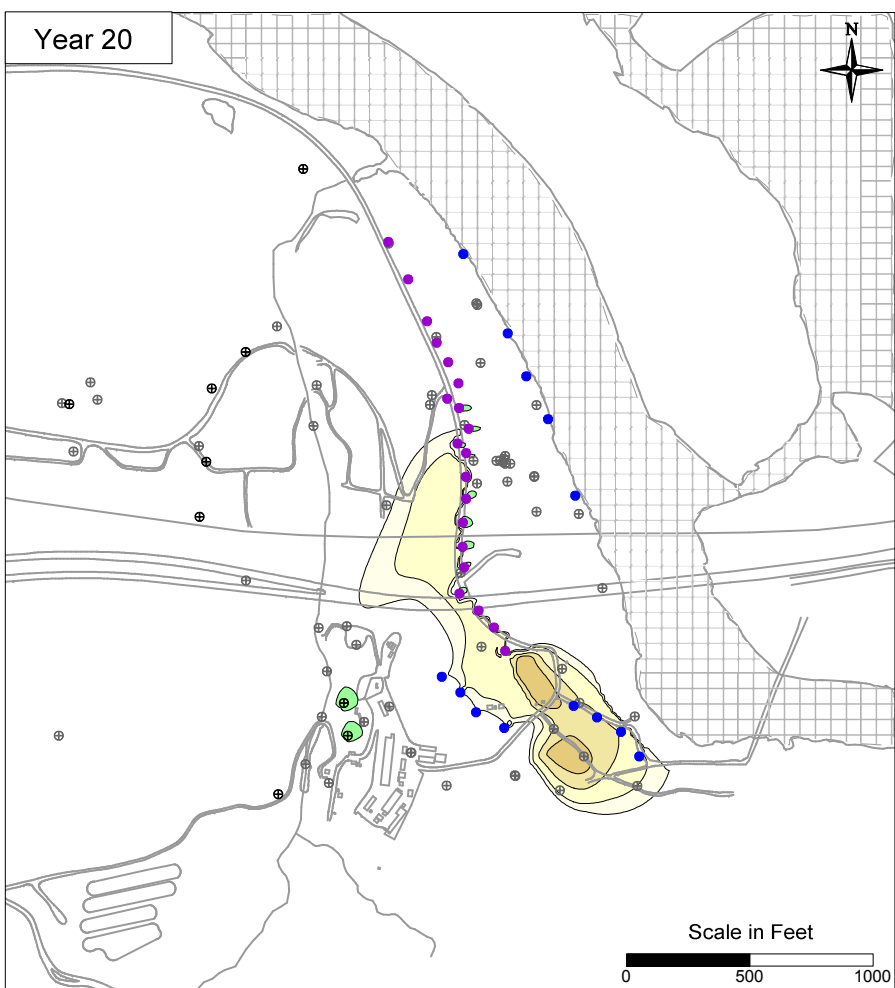
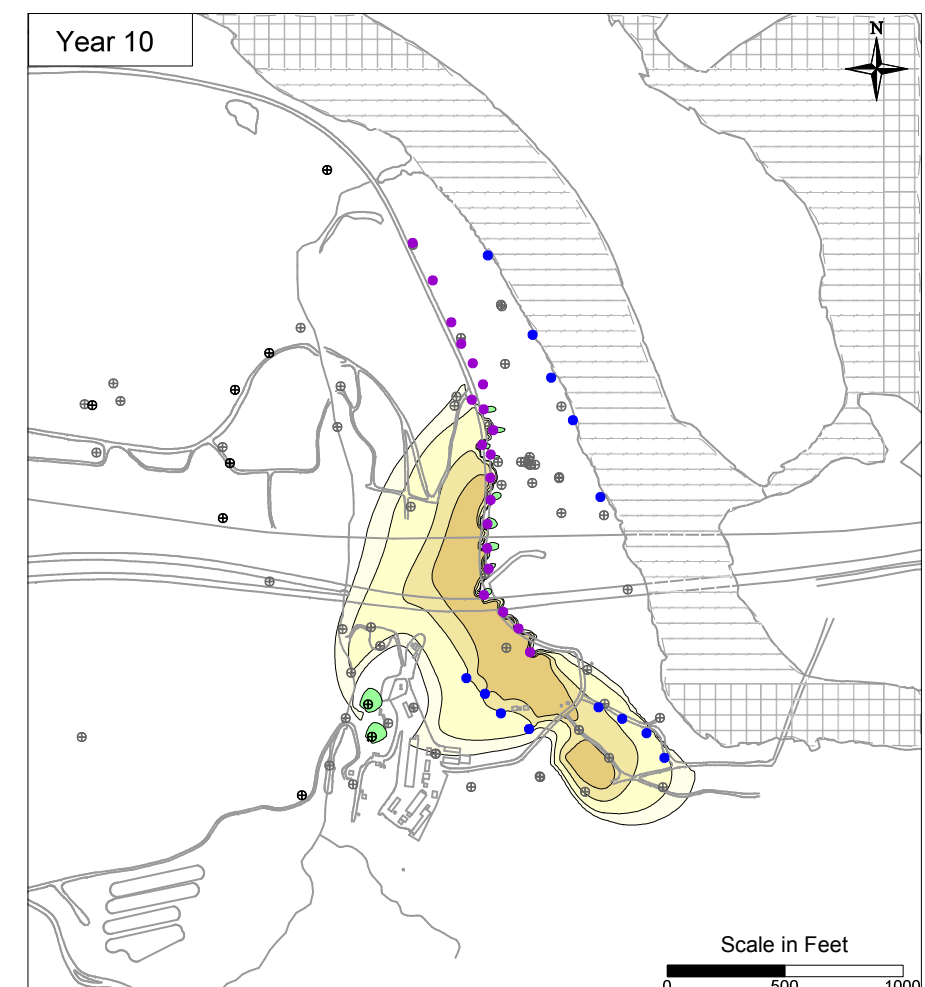
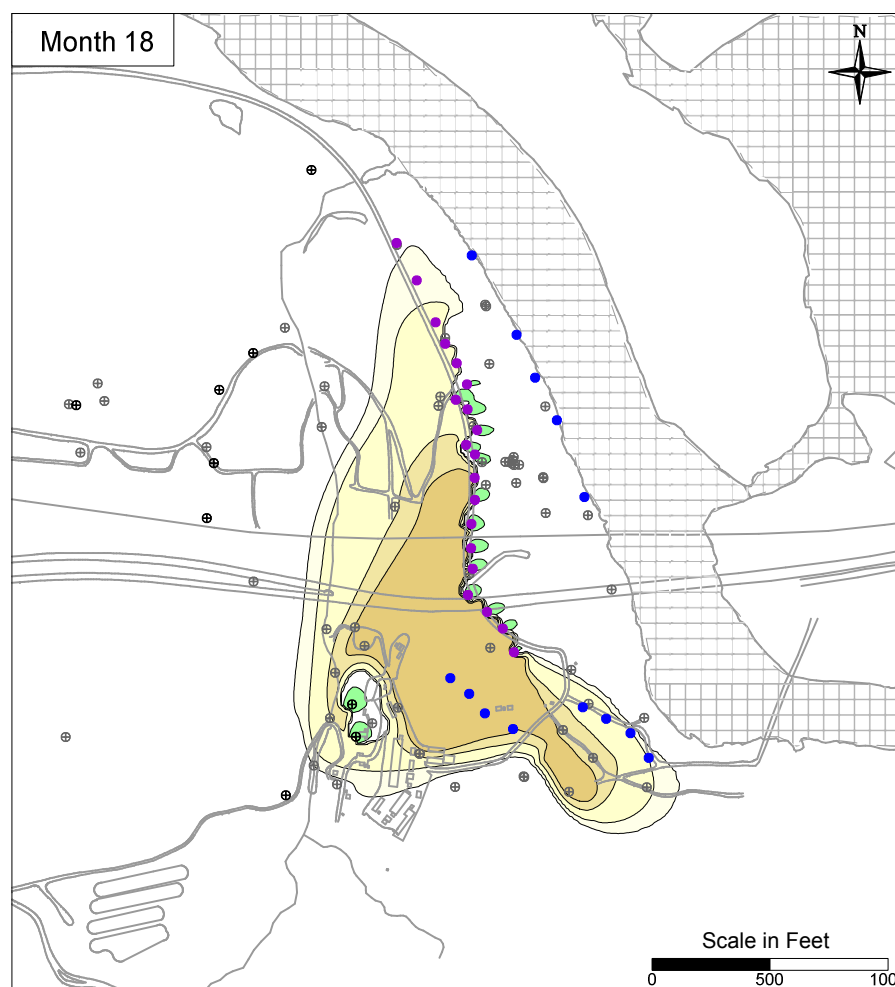
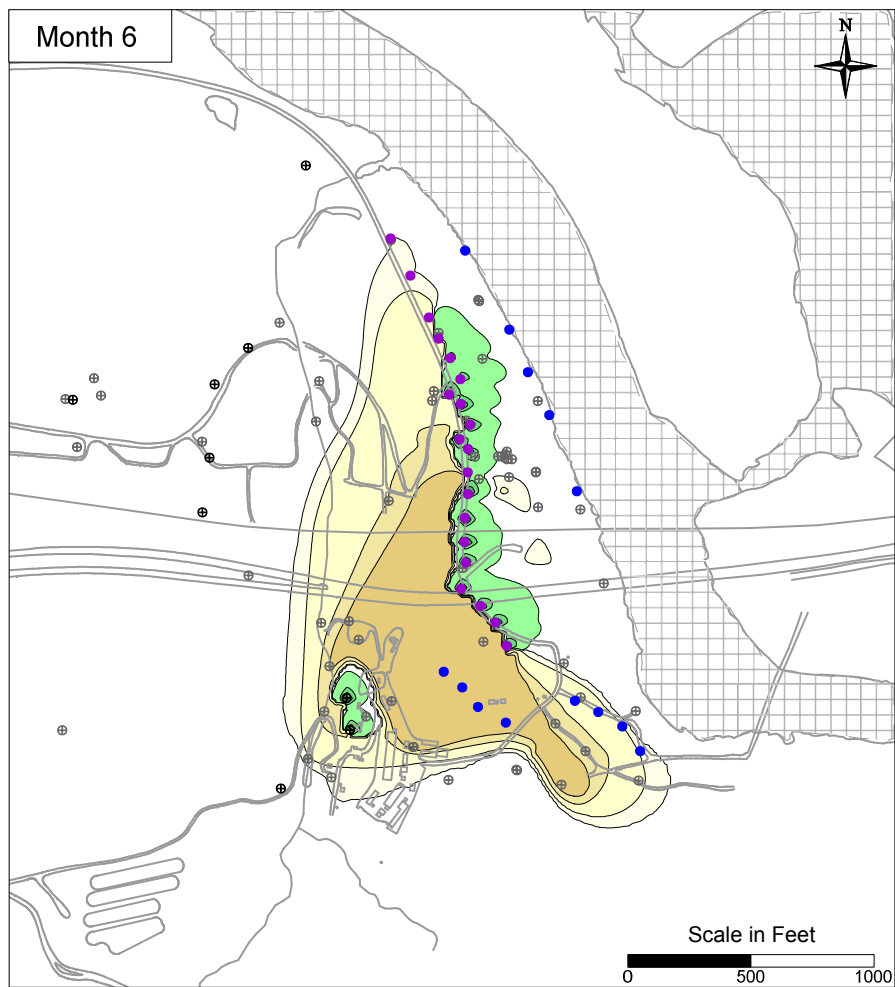
PG&E TOPOCK COMPRESSOR STATION NEEDLES, CALIFORNIA MODELING APPENDIX	
SIMULATED GROUNDWATER CONTOURS UNDER AMBIENT FLOW CONDITIONS	
	FIGURE B-25



LEGEND

- IRZ WELLS
- ⊕ UPGRADIENT INJECTION WELLS
- EXTRACTION WELLS
- ⊕ MONITORING WELLS
- -460- SIMULATED GROUNDWATER LEVELS (FT MSL)

PG&E TOPOCK COMPRESSOR STATION NEEDLES, CALIFORNIA MODELING APPENDIX	
SIMULATED GROUNDWATER CONTOURS UNDER ACTIVE REMEDY FLOW CONDITIONS	
	FIGURE B-26



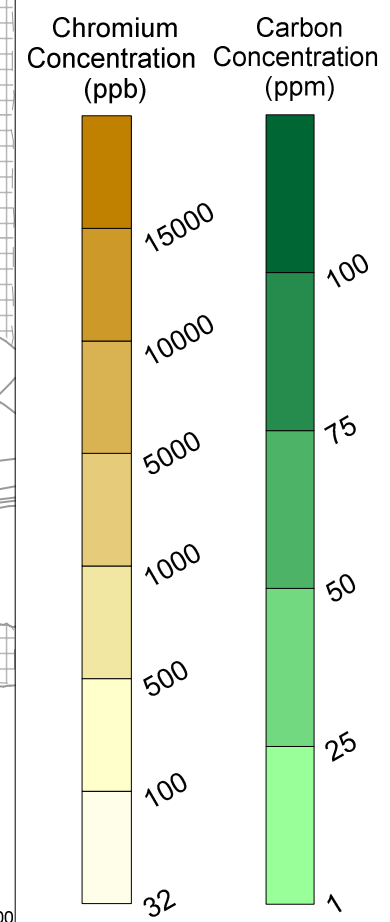
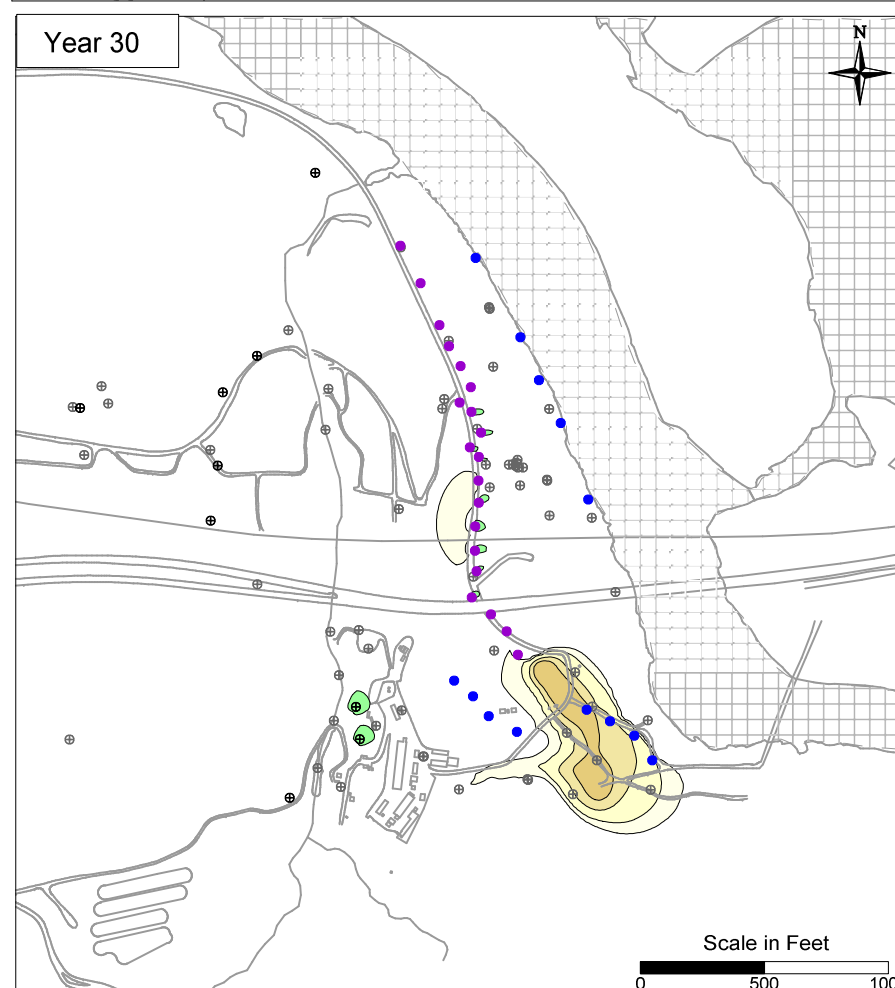
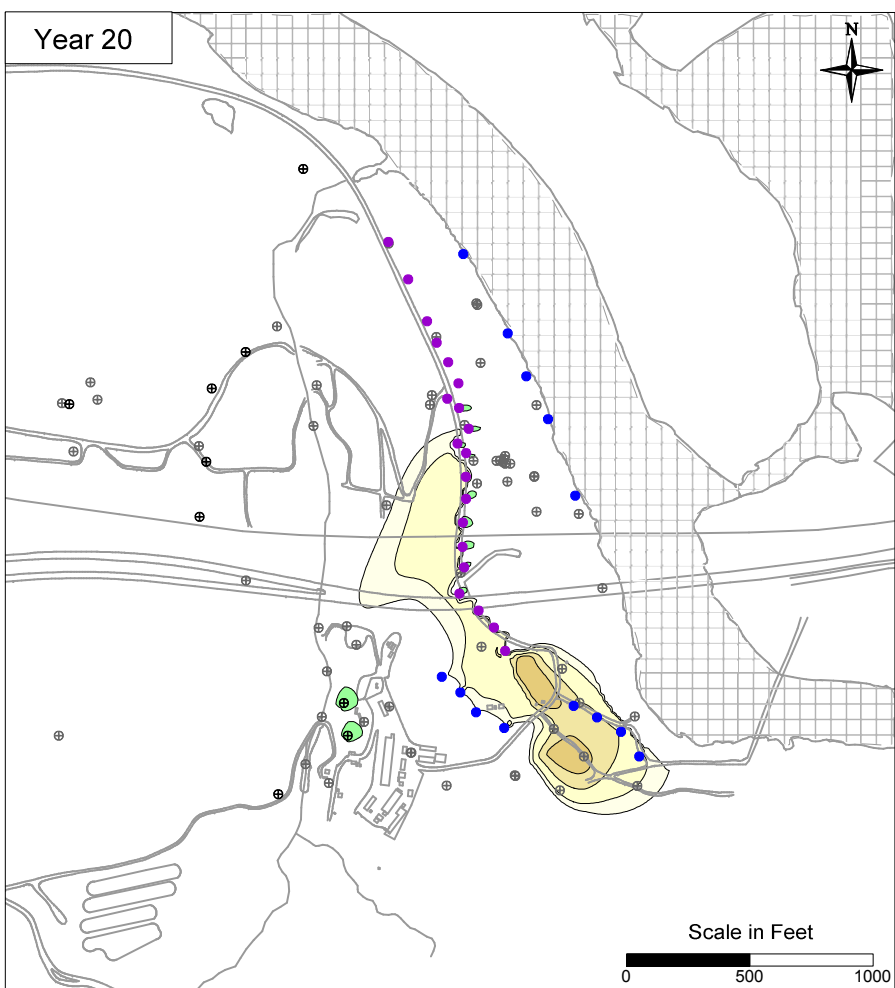
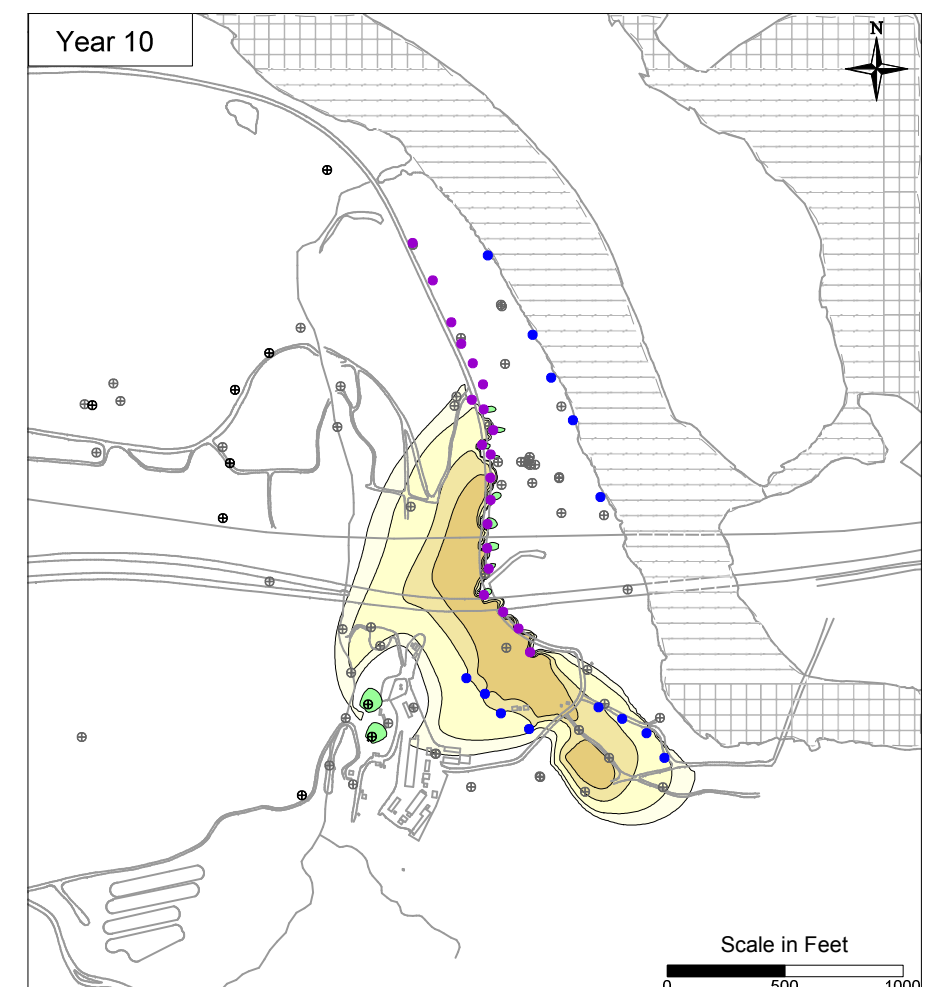
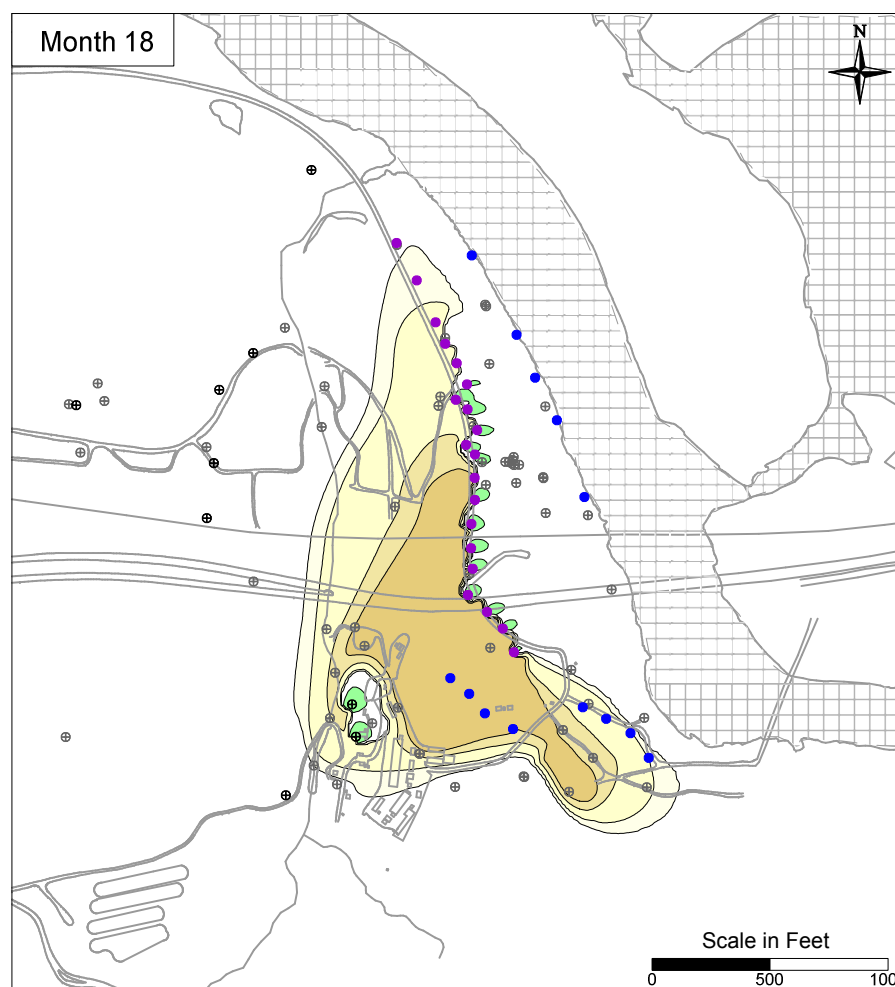
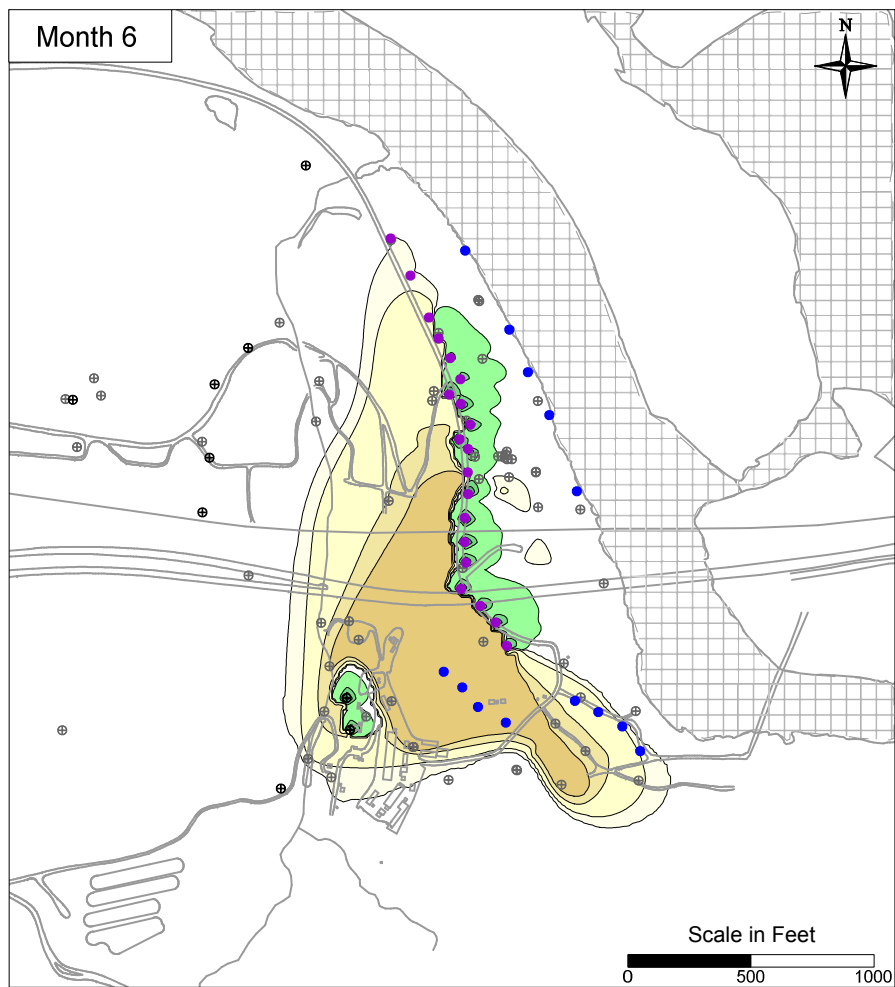
LEGEND

- IRZ WELLS
- ⊕ UPGRADIENT INJECTION WELLS
- EXTRACTION WELLS
- ⊕ MONITORING WELLS

PG&E
TOPOCK COMPRESSOR STATION
NEEDLES, CALIFORNIA
MODELING APPENDIX

SIMULATED HEXAVALENT CHROMIUM
TRANSPORT RESULTS IN
MODEL LAYER 1

FIGURE
B-27



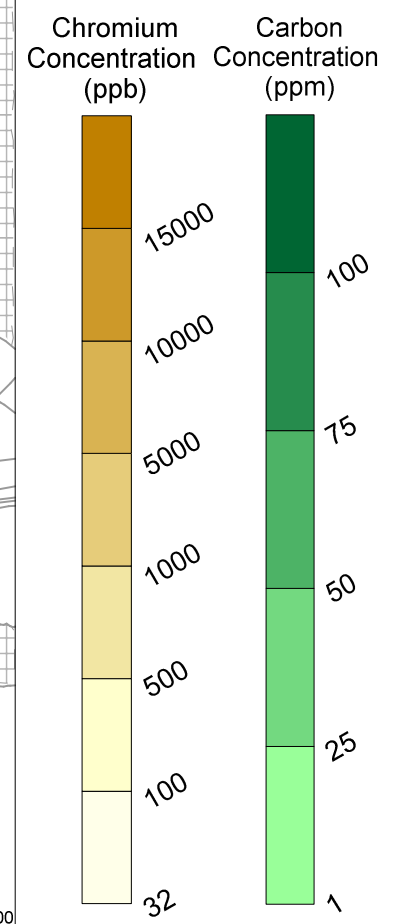
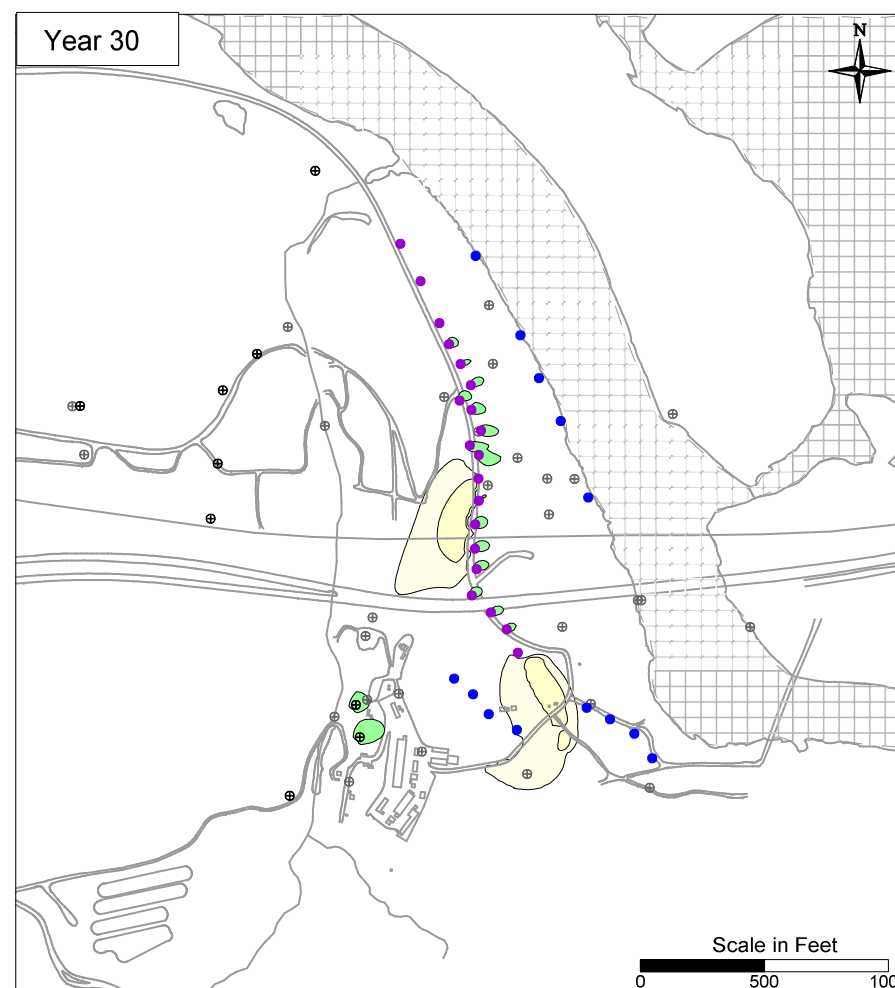
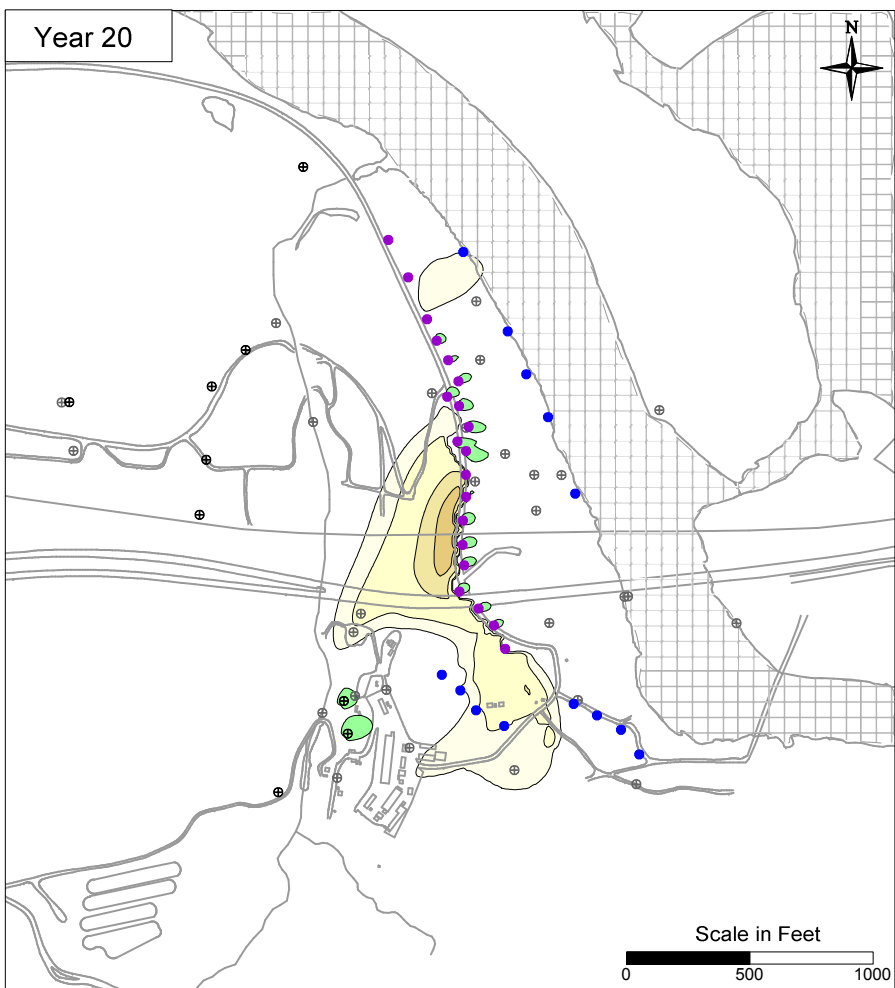
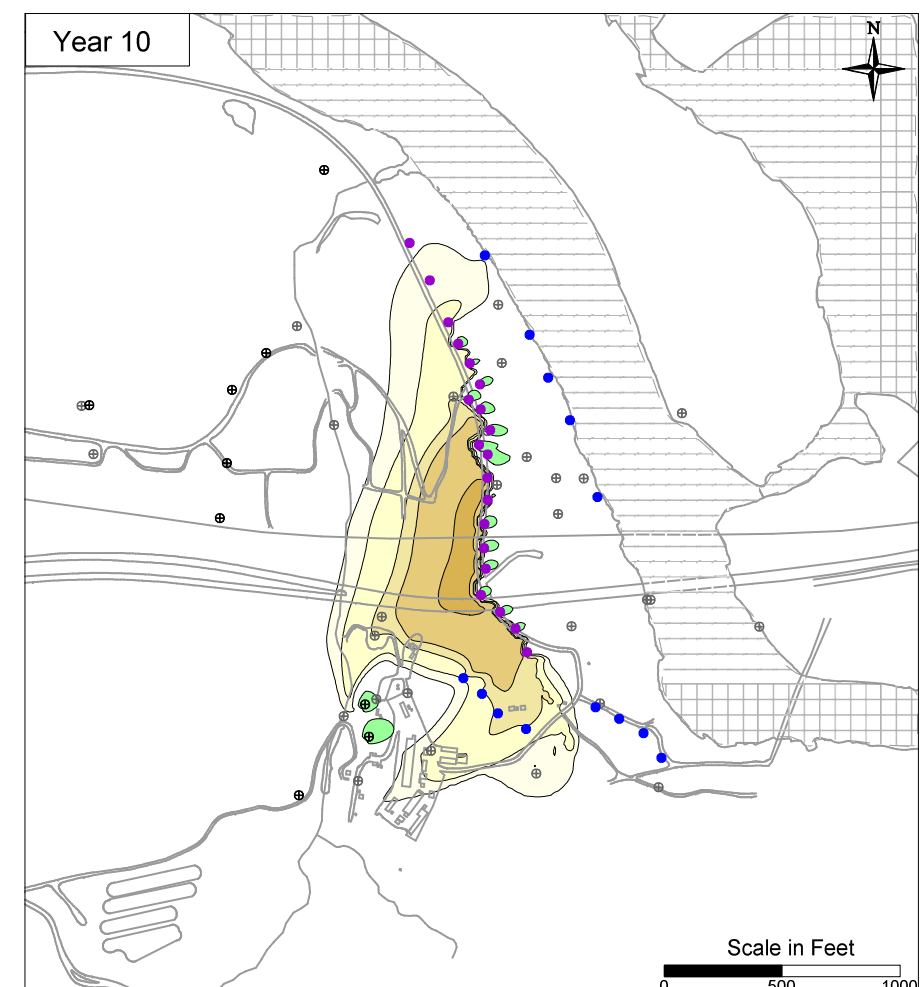
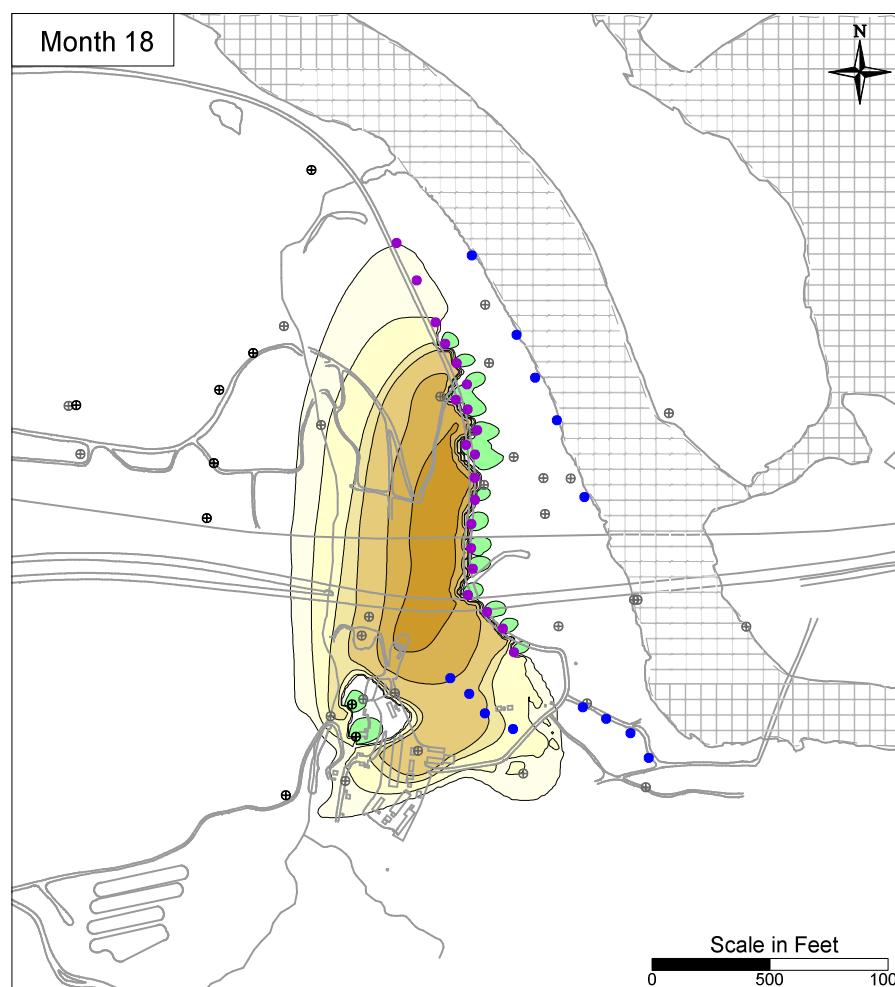
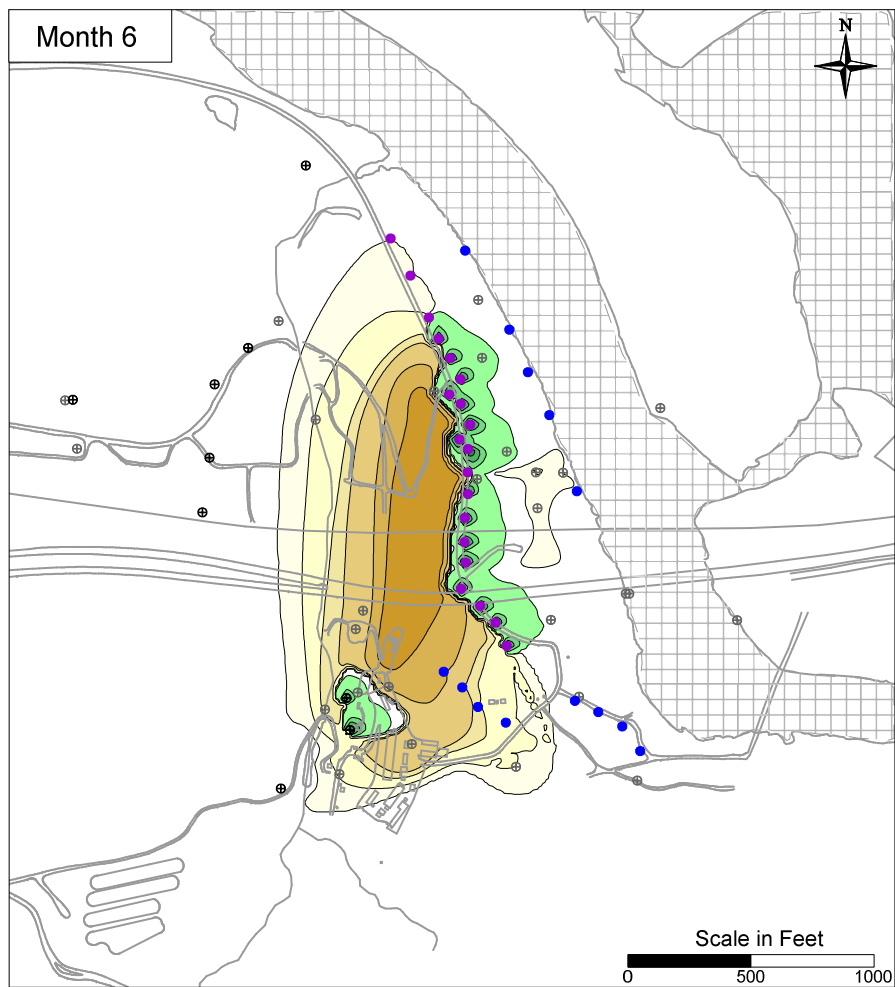
LEGEND

- IRZ WELLS
- ⊕ UPGRADIENT INJECTION WELLS
- EXTRACTION WELLS
- ⊕ MONITORING WELLS

PG&E
TOPOCK COMPRESSOR STATION
NEEDLES, CALIFORNIA
MODELING APPENDIX

SIMULATED HEXAVALENT CHROMIUM
TRANSPORT RESULTS IN
MODEL LAYER 1

FIGURE
B-27

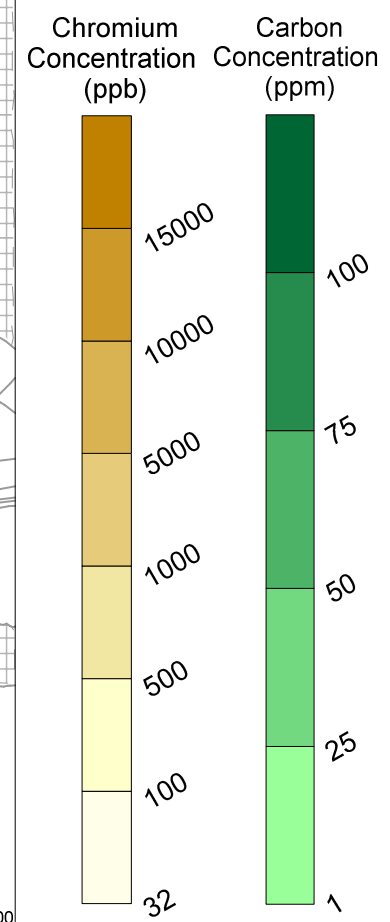
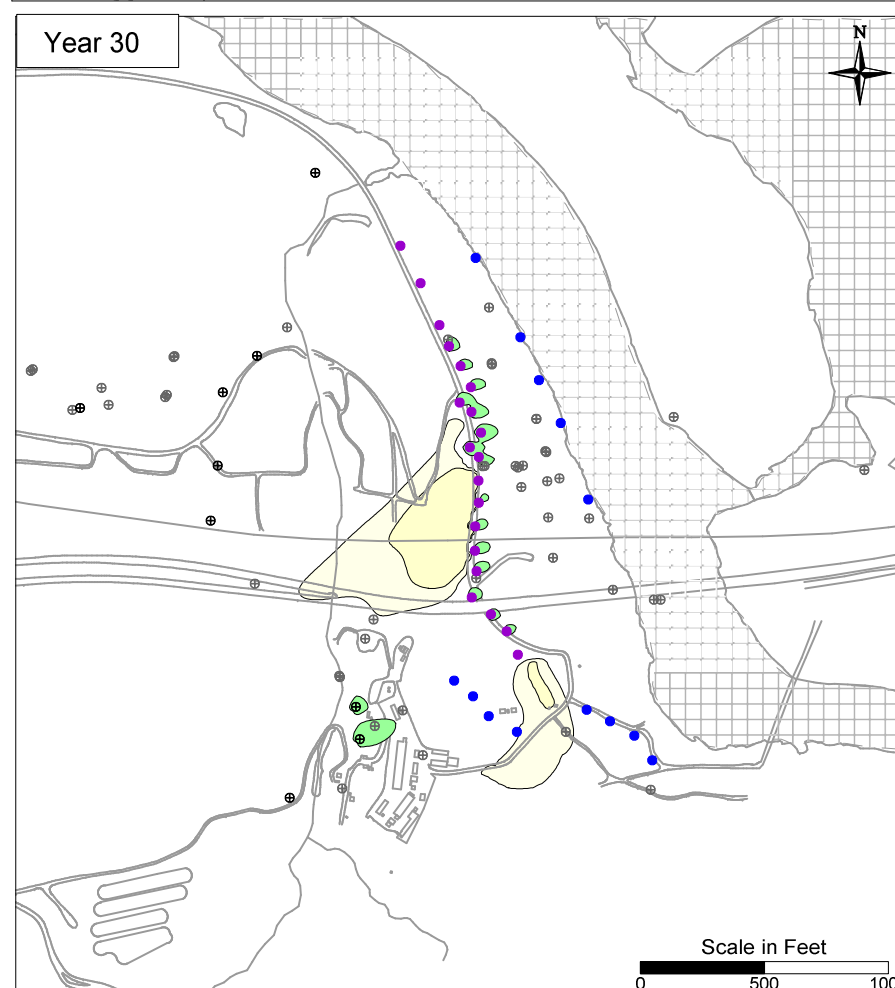
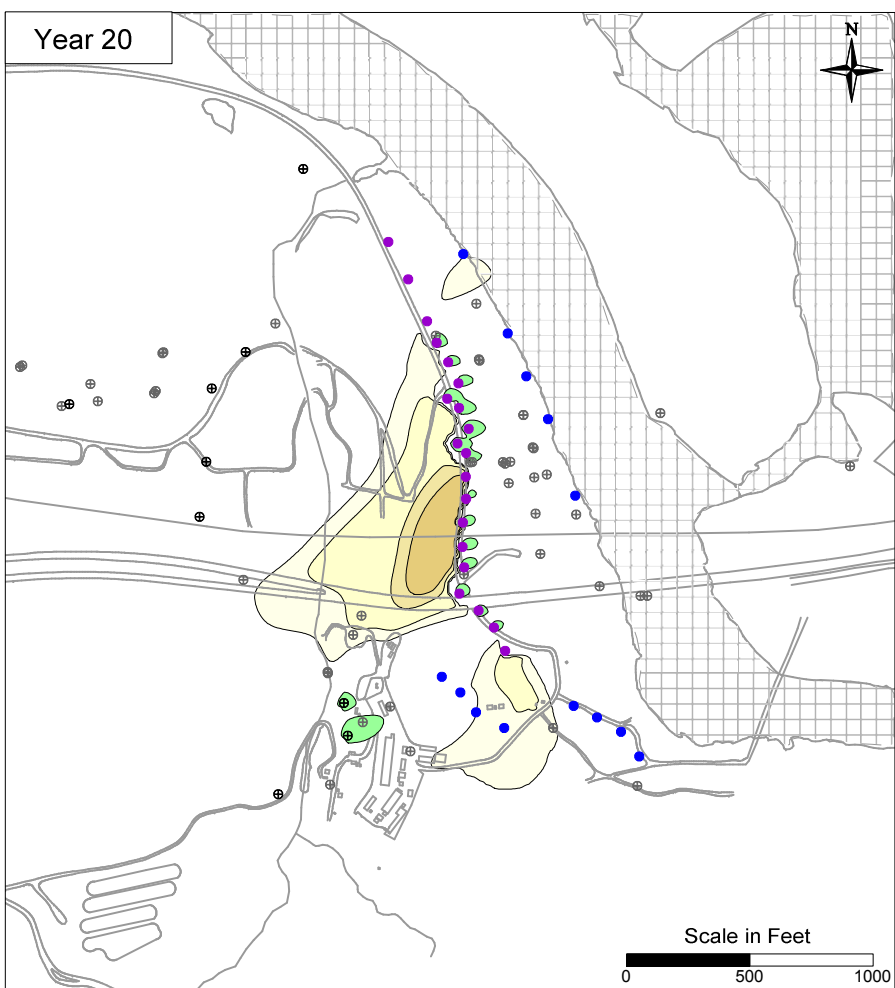
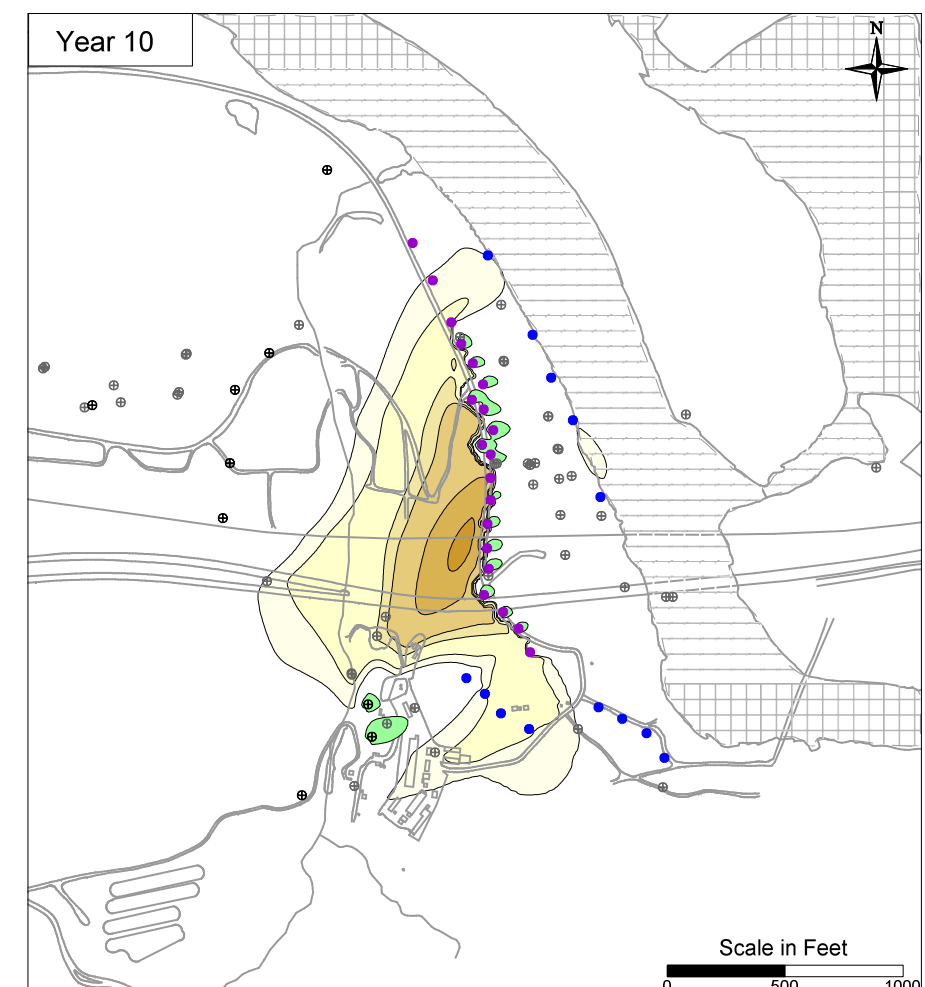
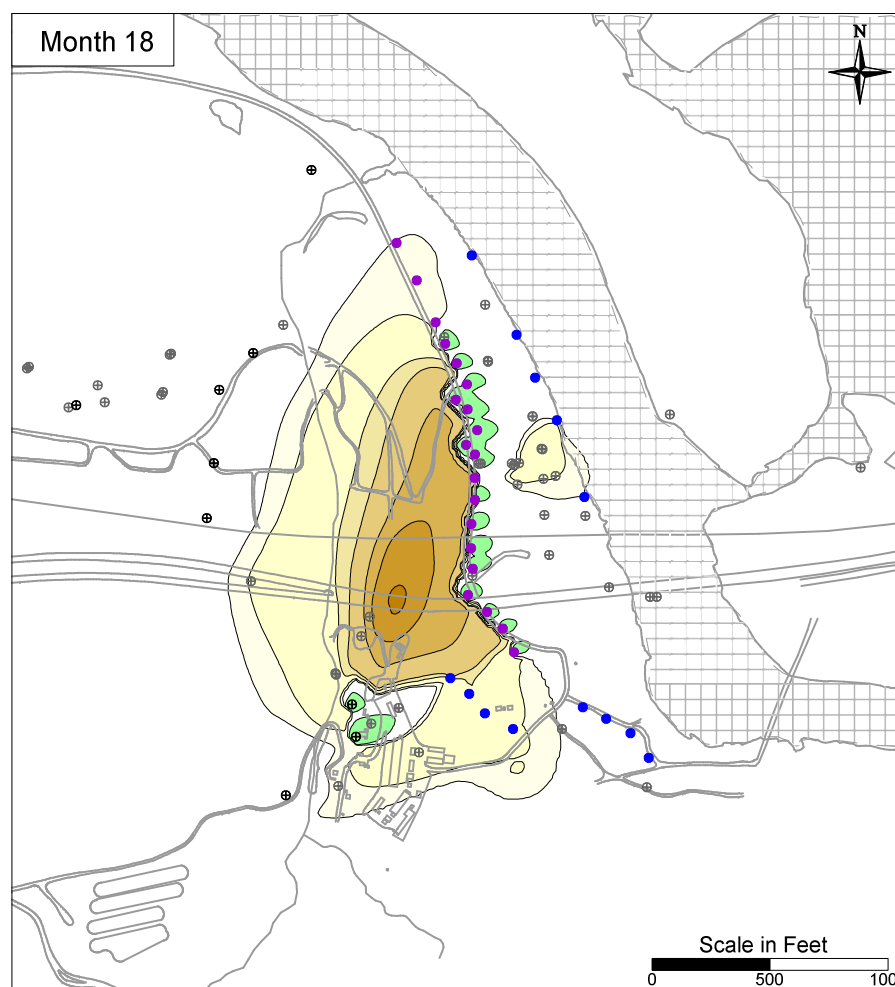
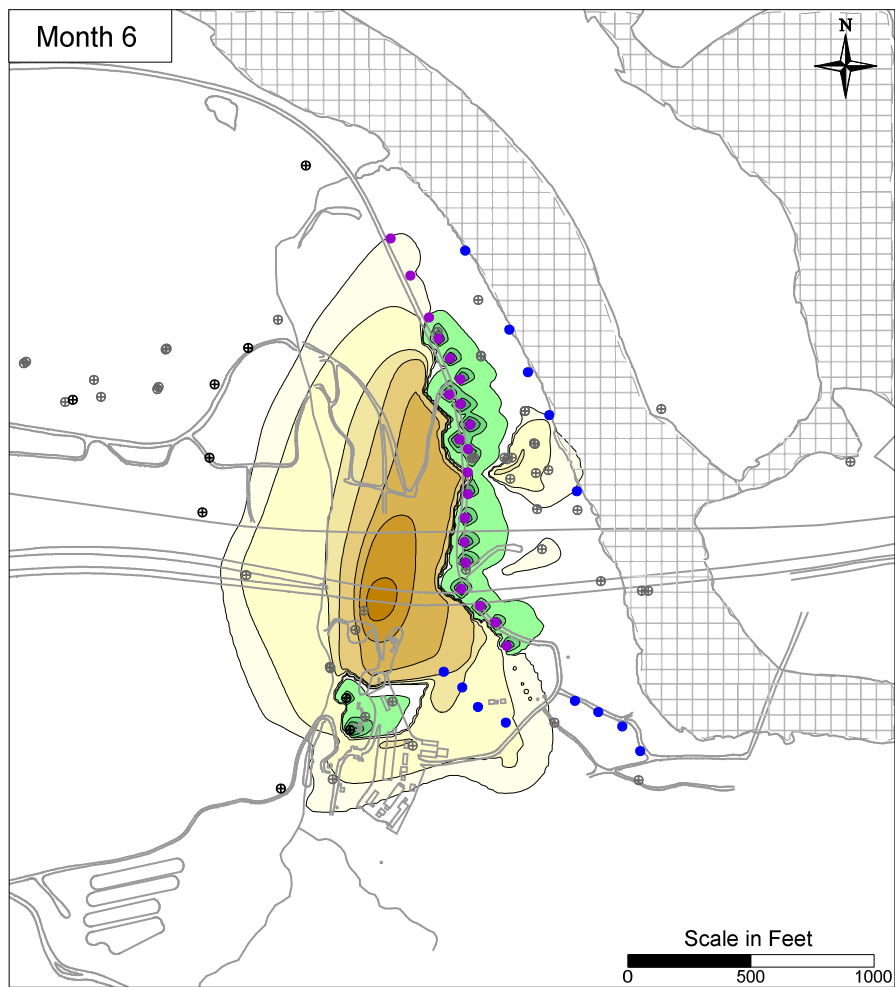


- LEGEND**
- IRZ WELLS
 - ⊕ UPGRADIENT INJECTION WELLS
 - EXTRACTION WELLS
 - ⊕ MONITORING WELLS

PG&E
TOPOCK COMPRESSOR STATION
NEEDLES, CALIFORNIA
MODELING APPENDIX

**SIMULATED HEXAVALENT CHROMIUM
TRANSPORT RESULTS IN
MODEL LAYER 3**

ARCADIS



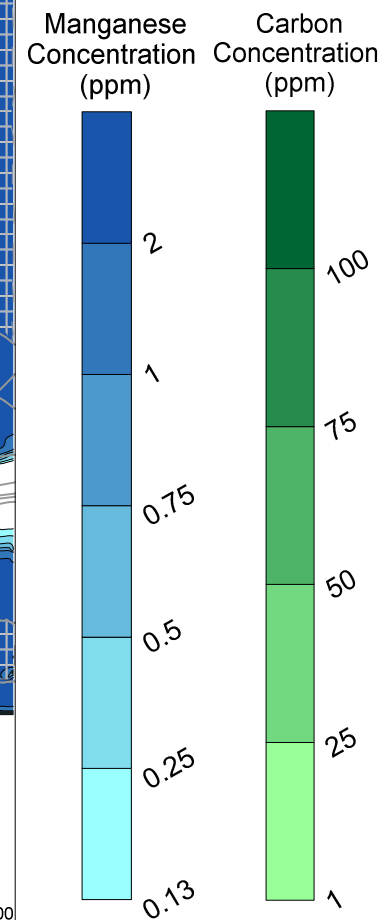
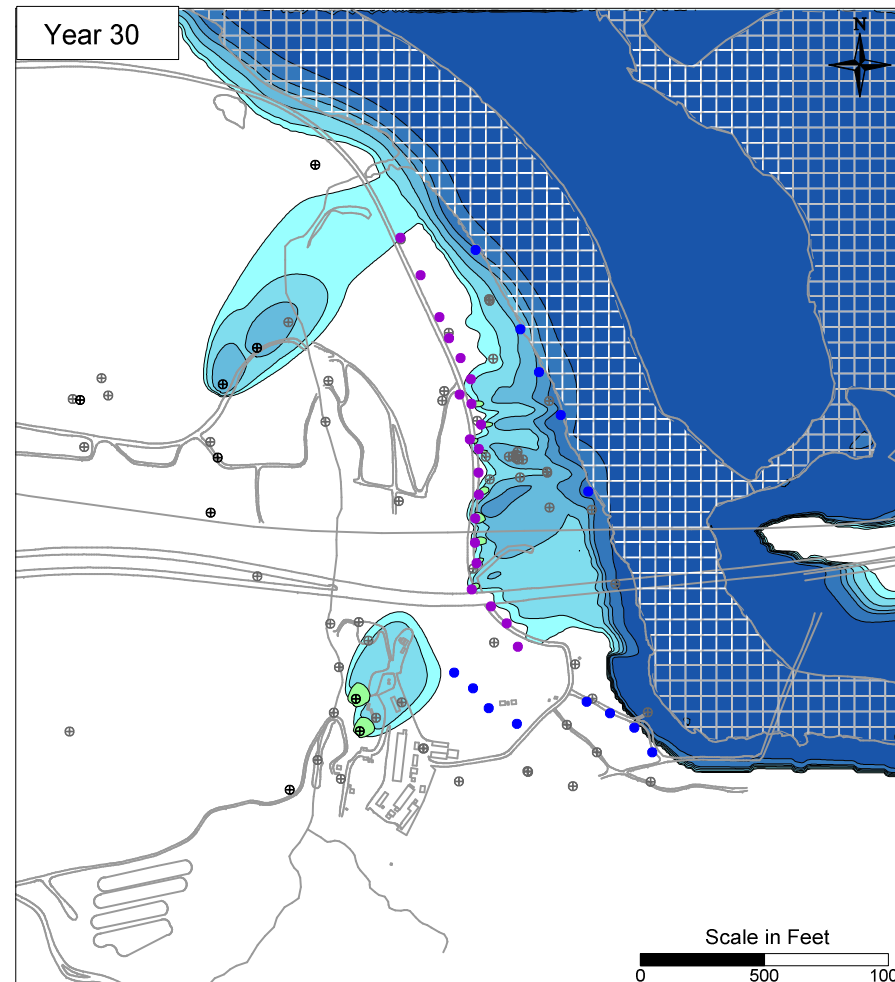
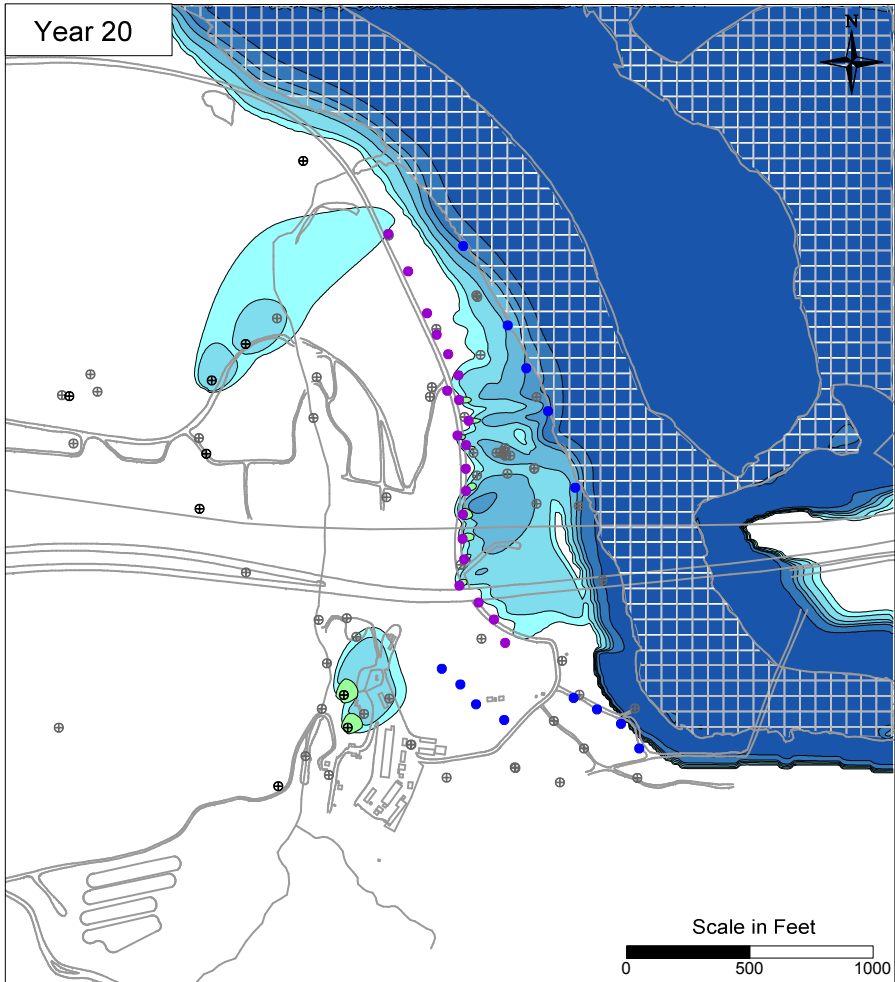
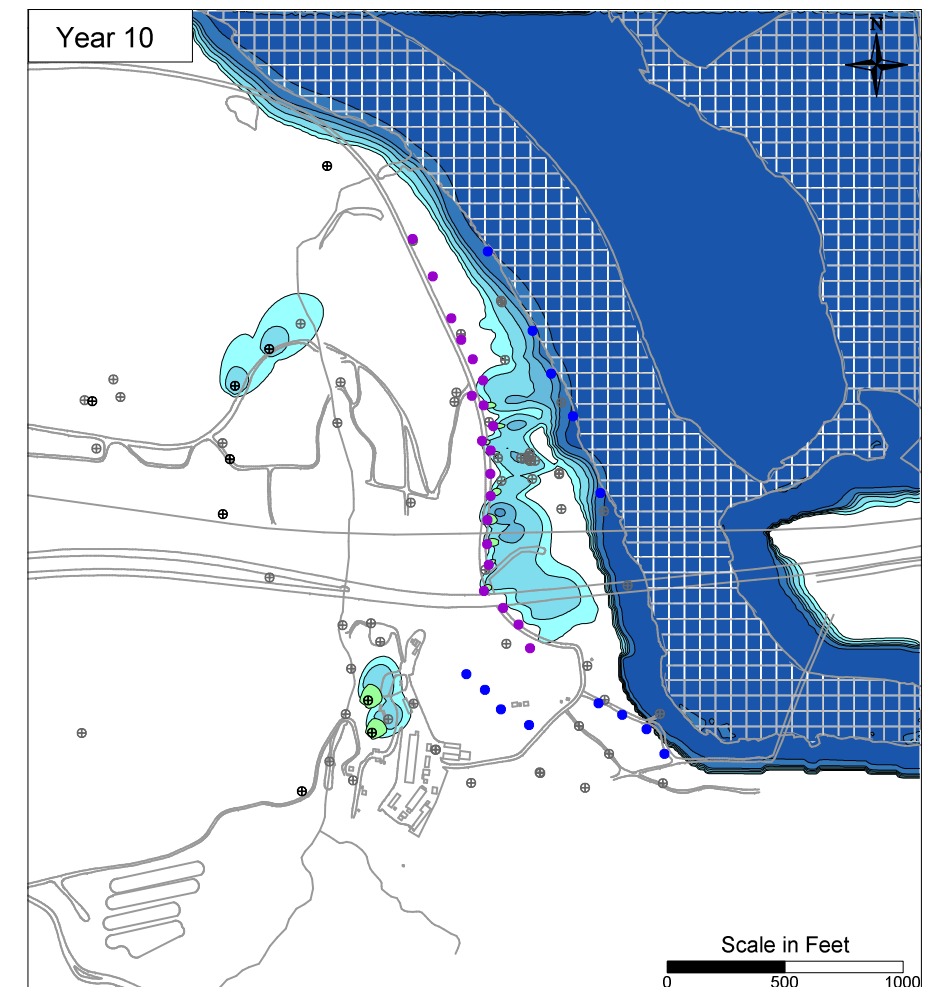
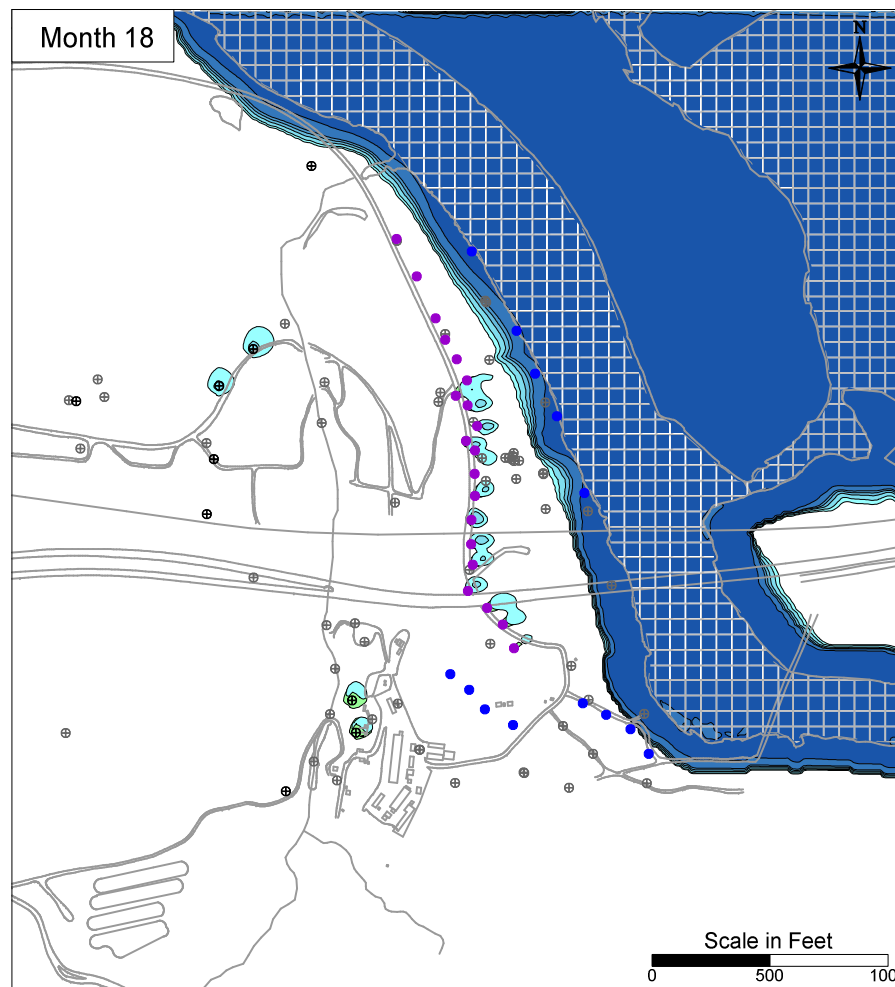
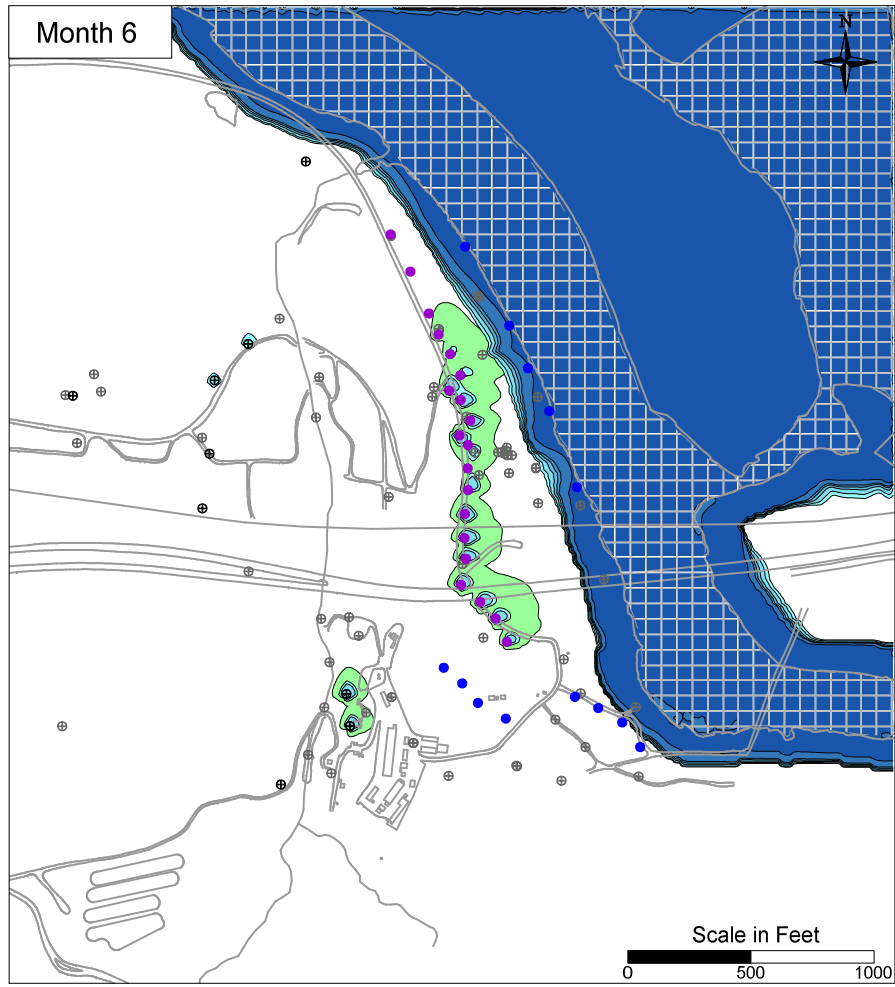
LEGEND

- IRZ WELLS
- ⊕ UPGRADIENT INJECTION WELLS
- EXTRACTION WELLS
- ⊕ MONITORING WELLS

PG&E
TOPOCK COMPRESSOR STATION
NEEDLES, CALIFORNIA
MODELING APPENDIX

SIMULATED HEXAVALENT CHROMIUM
TRANSPORT RESULTS IN
MODEL LAYER 4

FIGURE
B-30

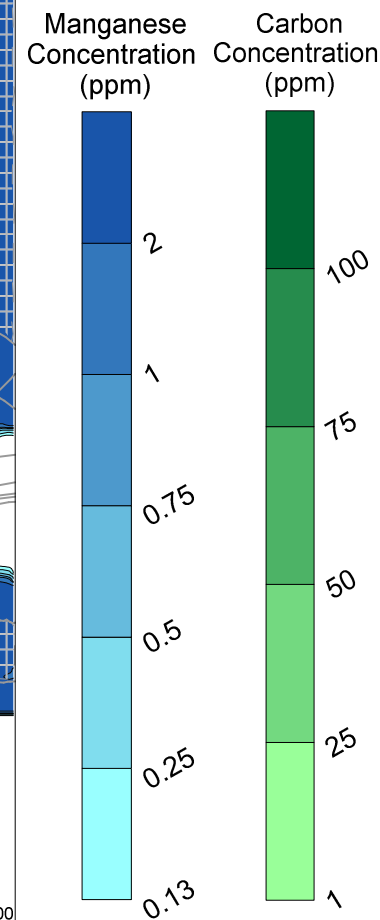
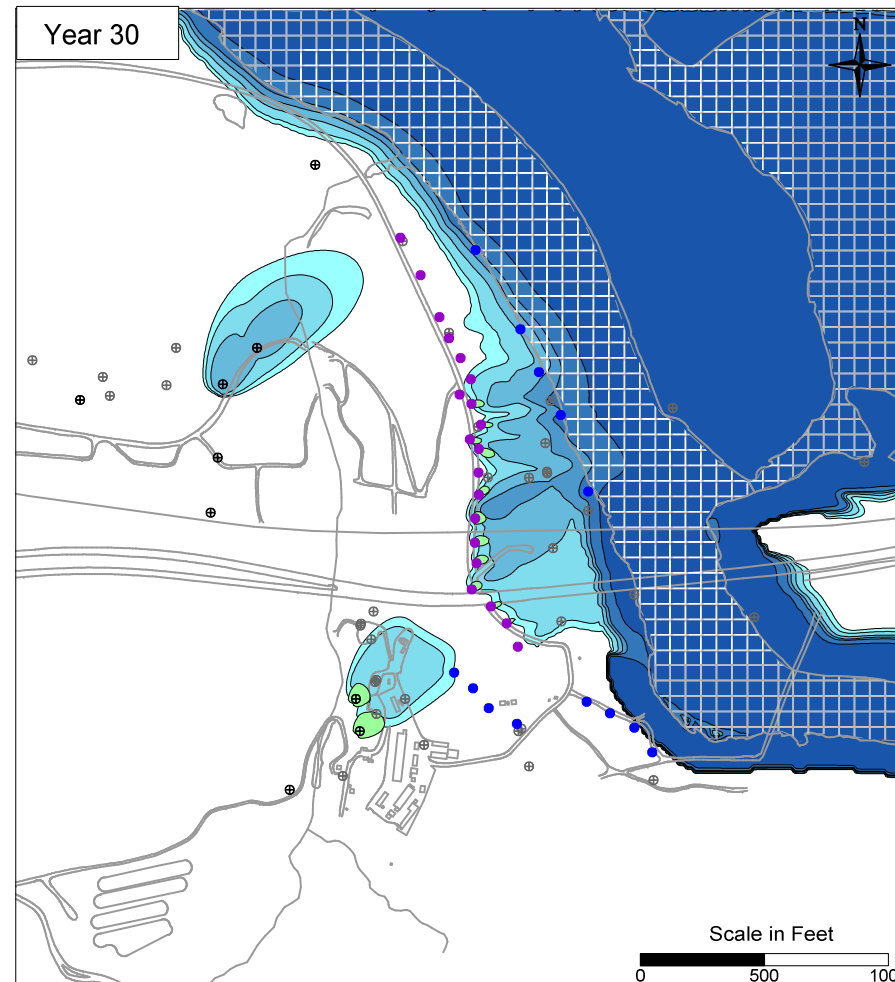
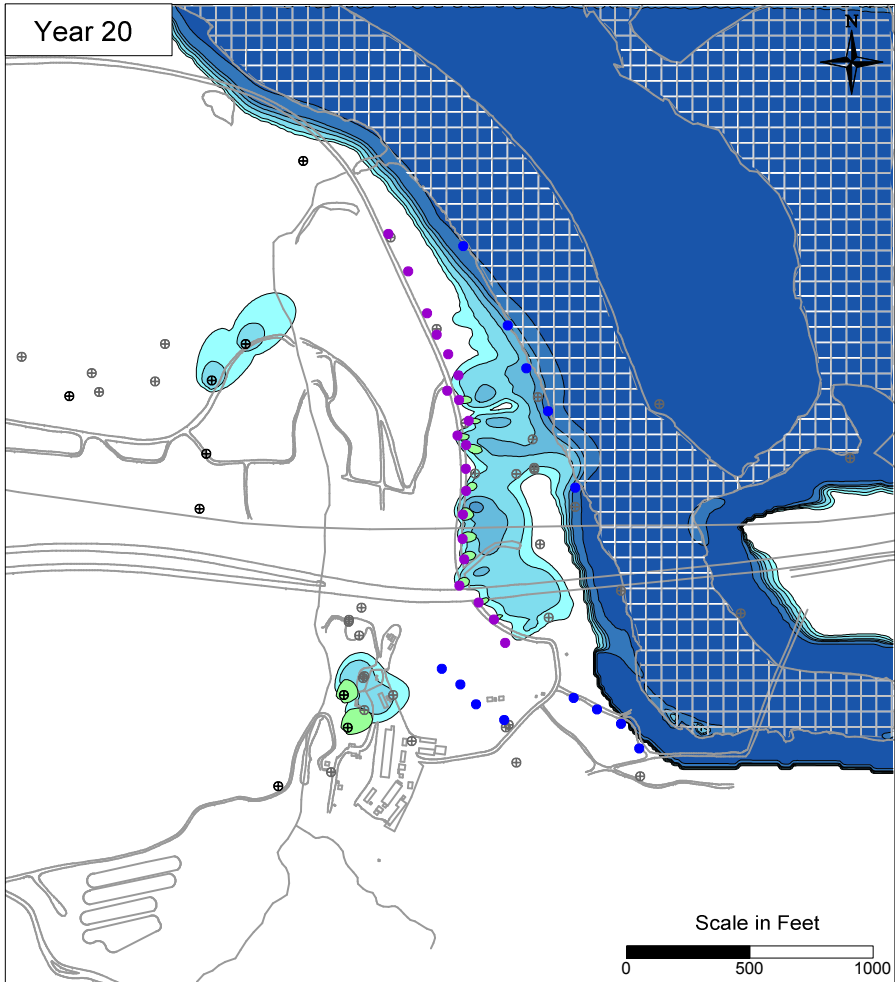
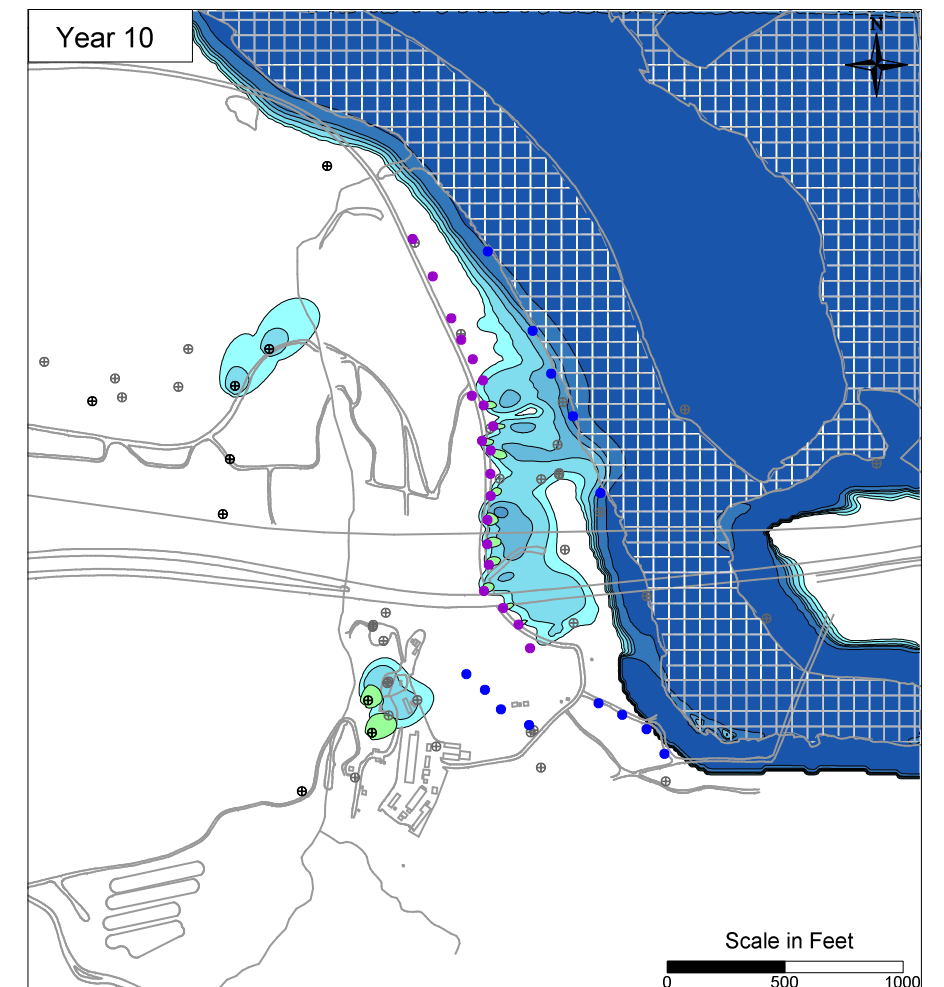
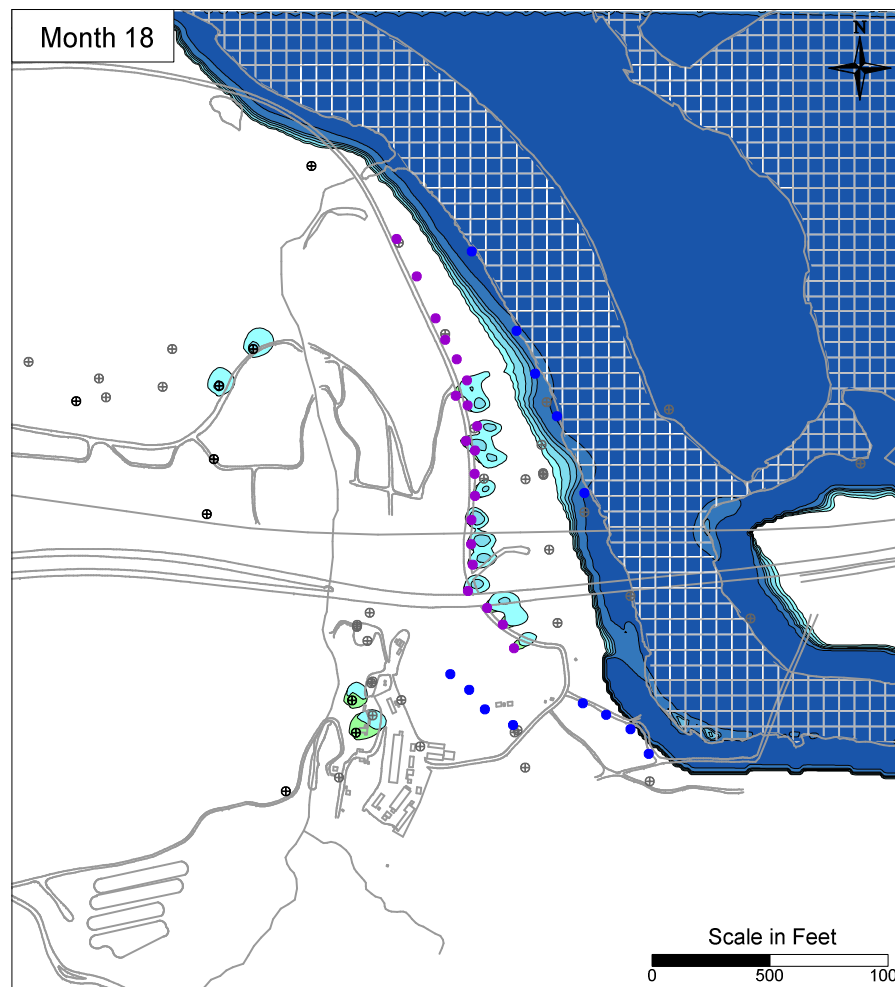
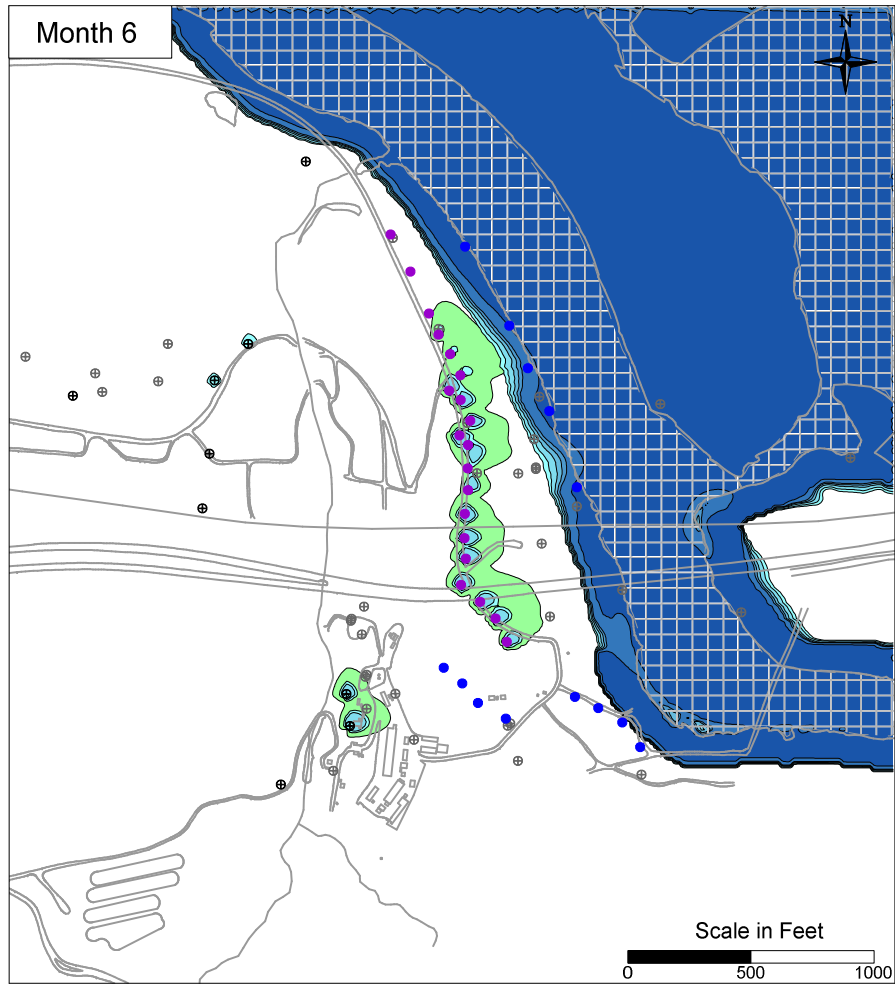


- LEGEND**
- IRZ WELLS
 - ⊕ UPGRADIENT INJECTION WELLS
 - EXTRACTION WELLS
 - ⊕ MONITORING WELLS

PG&E
TOPOCK COMPRESSOR STATION
NEEDLES, CALIFORNIA
MODELING APPENDIX

SIMULATED MANGANESE TRANSPORT
RESULTS IN MODEL LAYER 1

FIGURE
B-31

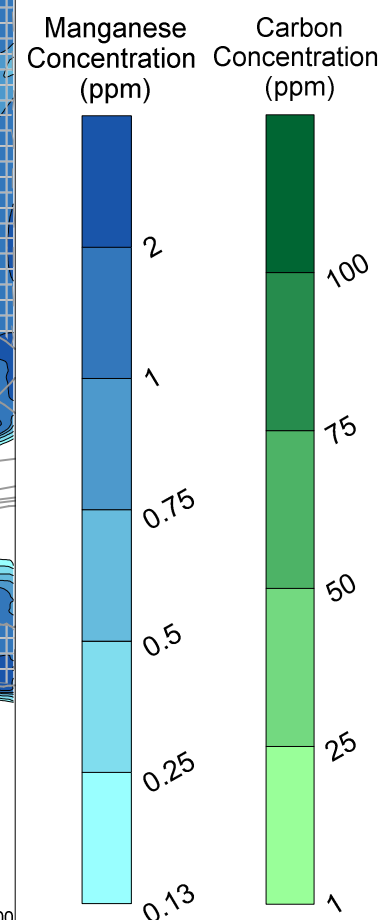
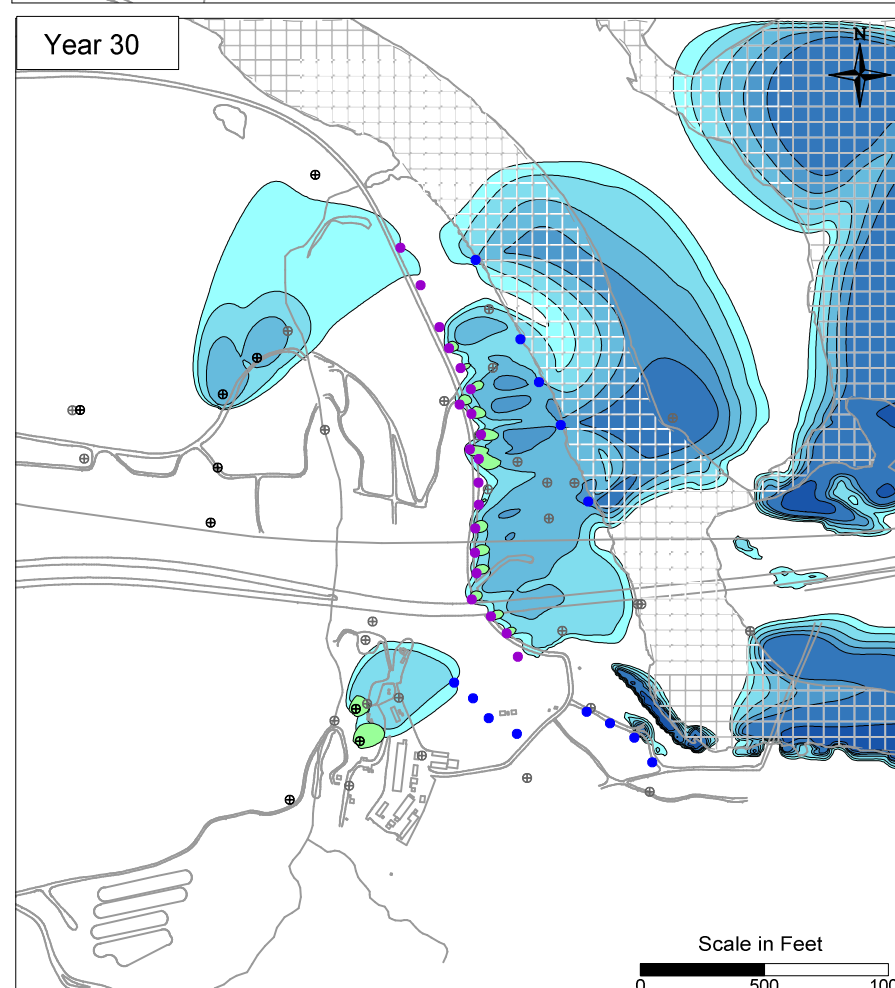
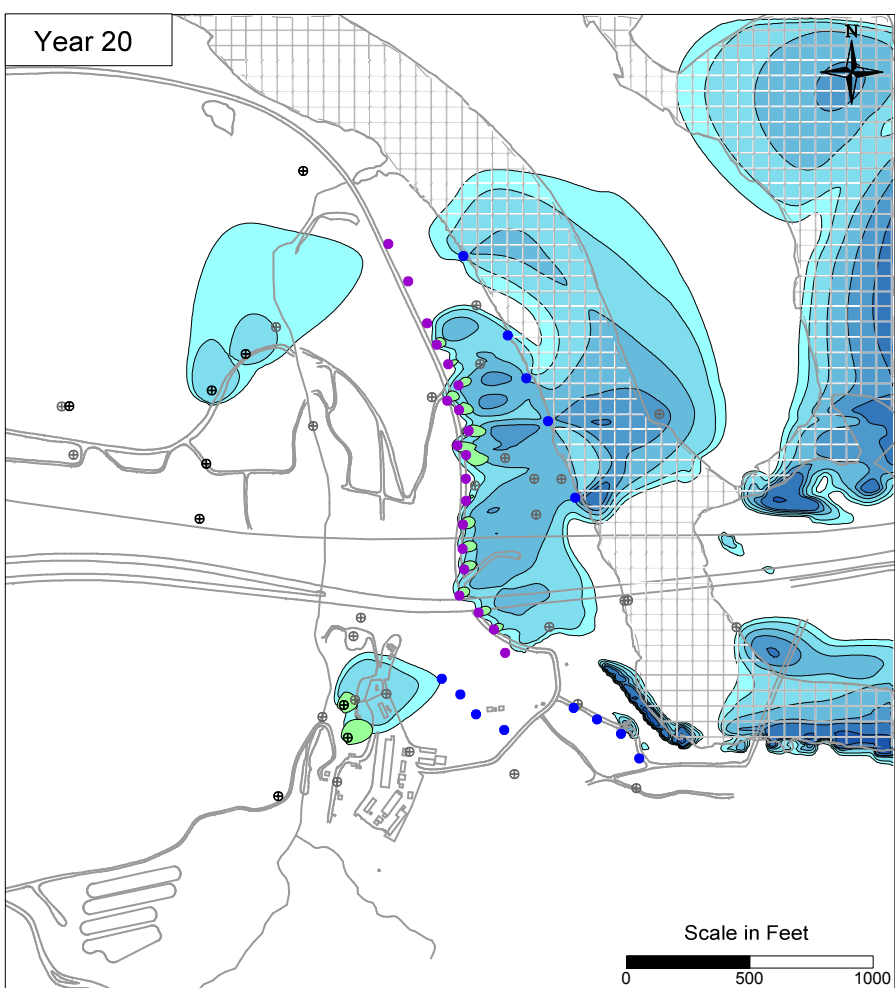
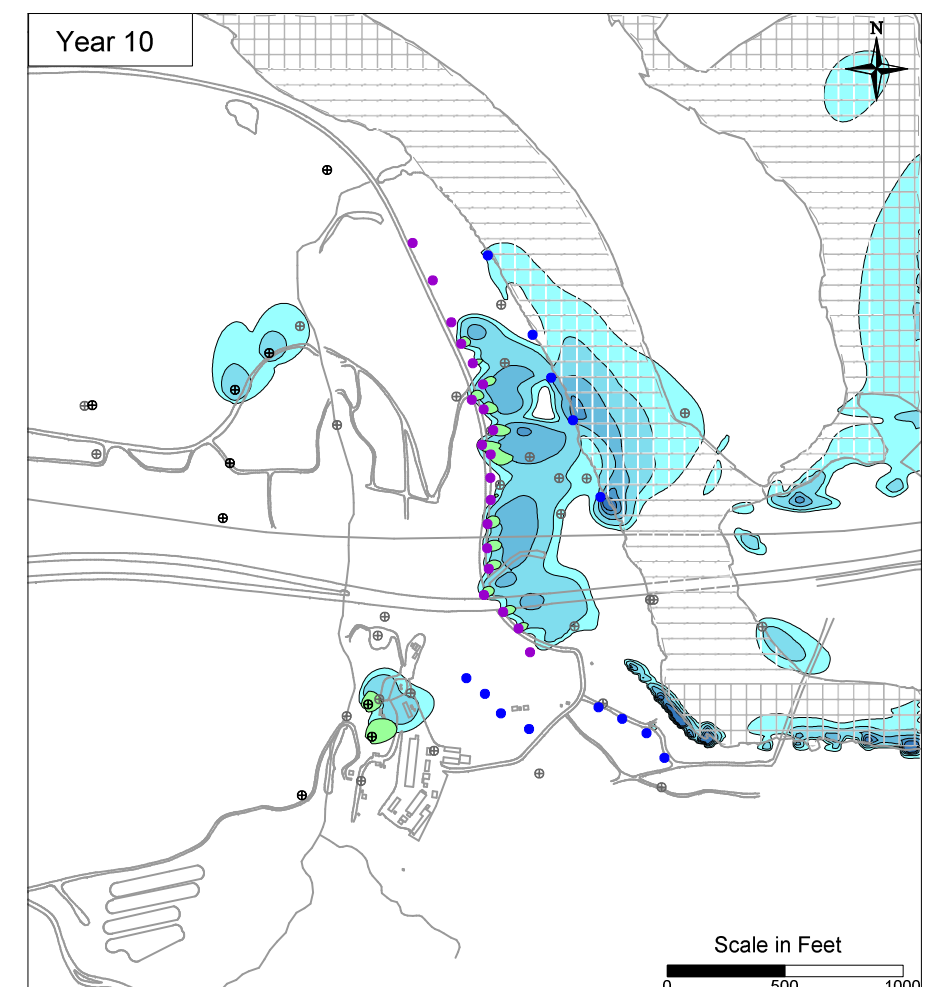
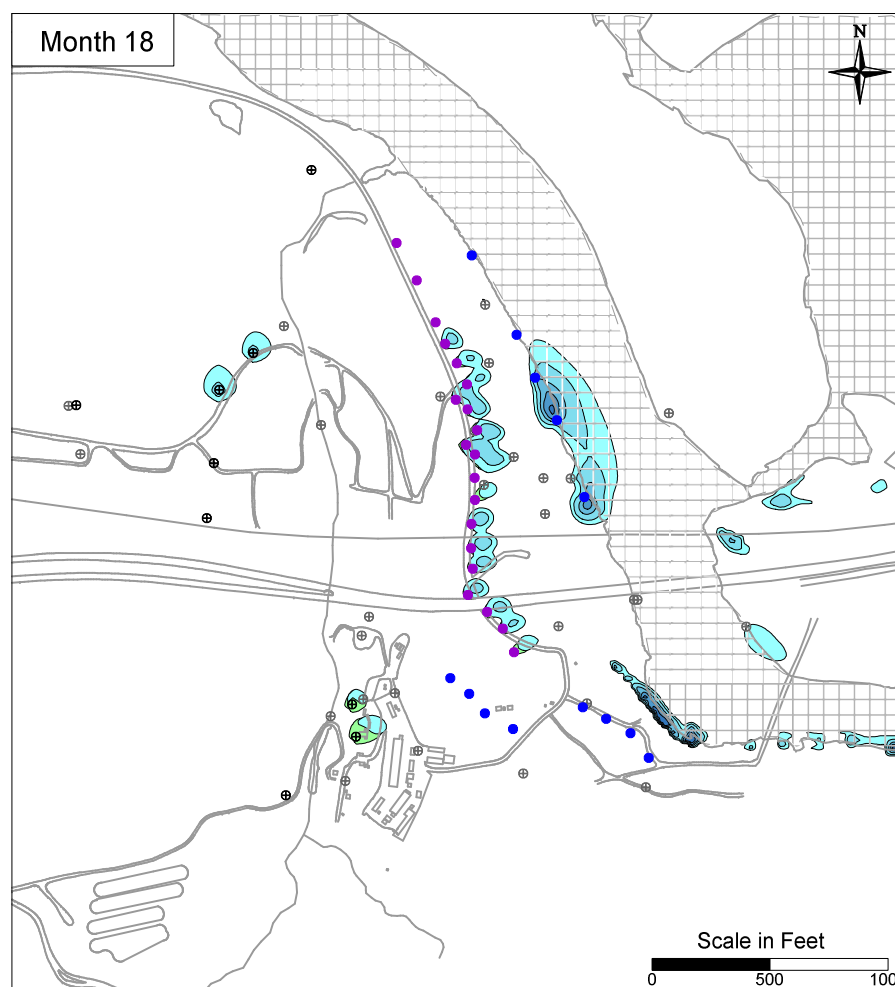
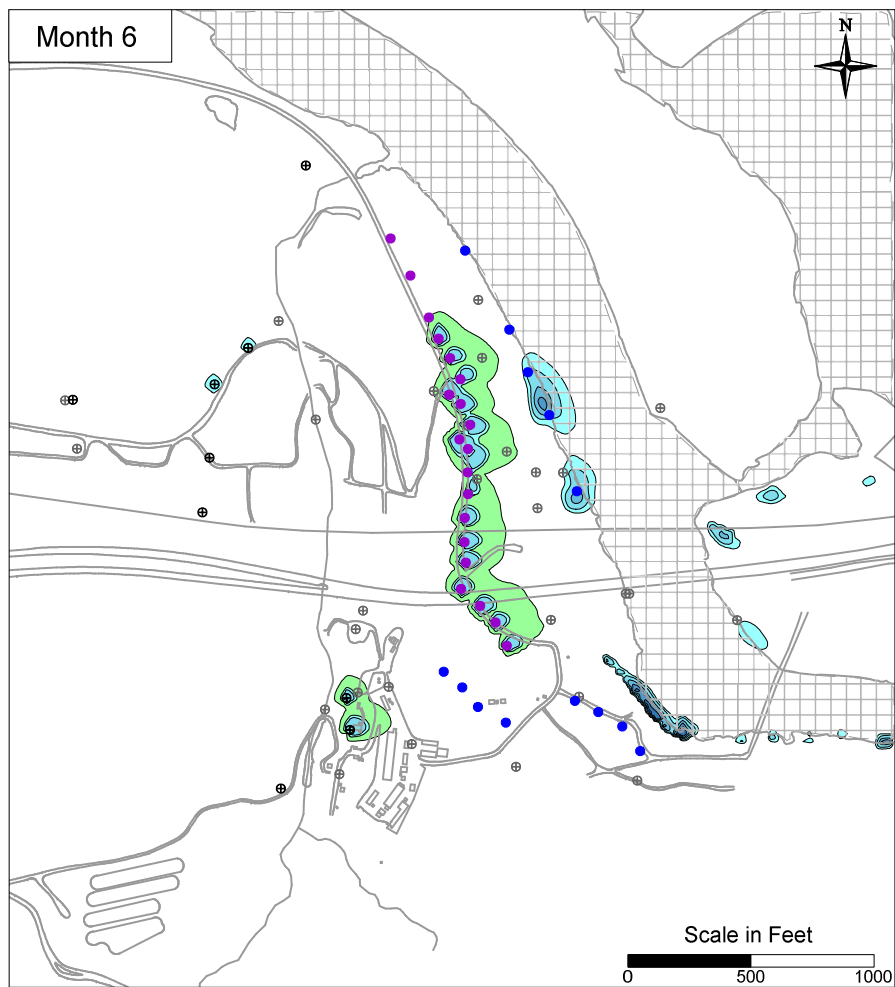


- LEGEND**
- IRZ WELLS
 - ⊕ UPGRADIENT INJECTION WELLS
 - EXTRACTION WELLS
 - ⊕ MONITORING WELLS

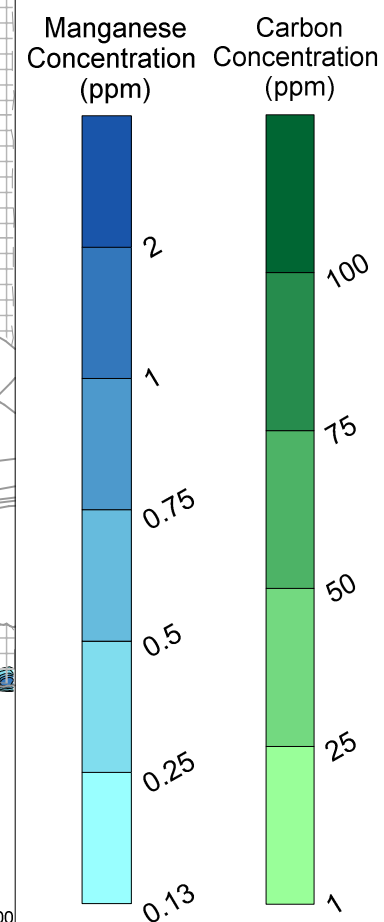
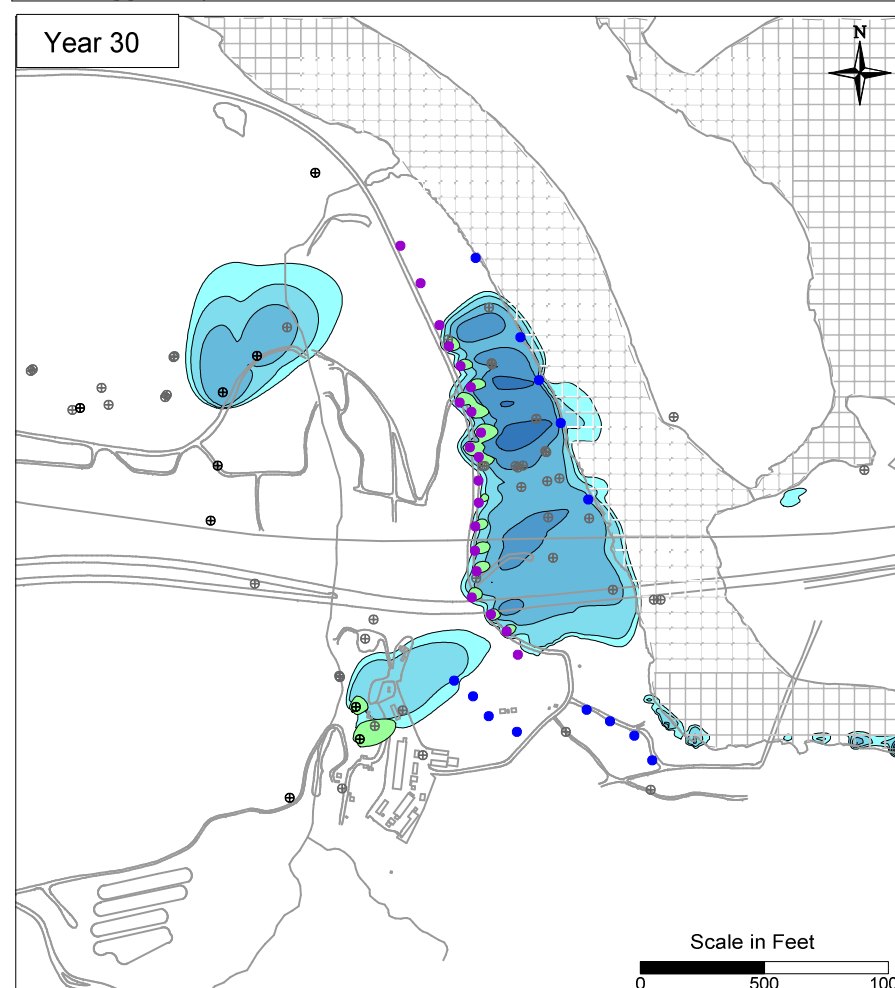
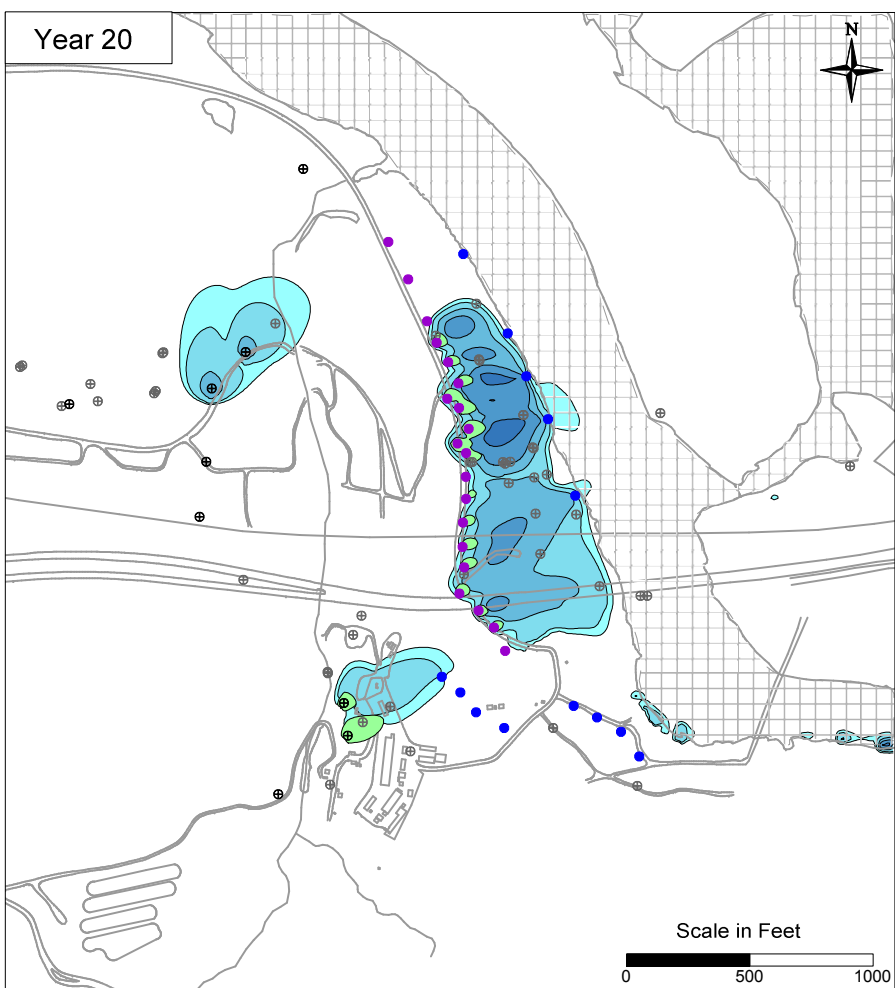
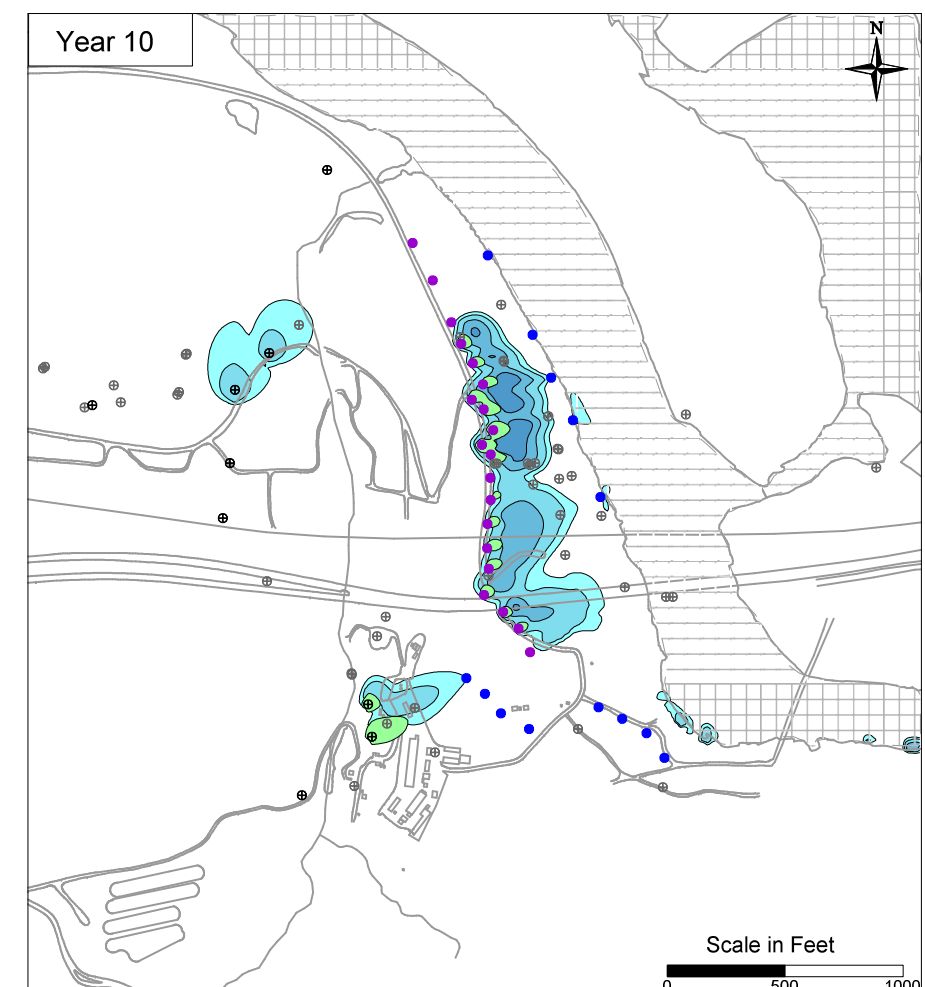
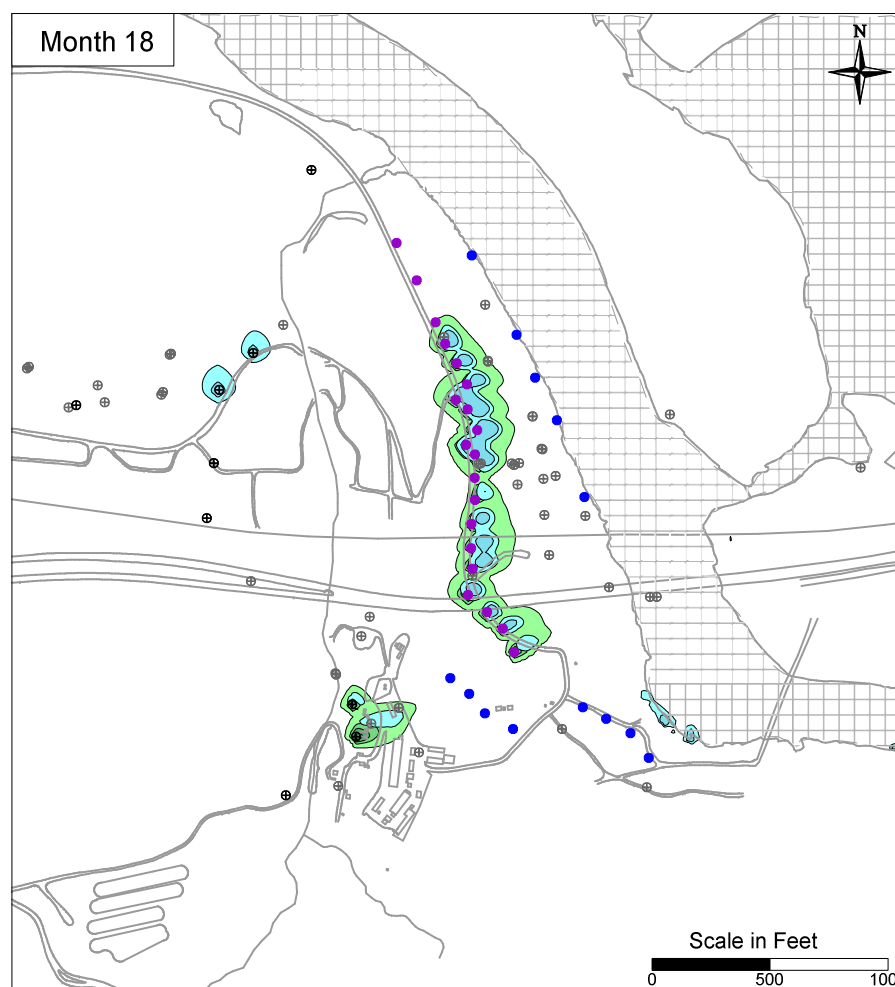
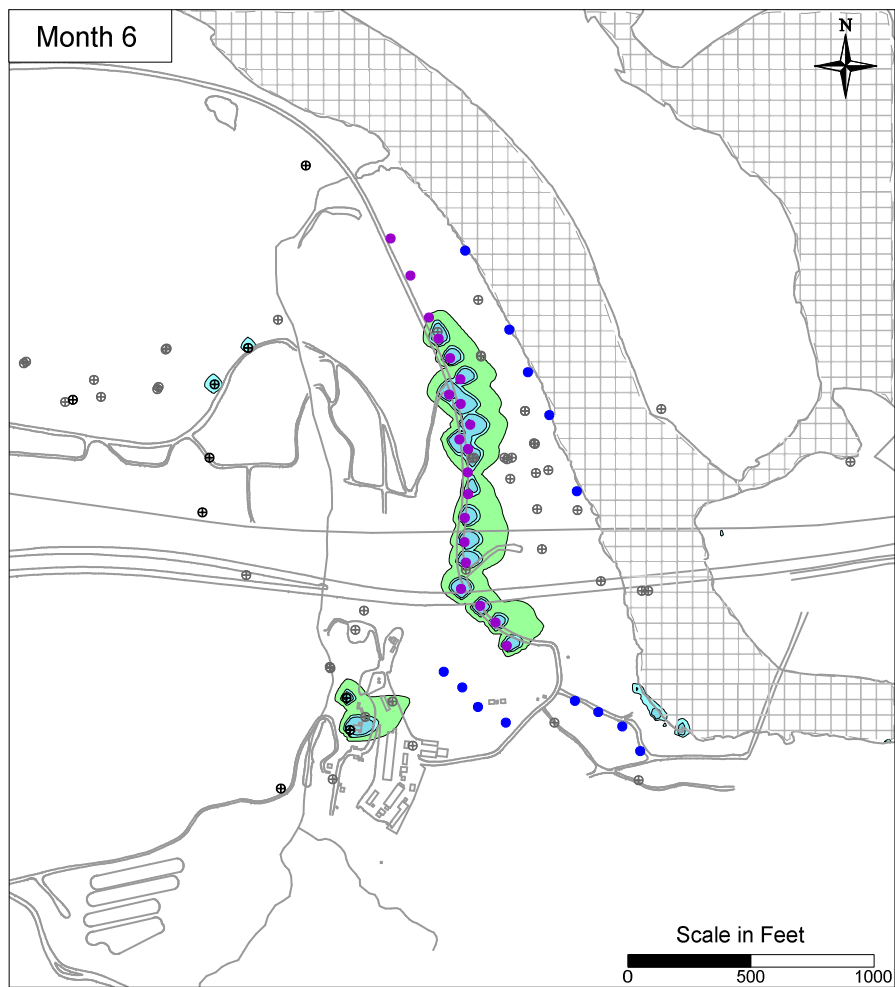
PG&E
TOPOCK COMPRESSOR STATION
NEEDLES, CALIFORNIA
MODELING APPENDIX

SIMULATED MANGANESE TRANSPORT
RESULTS IN MODEL LAYER 2

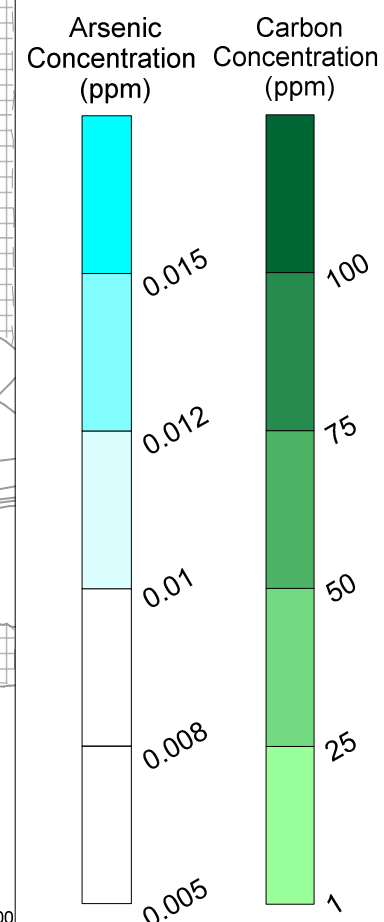
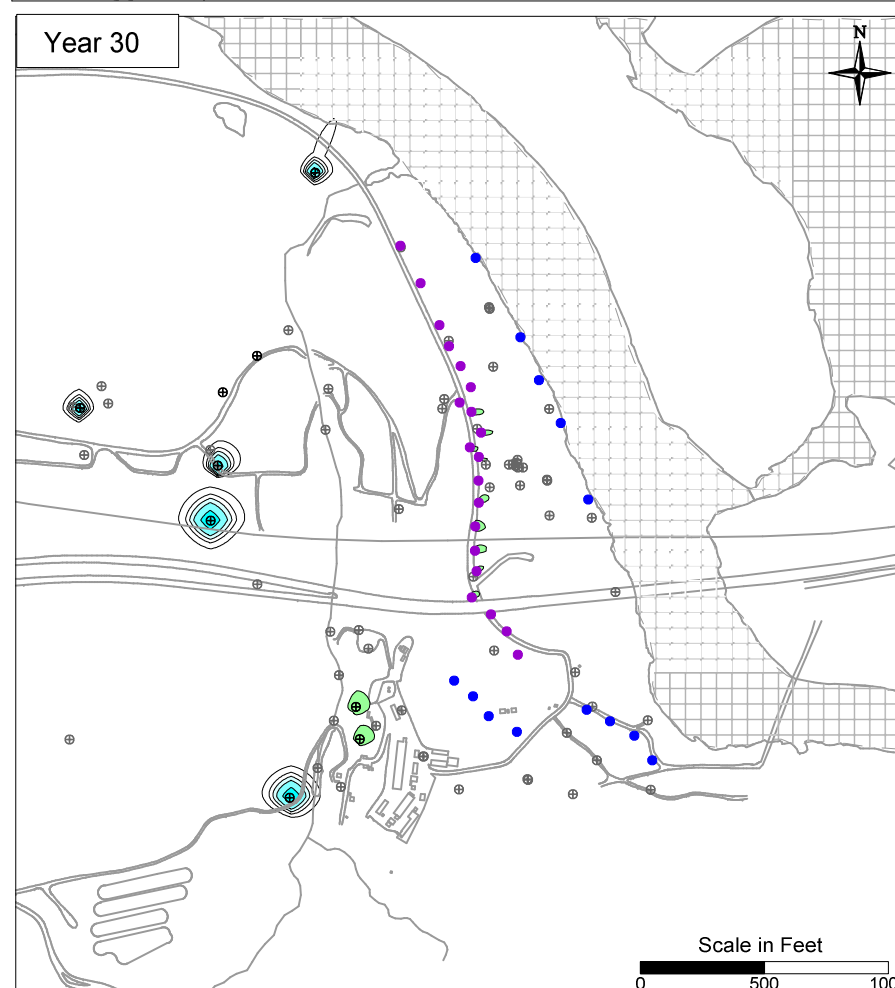
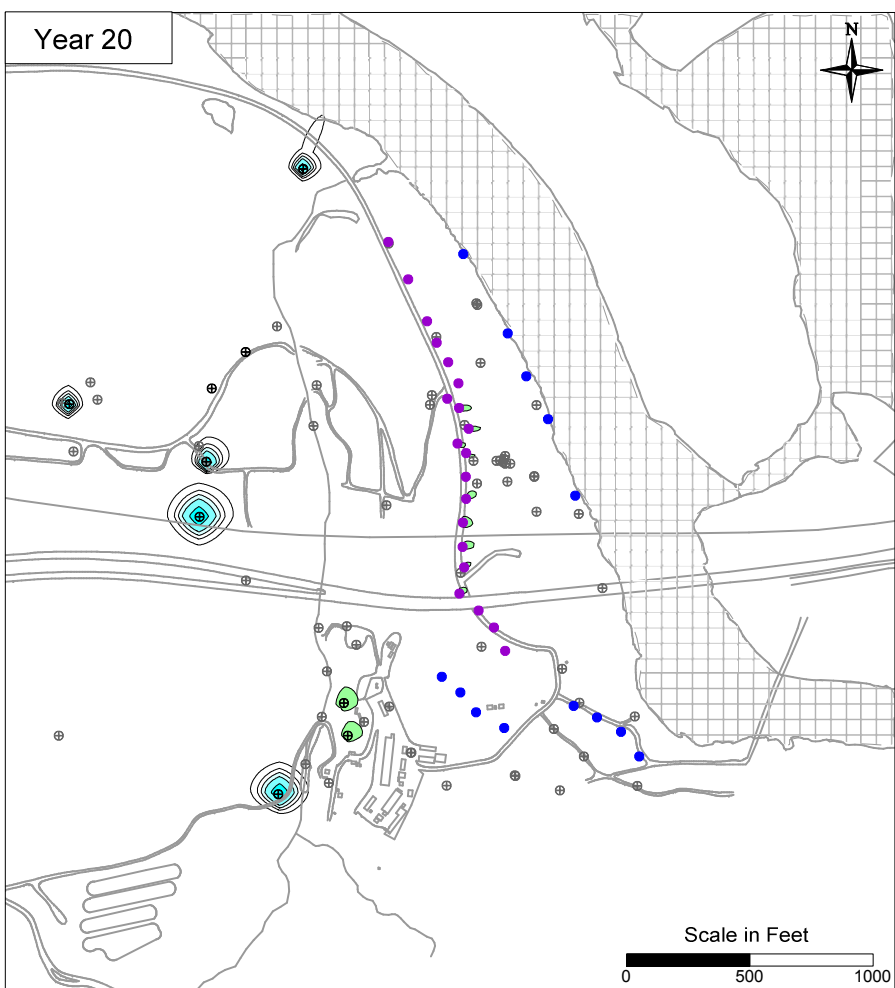
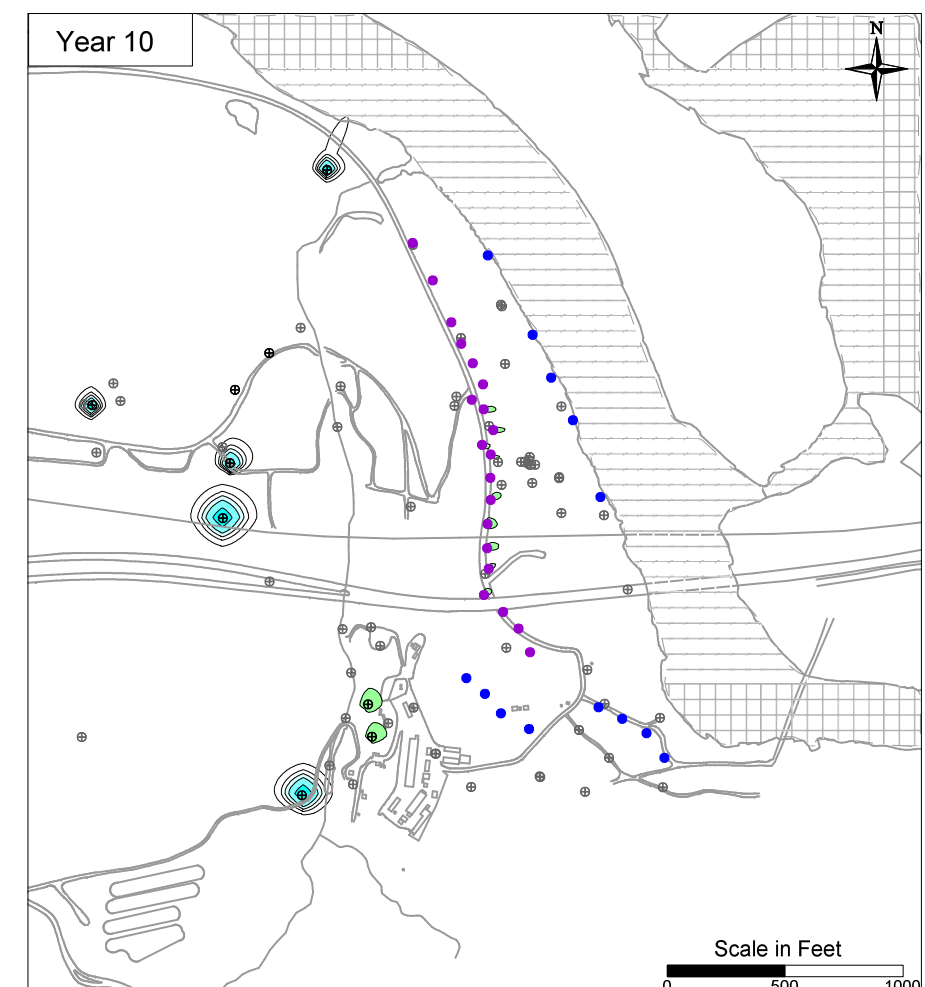
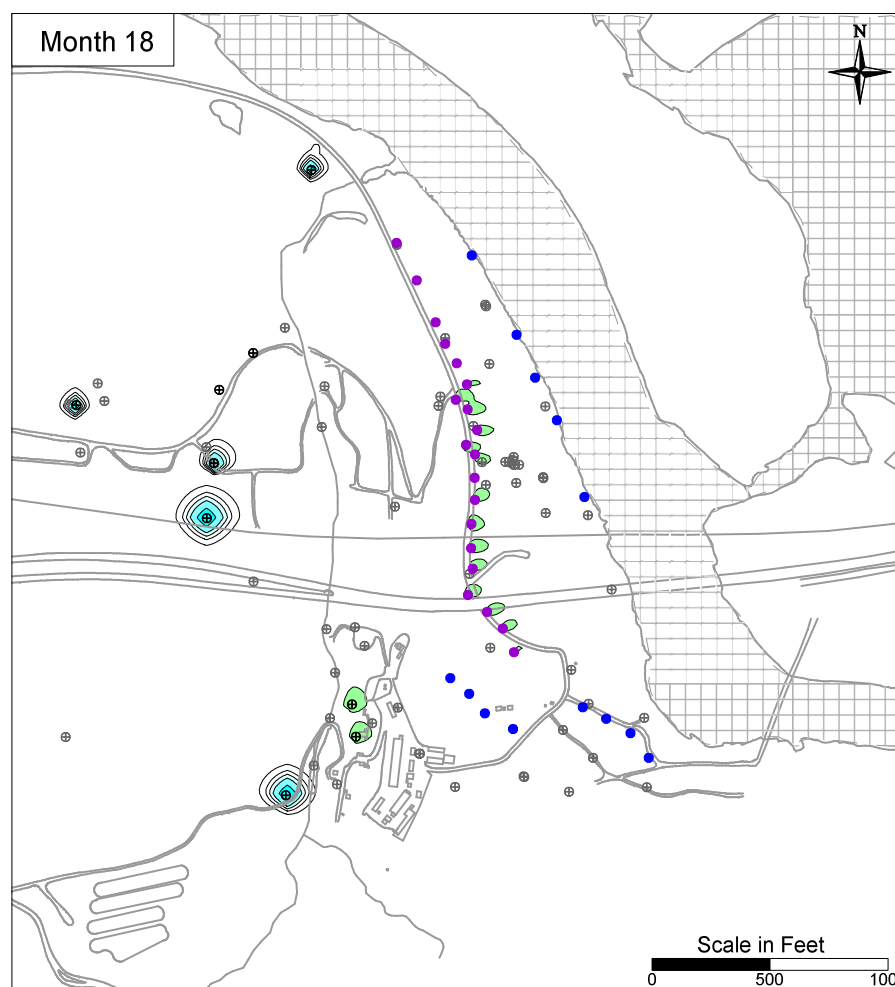
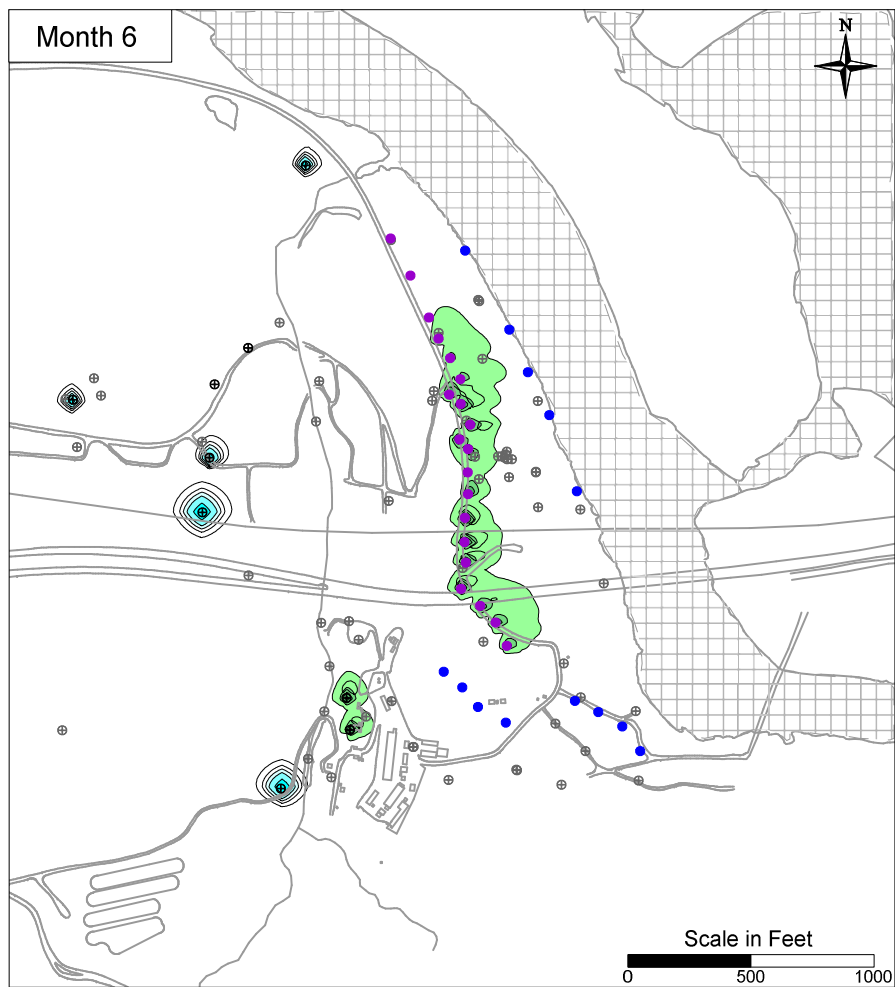
FIGURE
B-32



- LEGEND**
- IRZ WELLS
 - ⊕ UPGRADIENT INJECTION WELLS
 - EXTRACTION WELLS
 - ⊕ MONITORING WELLS



- LEGEND**
- IRZ WELLS
 - ⊕ UPGRADIENT INJECTION WELLS
 - EXTRACTION WELLS
 - ⊕ MONITORING WELLS

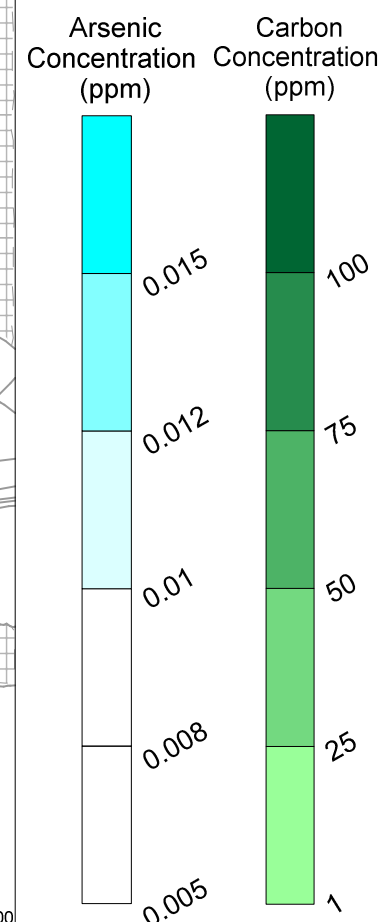
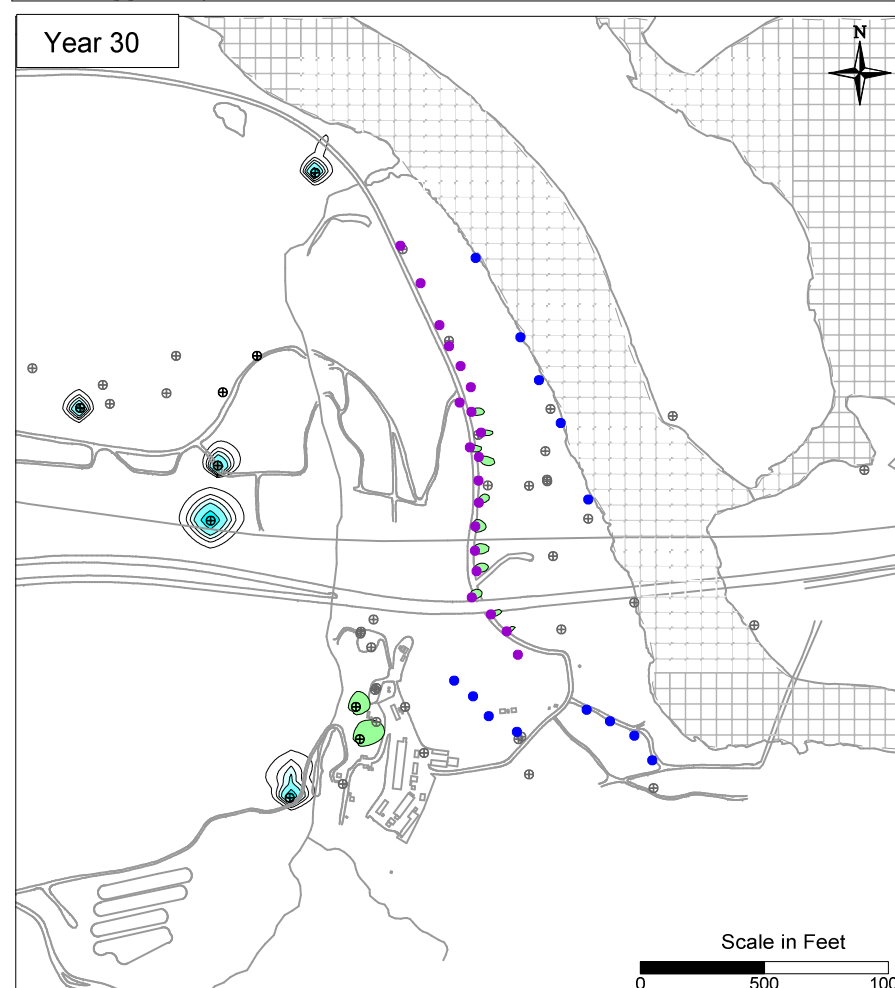
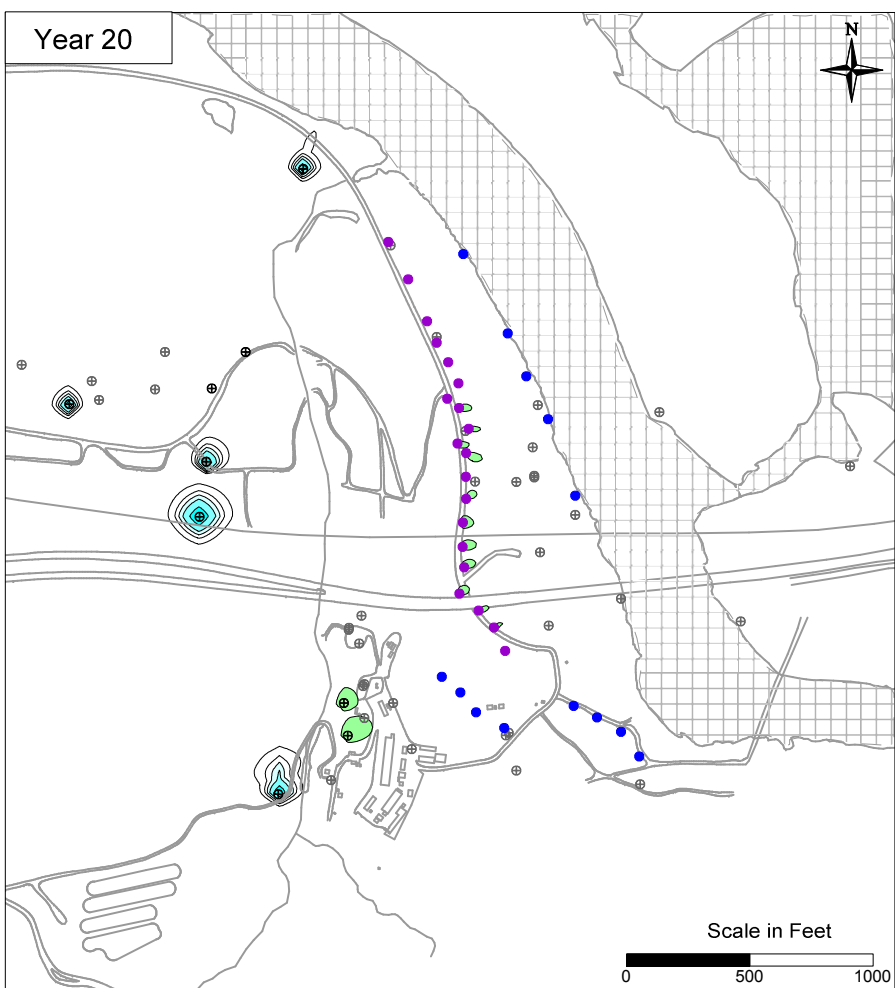
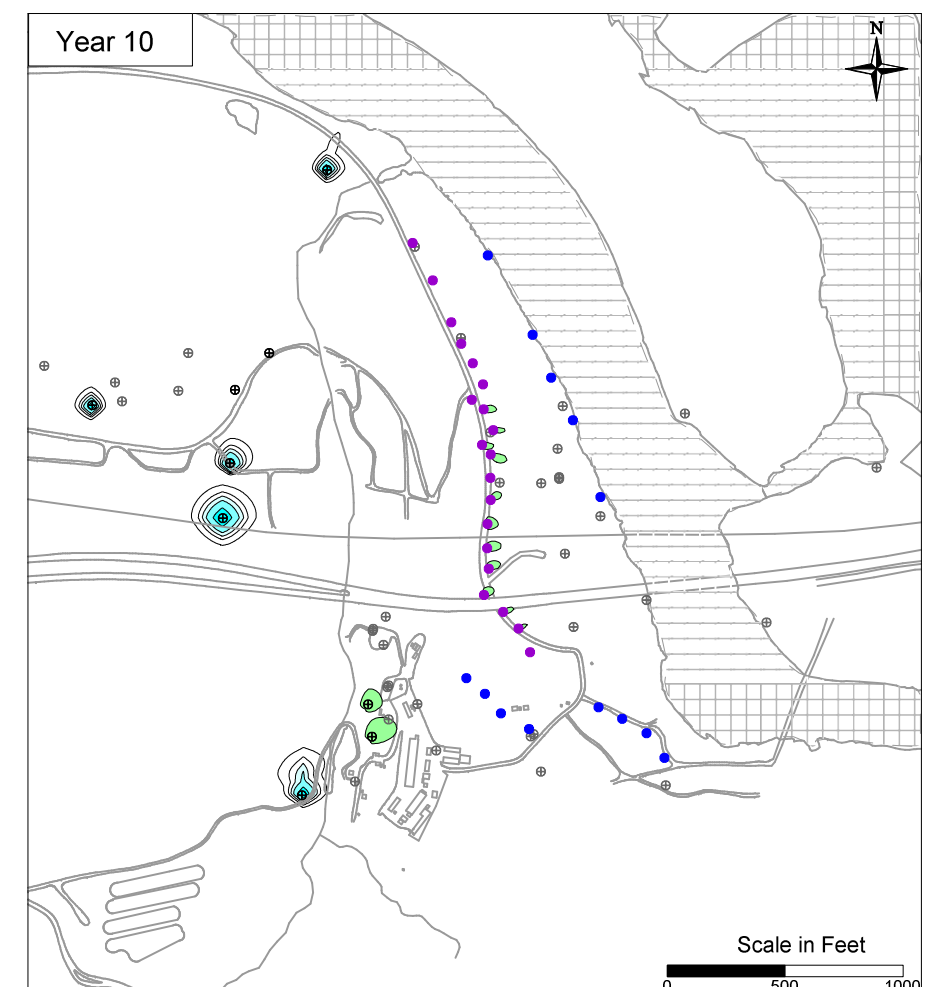
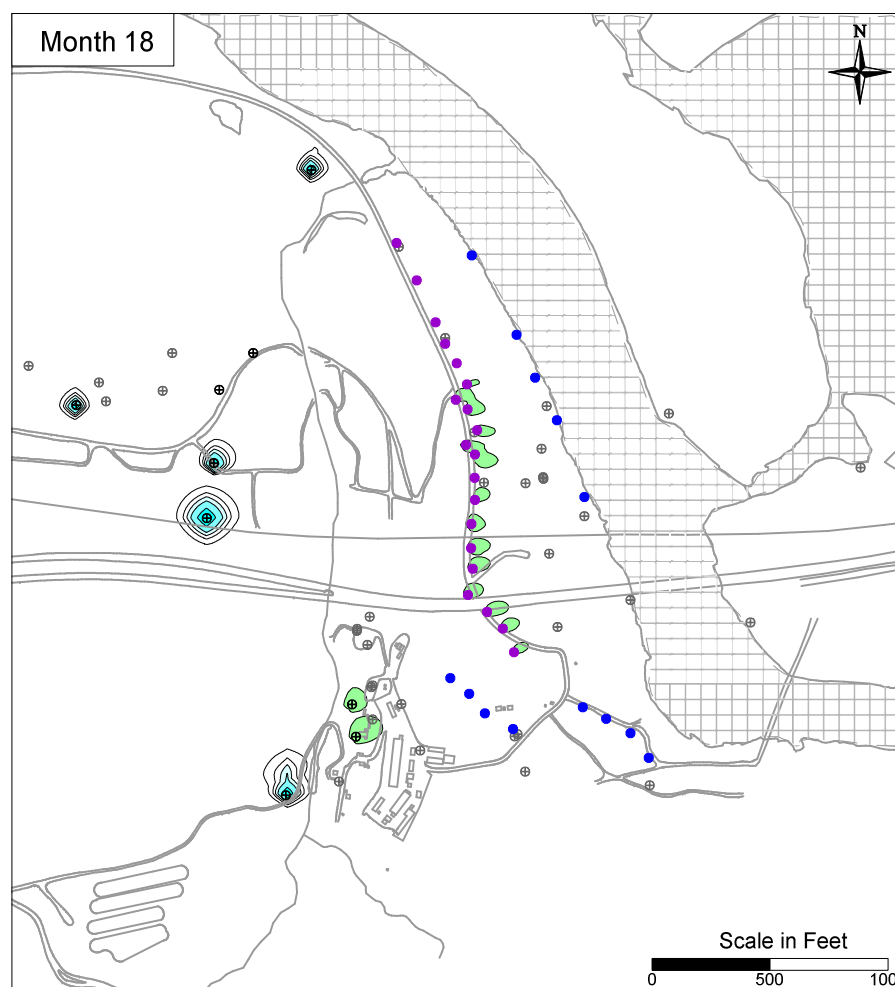
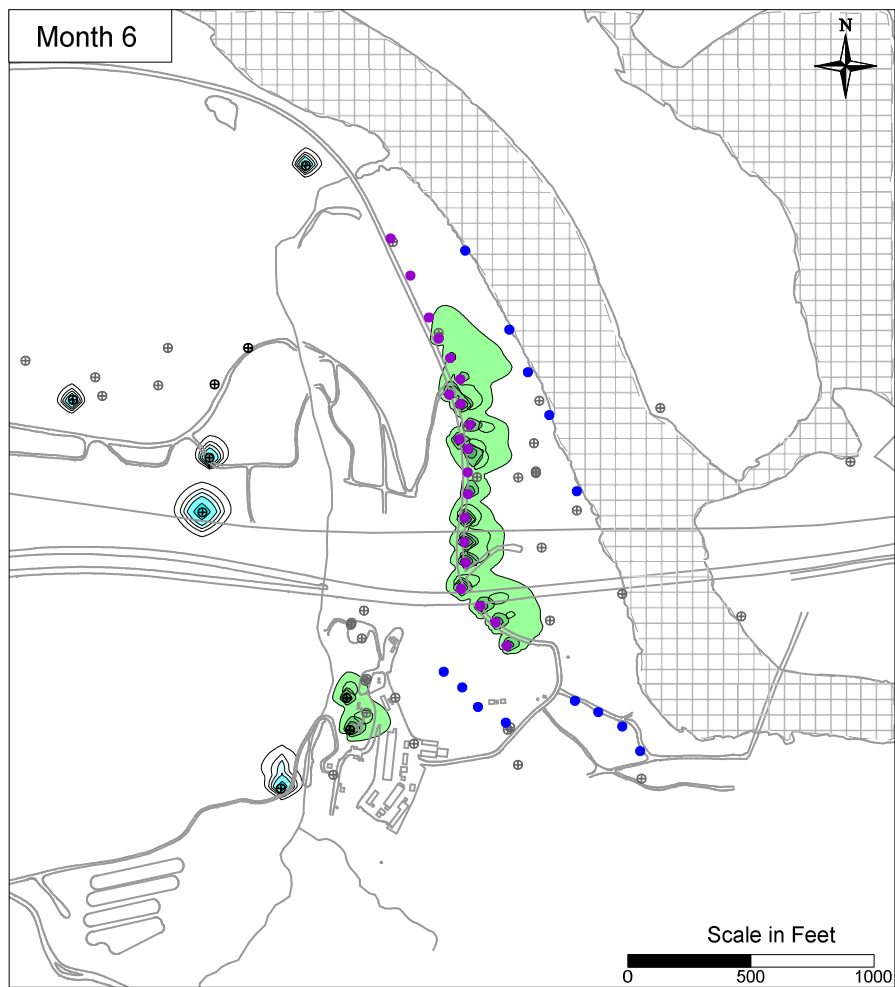


- LEGEND**
- IRZ WELLS
 - ⊕ UPGRADIENT INJECTION WELLS
 - EXTRACTION WELLS
 - ⊕ MONITORING WELLS

PG&E
TOPOCK COMPRESSOR STATION
NEEDLES, CALIFORNIA
MODELING APPENDIX

**SIMULATED ARSENIC TRANSPORT
RESULTS IN MODEL LAYER 1**

ARCADIS



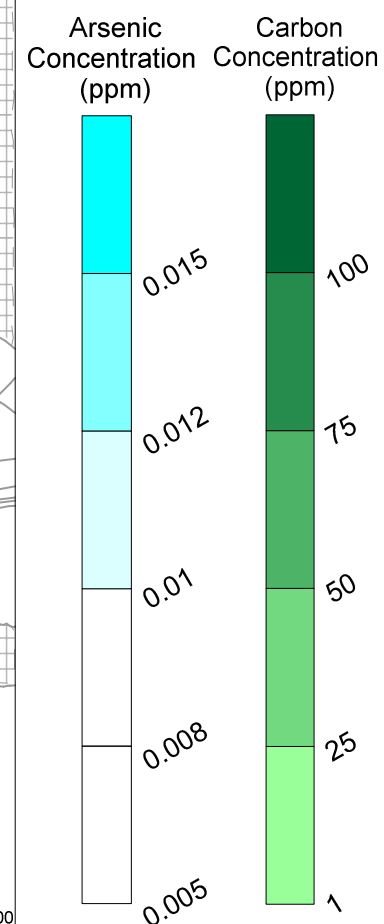
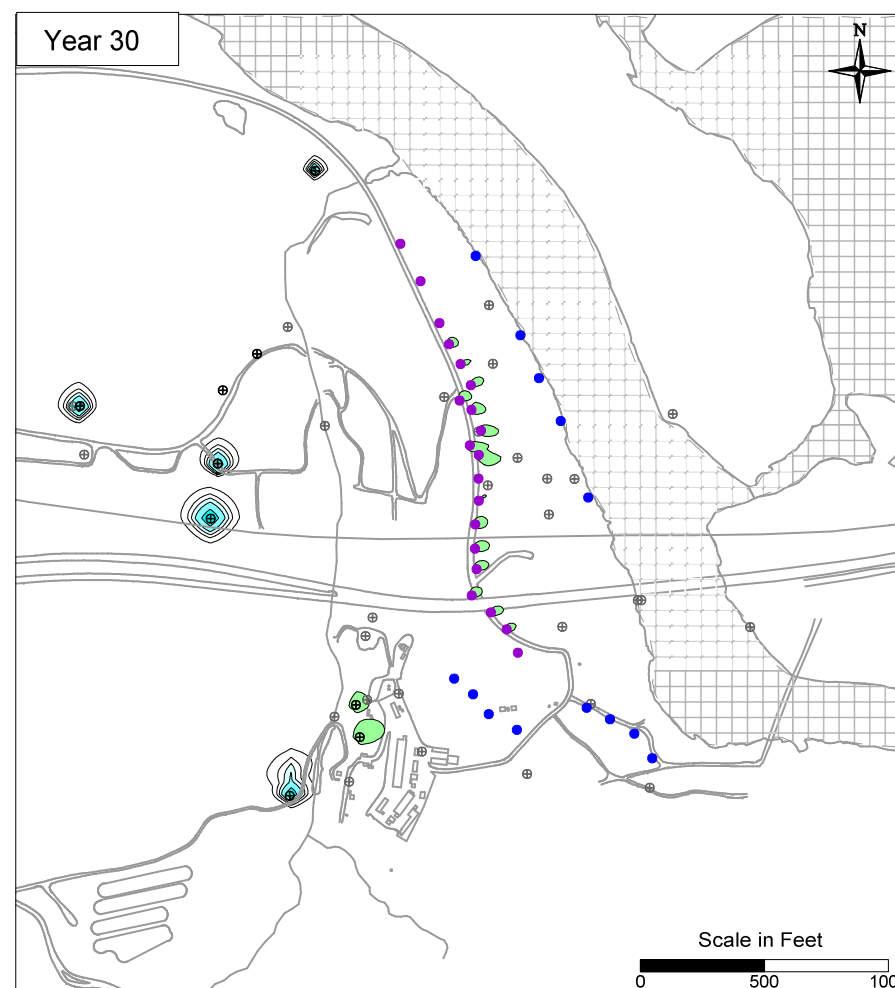
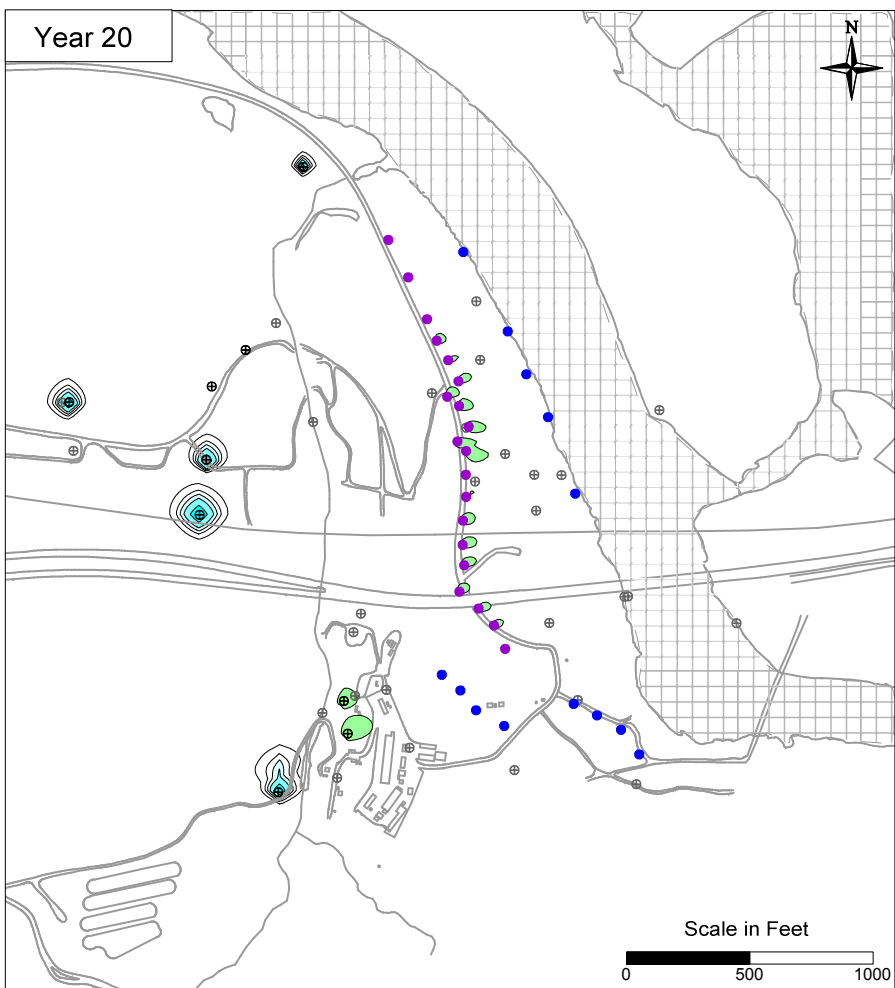
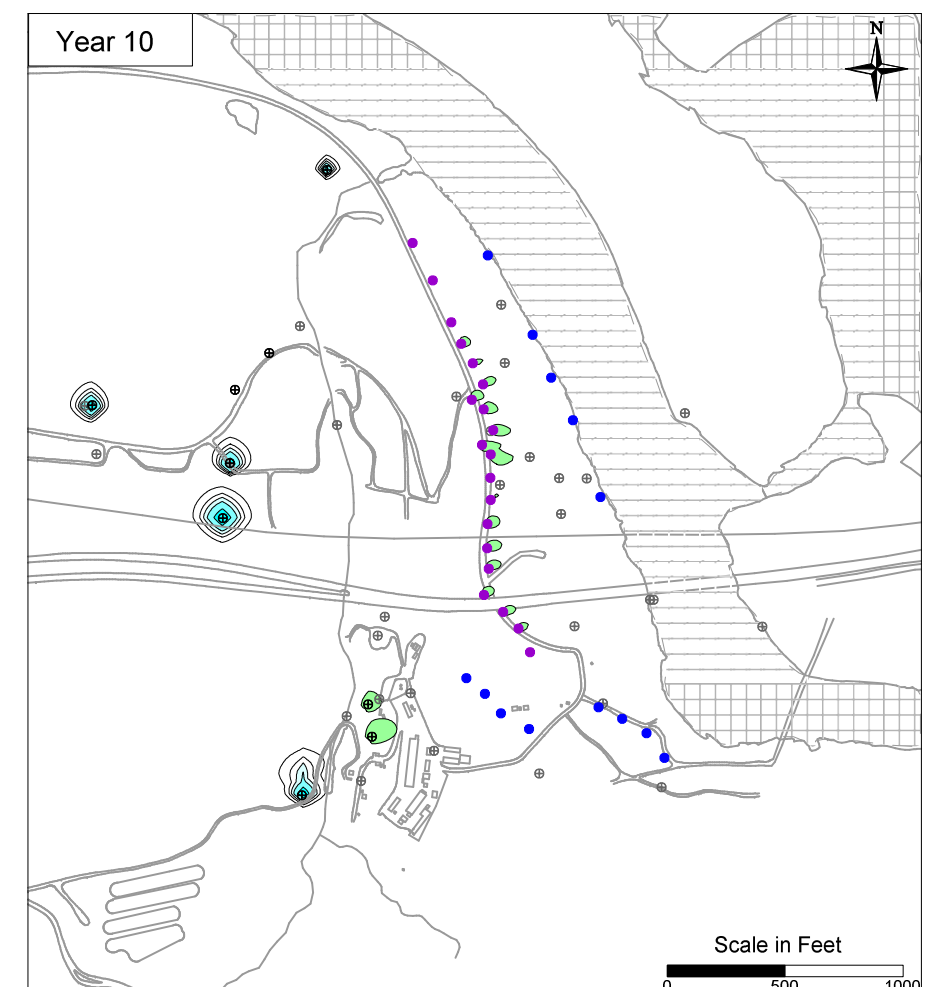
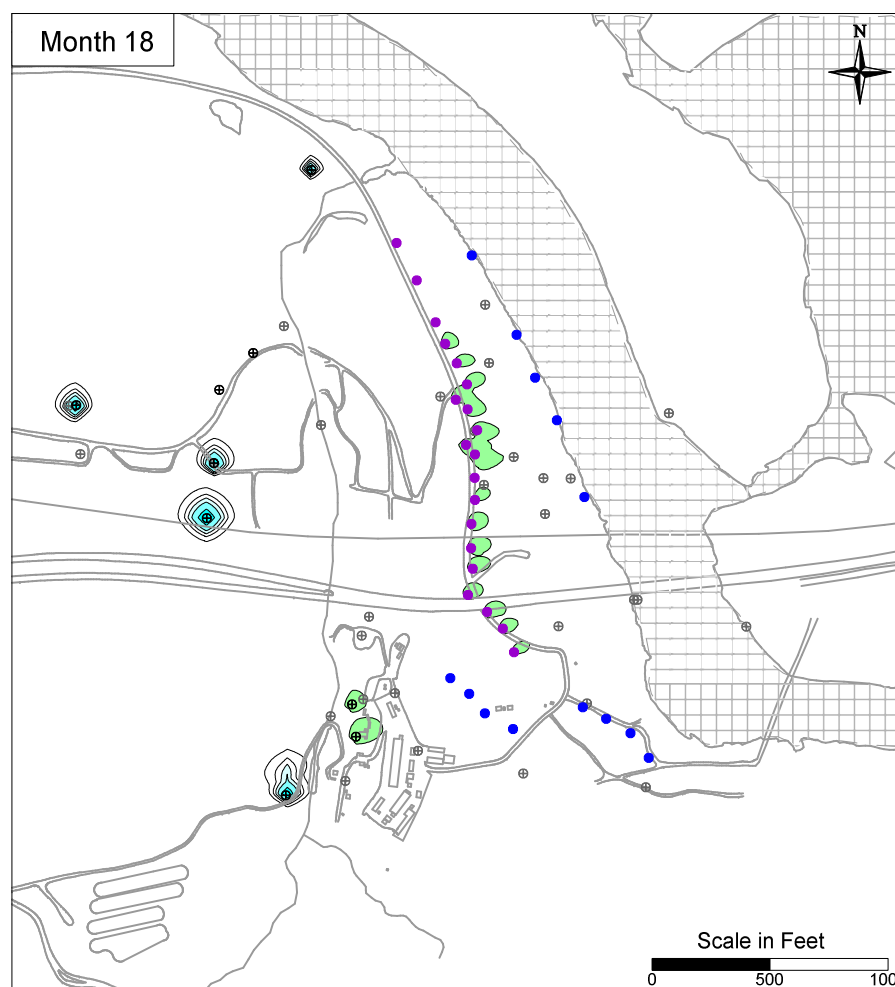
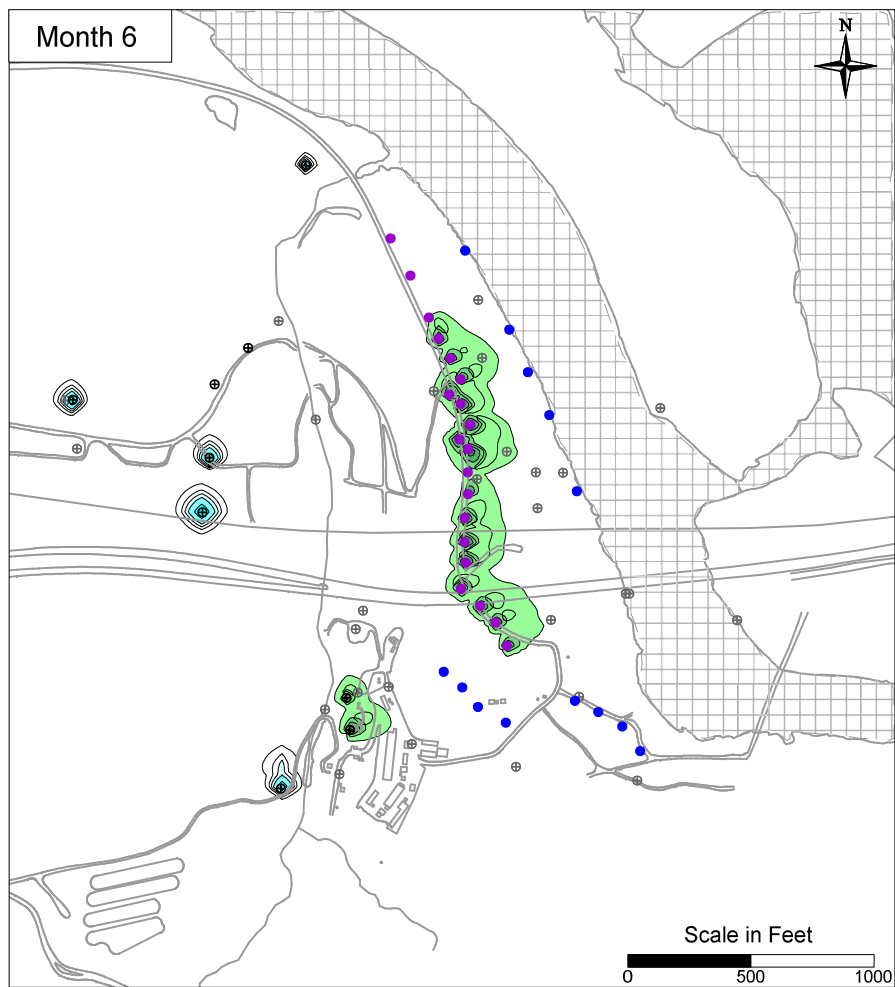
- LEGEND**
- IRZ WELLS
 - ⊕ UPGRADIENT INJECTION WELLS
 - EXTRACTION WELLS
 - ⊕ MONITORING WELLS

PG&E
TOPOCK COMPRESSOR STATION
NEEDLES, CALIFORNIA
MODELING APPENDIX

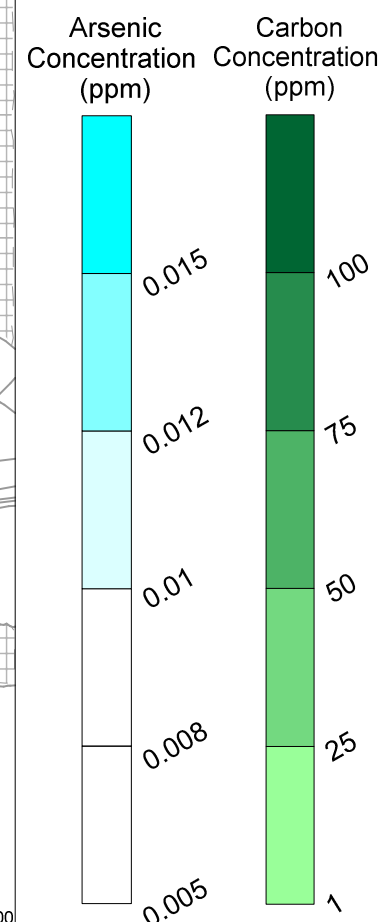
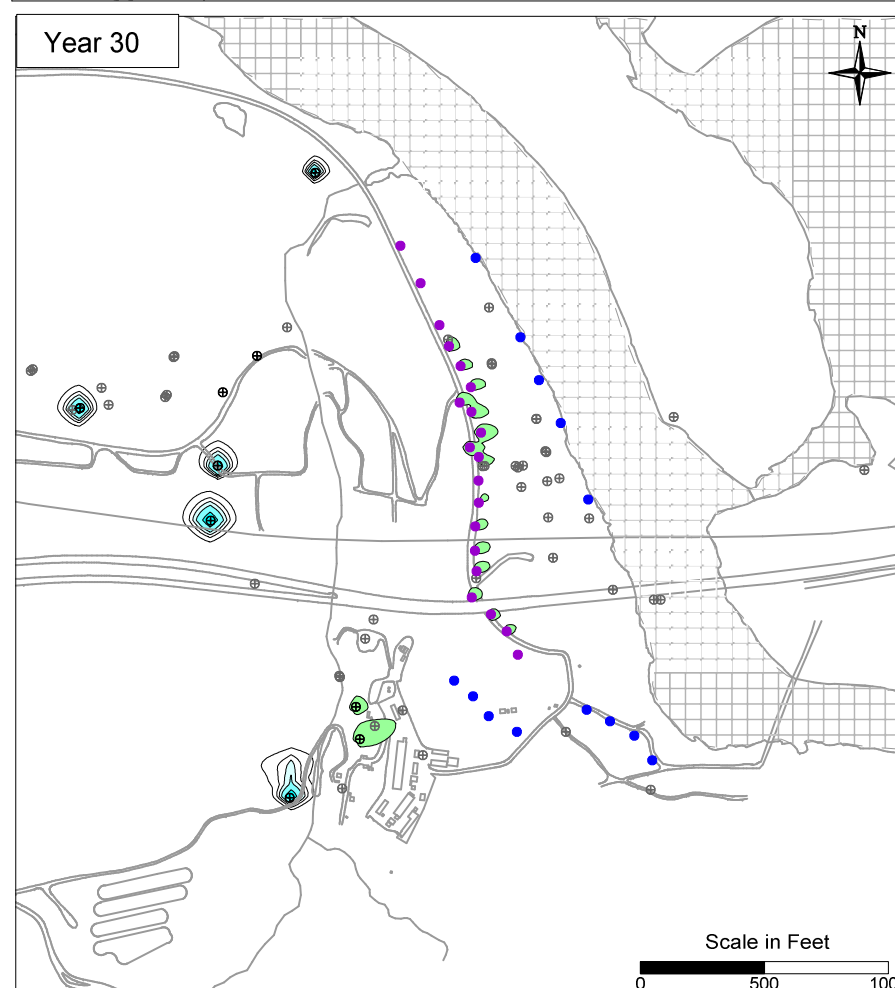
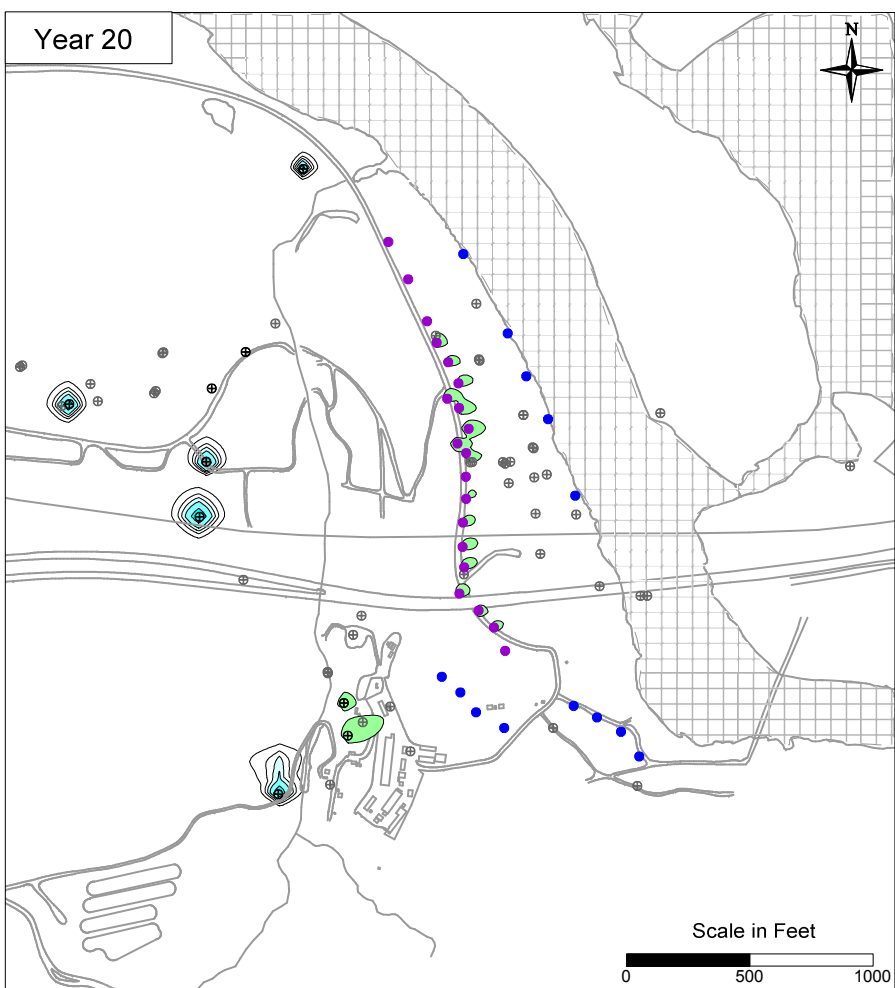
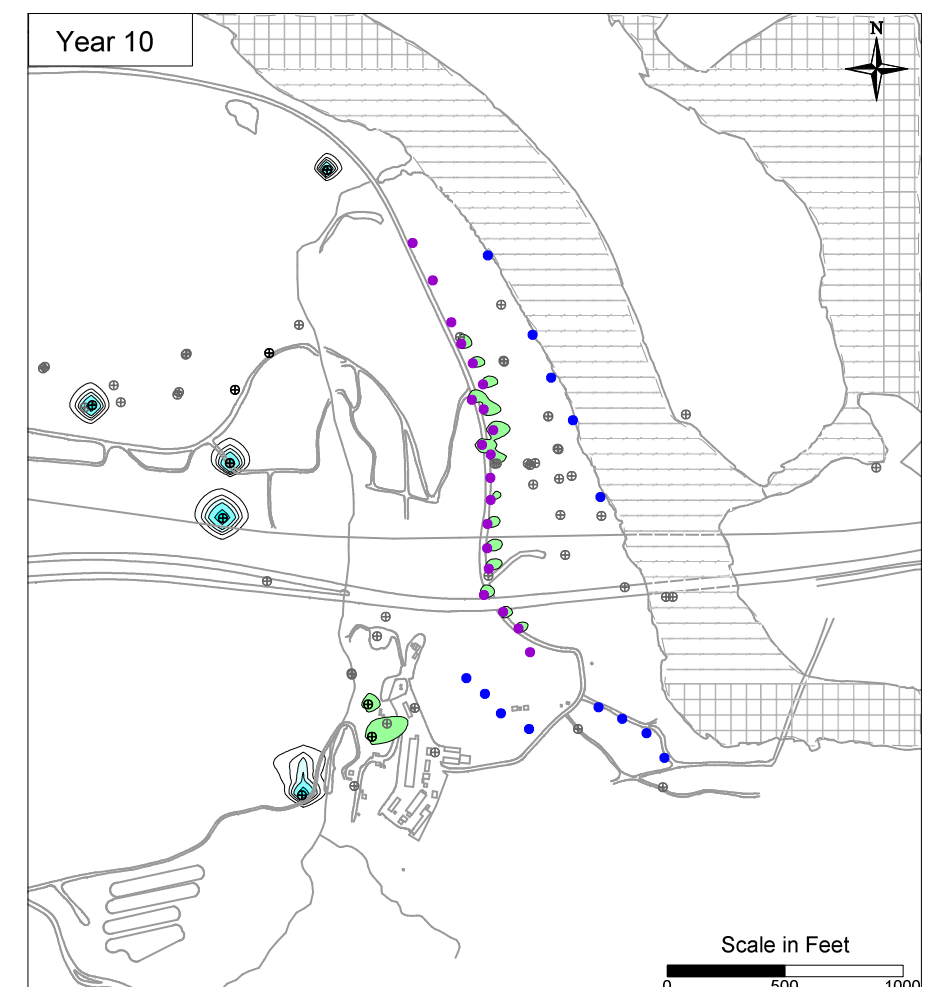
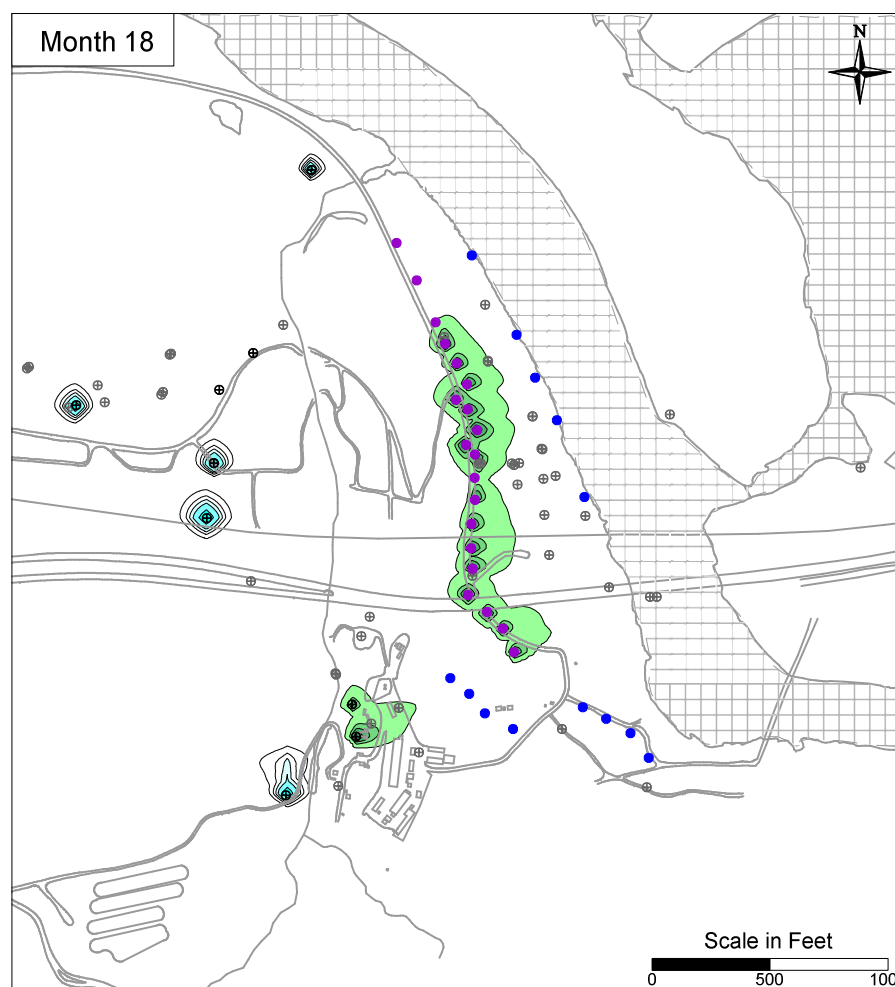
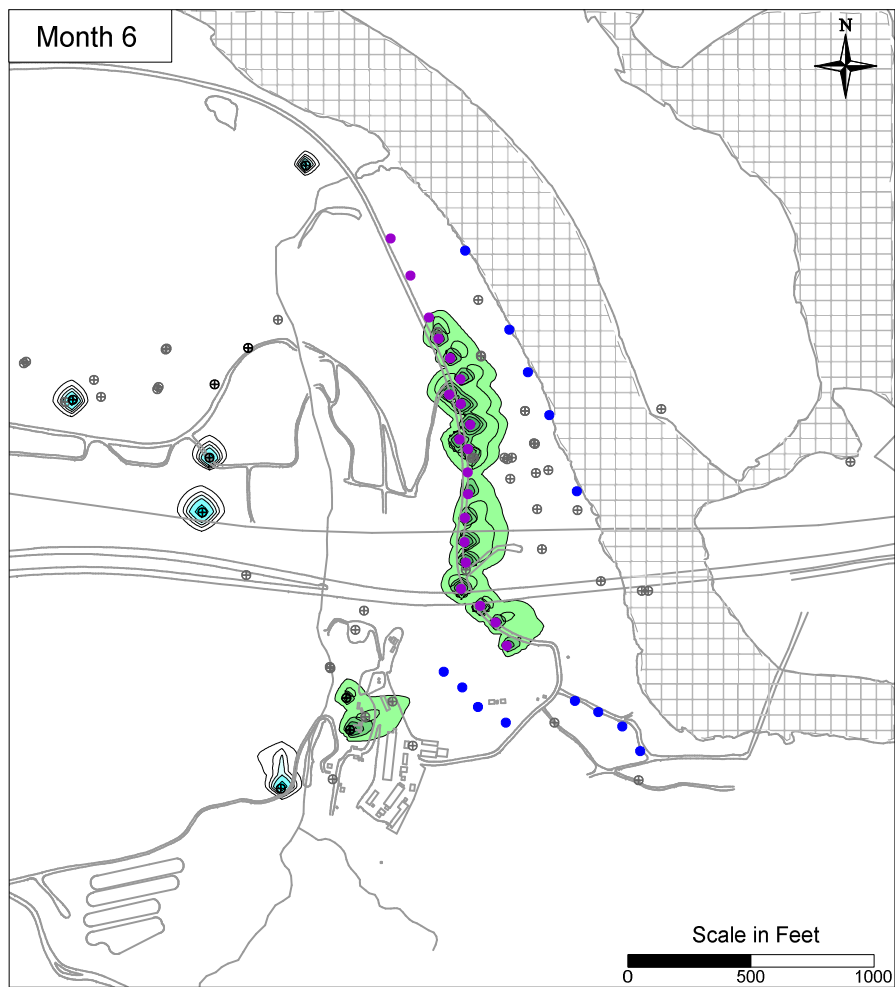
**SIMULATED ARSENIC TRANSPORT
RESULTS IN MODEL LAYER 2**

ARCADIS

FIGURE
B-36



- LEGEND**
- IRZ WELLS
 - ⊕ UPGRADIENT INJECTION WELLS
 - EXTRACTION WELLS
 - ⊕ MONITORING WELLS

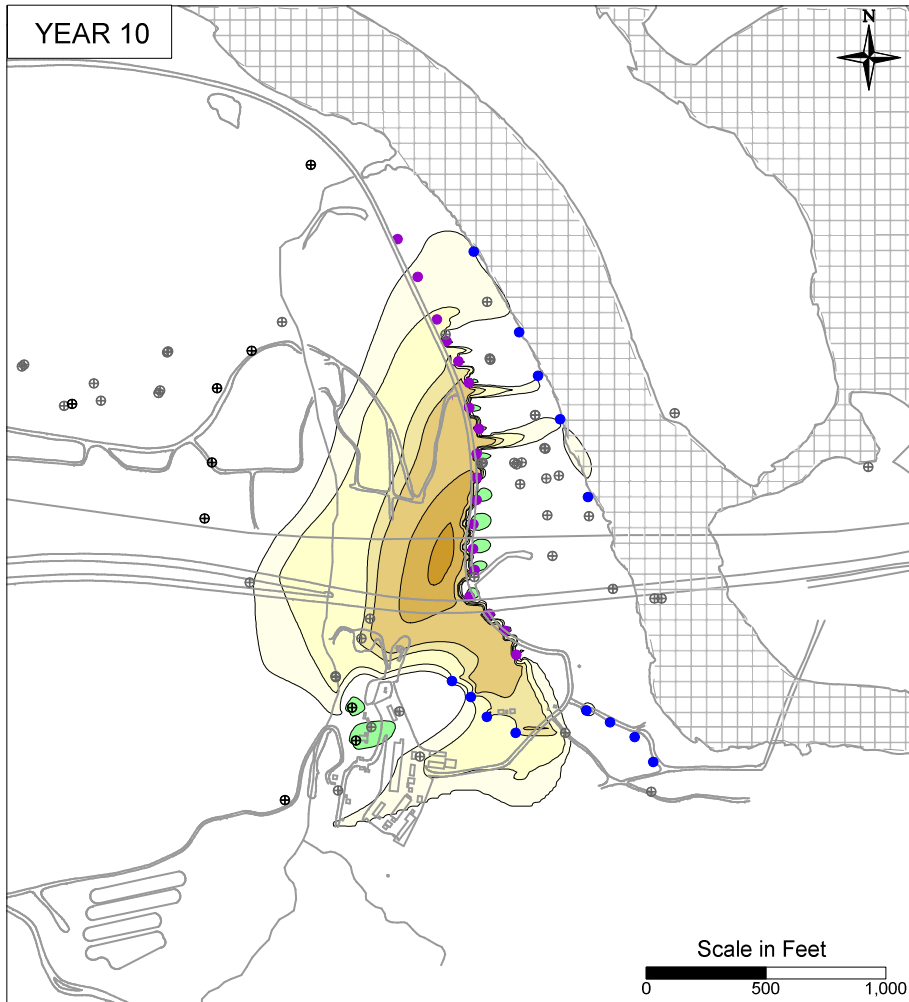


- LEGEND**
- IRZ WELLS
 - ⊕ UPGRADIENT INJECTION WELLS
 - EXTRACTION WELLS
 - ⊕ MONITORING WELLS

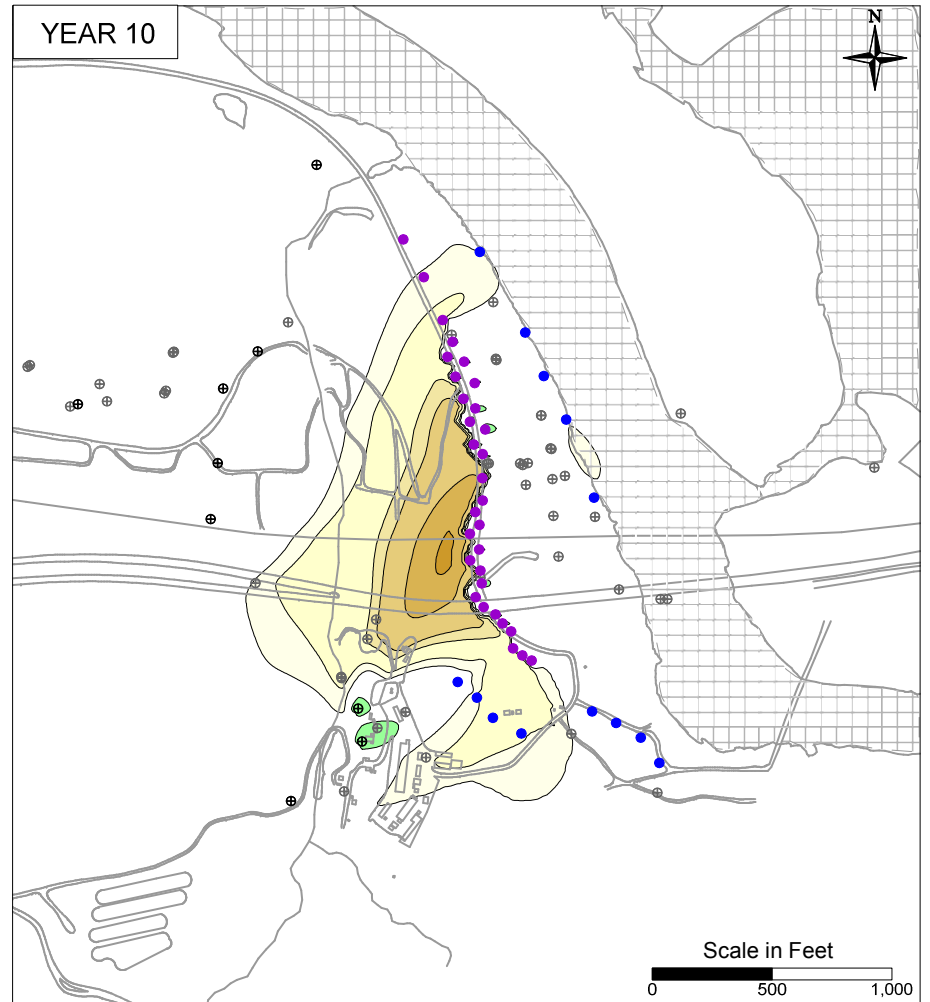
PG&E
TOPOCK COMPRESSOR STATION
NEEDLES, CALIFORNIA
MODELING APPENDIX

SIMULATED ARSENIC TRANSPORT
RESULTS IN MODEL LAYER 4

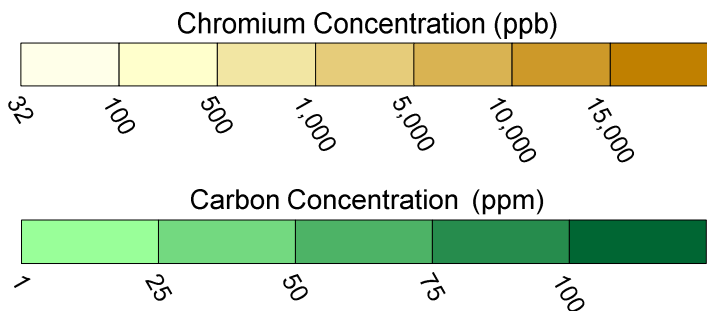
FIGURE
B-38



Initial Run: 150 ft NTH IRZ Well Spacing



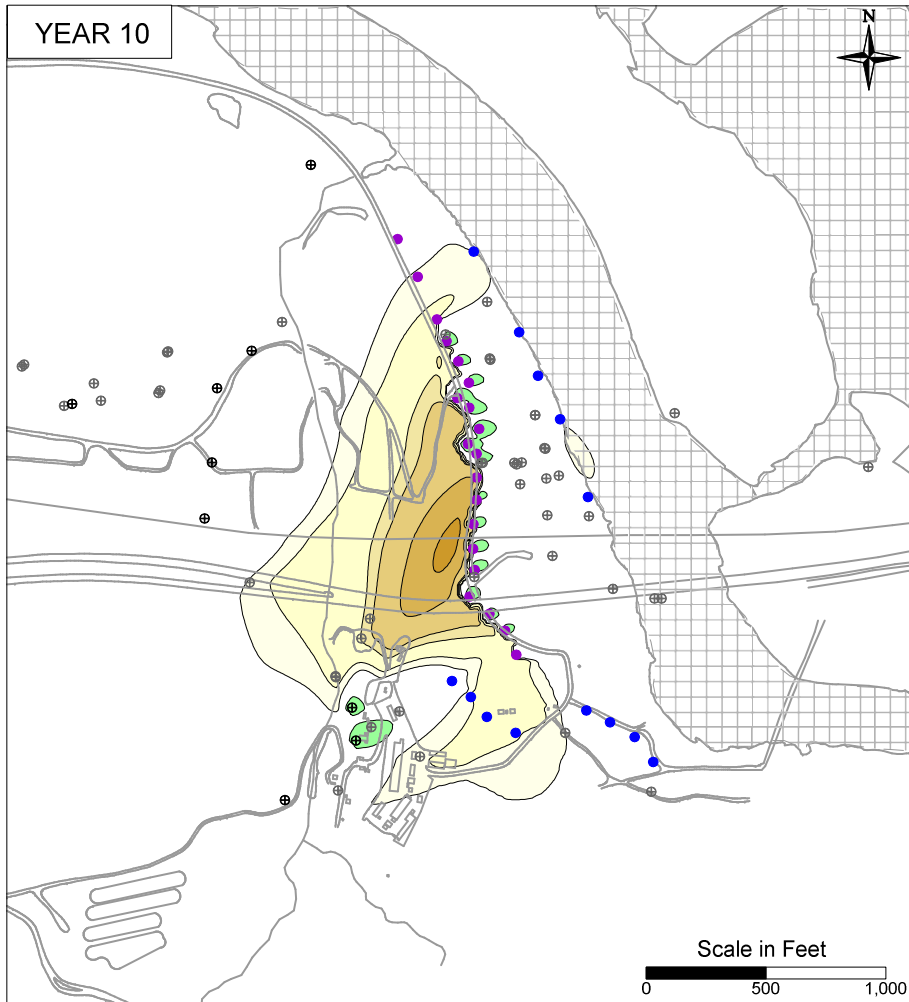
Decreased Spacing: 75 ft NTH IRZ Well Spacing



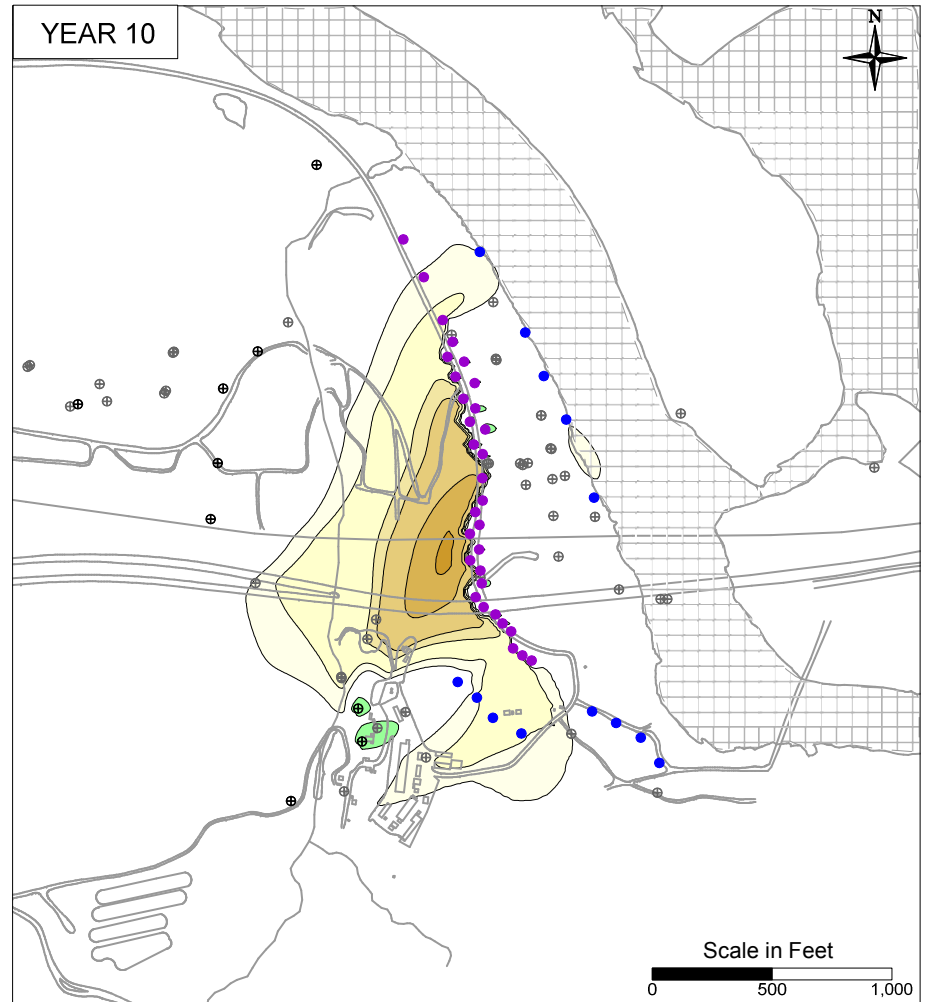
LEGEND

- IRZ WELLS
- ⊕ UPGRADE INJECTION WELLS
- EXTRACTION WELLS
- ⊕ MONITORING WELLS

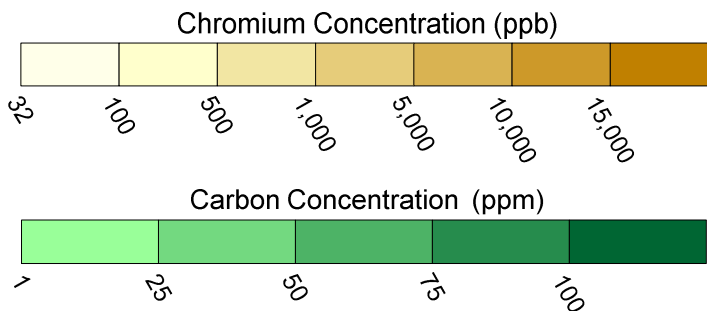
PG&E TOPOCK COMPRESSOR STATION NEEDLES, CALIFORNIA MODELING APPENDIX	
NTH IRZ WELL SPACING SENSITIVITY: INITIAL 150 FT AND 75 FT SPACING WITH SIMULATED HEXAVALENT CHROMIUM TRANSPORT RESULTS IN MODEL LAYER 4	
	FIGURE B-39



Base: 150 ft NTH IRZ Well Spacing with Filled Gaps



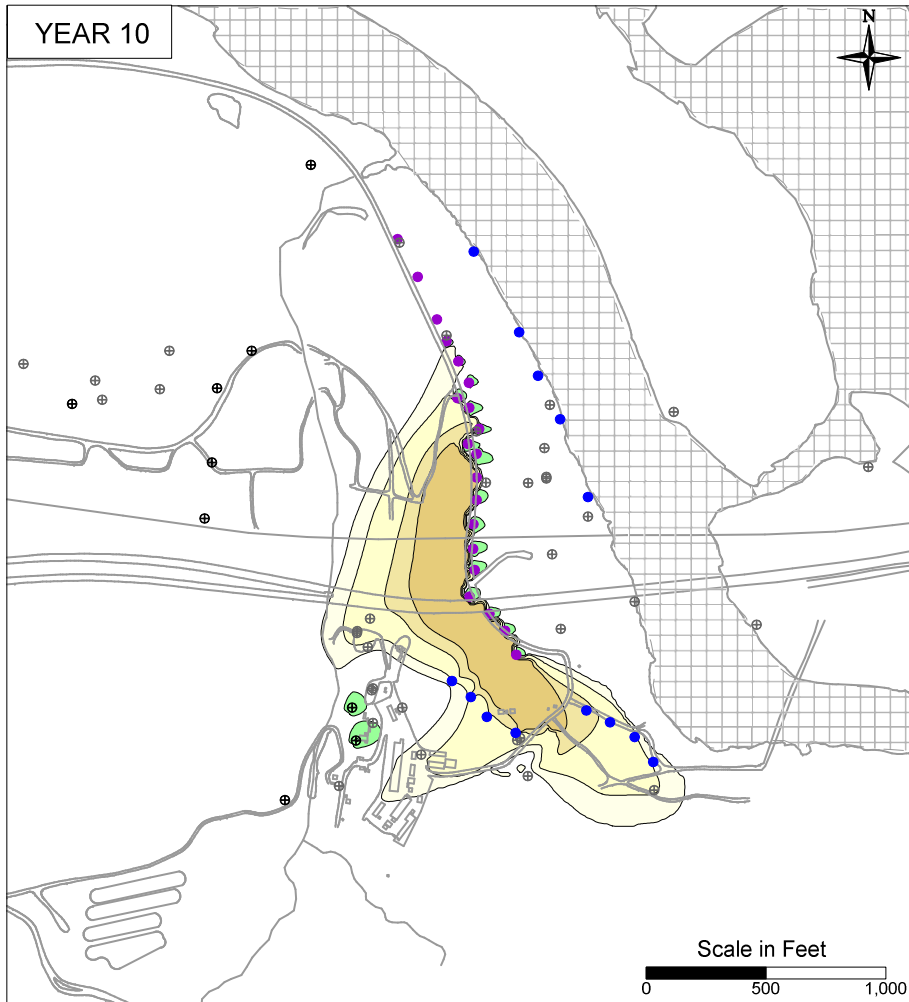
Decreased Spacing: 75 ft NTH IRZ Well Spacing



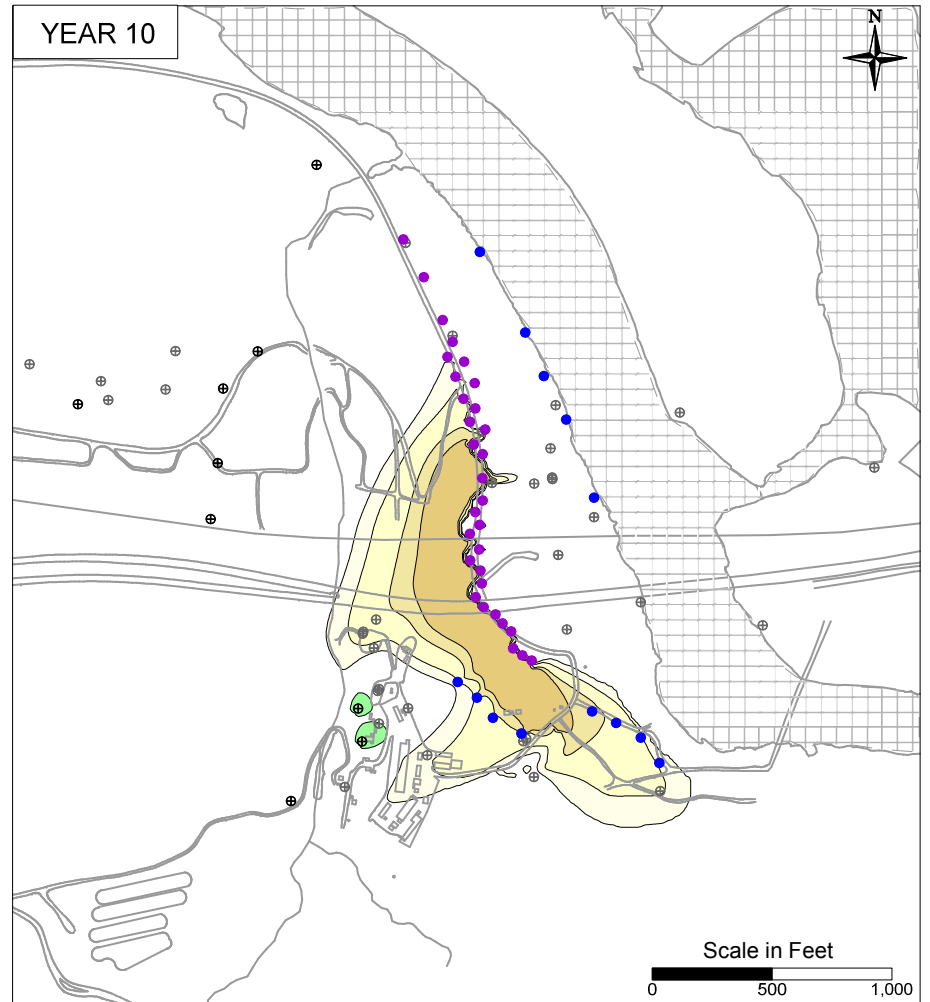
LEGEND

- IRZ WELLS
- ⊕ UPGRADE INJECTION WELLS
- EXTRACTION WELLS
- ⊕ MONITORING WELLS

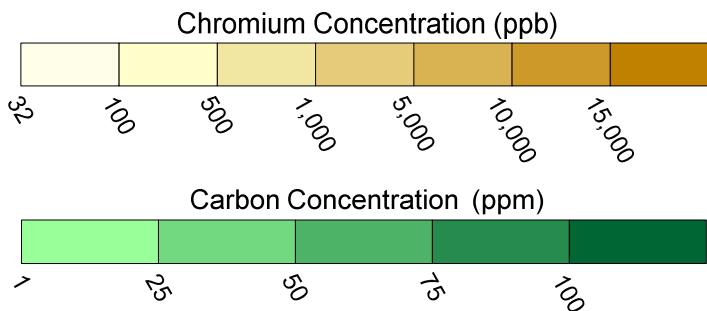
PG&E TOPOCK COMPRESSOR STATION NEEDLES, CALIFORNIA MODELING APPENDIX	
NTH IRZ WELL SPACING SENSITIVITY: REVISED 150 FT AND 75 FT SPACING WITH SIMULATED HEXAVALENT CHROMIUM TRANSPORT RESULTS IN MODEL LAYER 4	
	FIGURE B-40



Base: 150 ft NTH IRZ Well Spacing with Filled Gaps



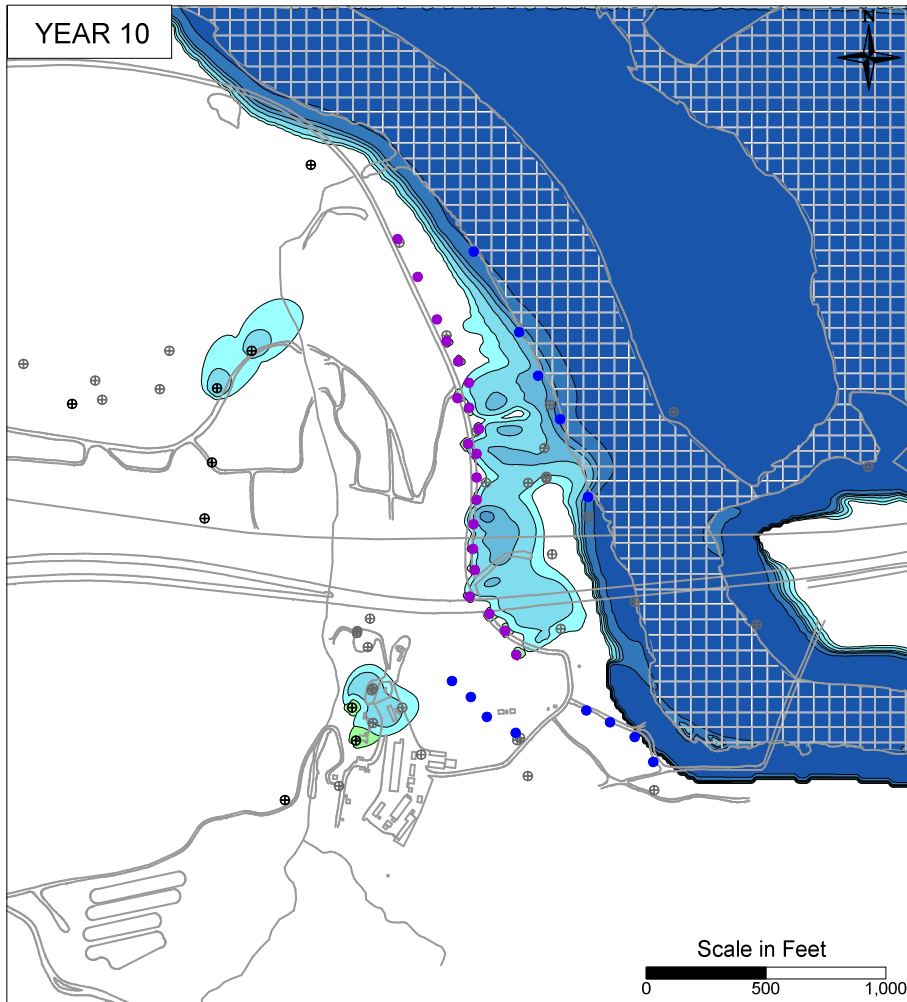
Decreased Spacing: 75 ft NTH IRZ Well Spacing



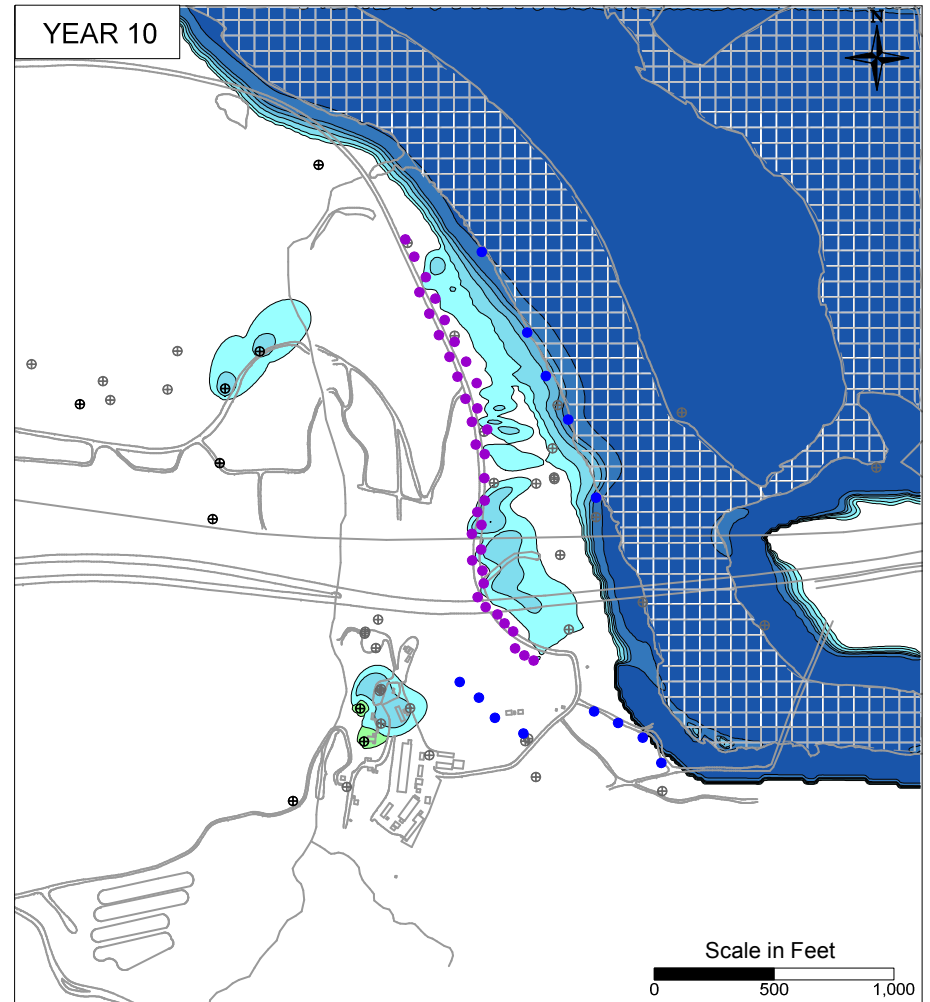
LEGEND

- IRZ WELLS
- ⊕ UPGRADIENT INJECTION WELLS
- EXTRACTION WELLS
- ⊕ MONITORING WELLS

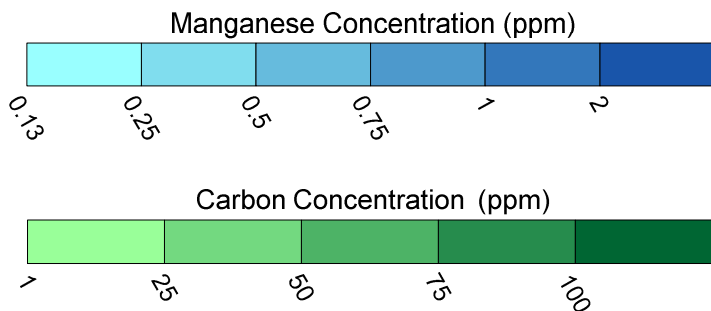
PG&E TOPOCK COMPRESSOR STATION NEEDLES, CALIFORNIA MODELING APPENDIX	
NTH IRZ WELL SPACING SENSITIVITY: REVISED 150 FT AND 75 FT SPACING WITH SIMULATED HEXAVALENT CHROMIUM TRANSPORT RESULTS IN MODEL LAYER 2	
	FIGURE B-41



Base: 150 ft NTH IRZ Well Spacing with Filled Gaps



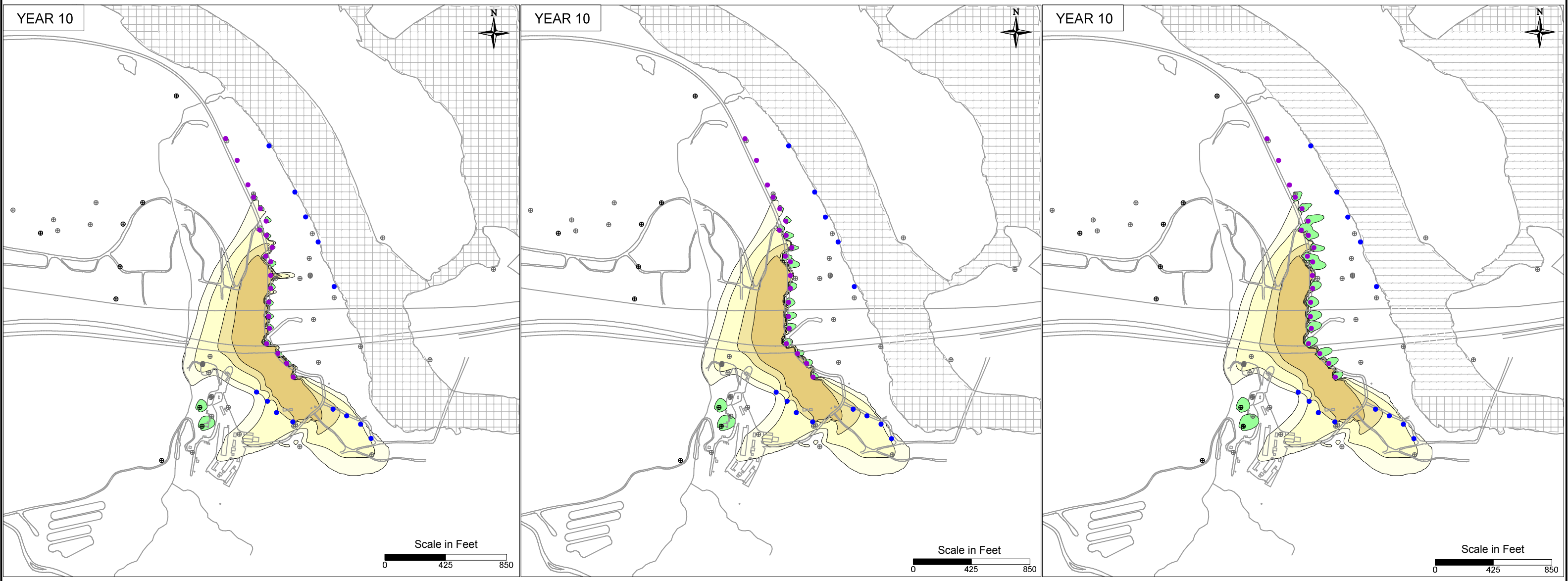
Decreased Spacing: 75 ft NTH IRZ Well Spacing



LEGEND

- IRZ WELLS
- ⊕ UPGRADIENT INJECTION WELLS
- EXTRACTION WELLS
- ⊕ MONITORING WELLS

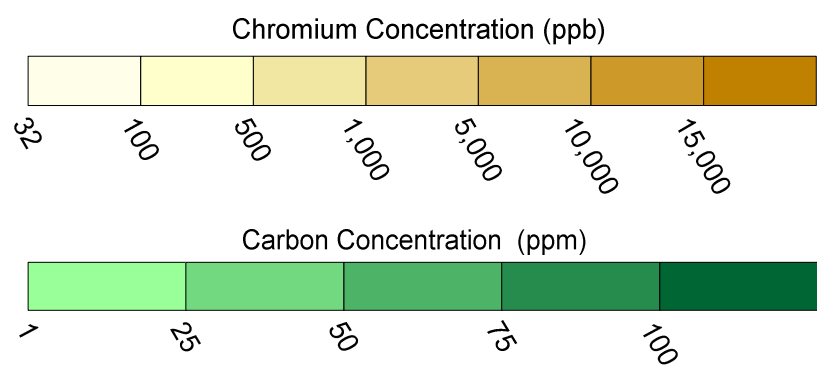
PG&E TOPOCK COMPRESSOR STATION NEEDLES, CALIFORNIA MODELING APPENDIX	
NTH IRZ WELL SPACING SENSITIVITY: REVISED 150 FT AND 75 FT SPACING WITH SIMULATED MANGANESE TRANSPORT RESULTS IN MODEL LAYER 2	
	FIGURE B-42



LOW TOC = 50 ppm

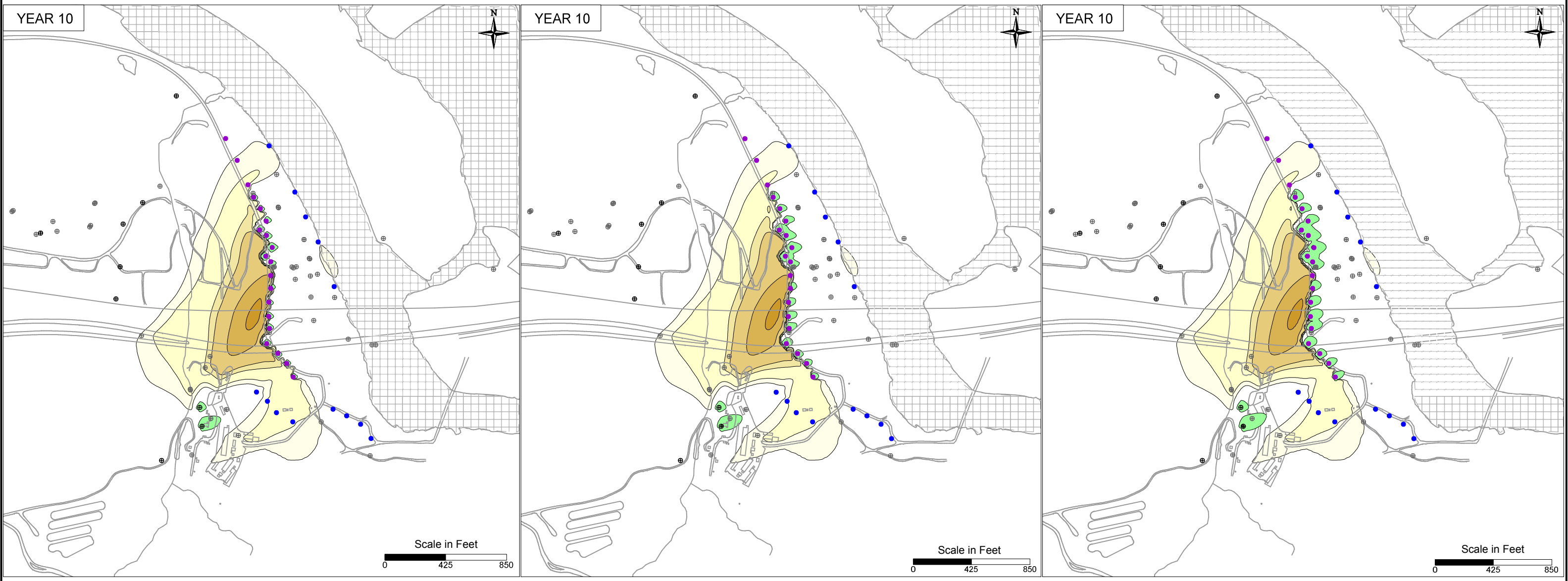
BASE TOC = 100 ppm

HIGH TOC = 150 ppm



- LEGEND**
- IRZ WELLS
 - ⊕ UPGRADIENT INJECTION WELLS
 - EXTRACTION WELLS
 - ⊕ MONITORING WELLS

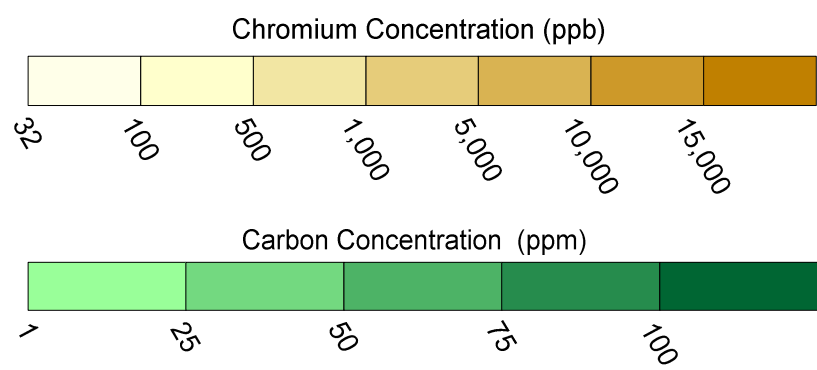
PG&E TOPOCK COMPRESSOR STATION NEEDLES, CALIFORNIA MODELING APPENDIX	
TOC CONCENTRATION SENSITIVITY: SIMULATED HEXAVALENT CHROMIUM TRANSPORT RESULTS IN MODEL LAYER 2	
	FIGURE B-43



LOW TOC = 50 ppm

BASE TOC = 100 ppm

HIGH TOC = 150 ppm



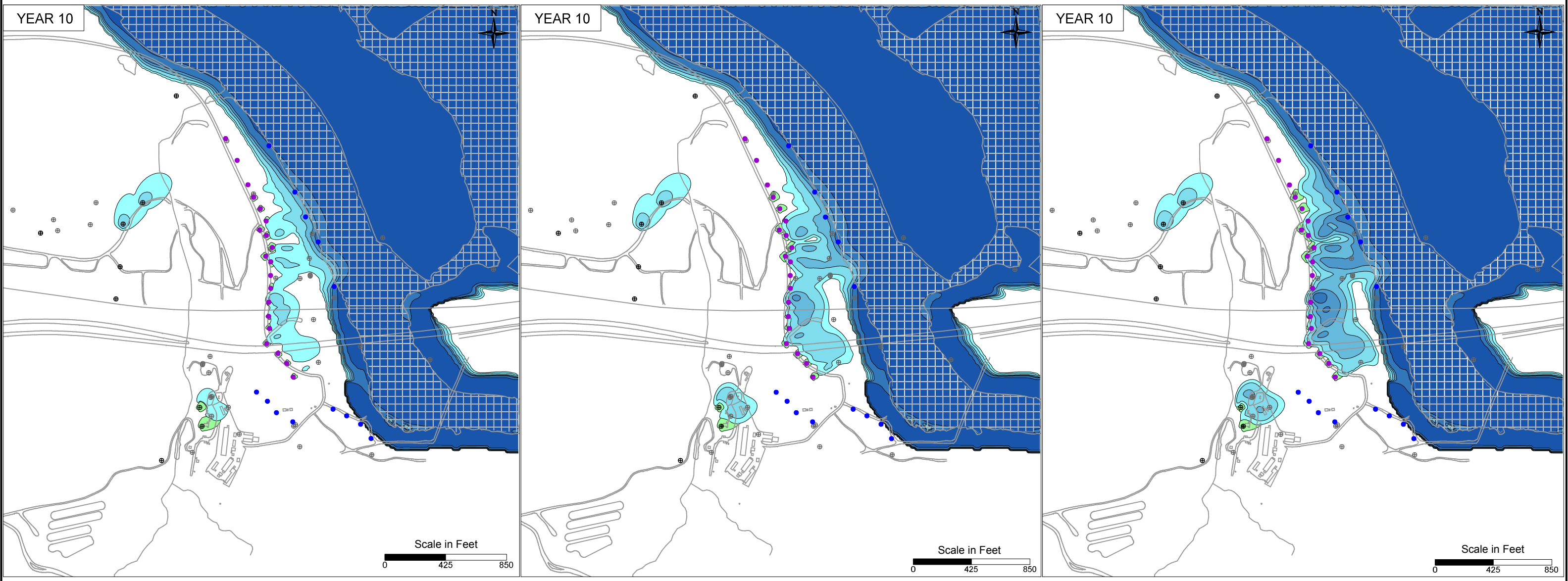
- LEGEND**
- IRZ WELLS
 - ⊕ UPGRADIENT INJECTION WELLS
 - EXTRACTION WELLS
 - ⊕ MONITORING WELLS

PG&E
TOPOCK COMPRESSOR STATION
NEEDLES, CALIFORNIA
MODELING APPENDIX

**TOC CONCENTRATION SENSITIVITY:
SIMULATED HEXAVALENT CHROMIUM
TRANSPORT RESULTS IN MODEL LAYER 4**



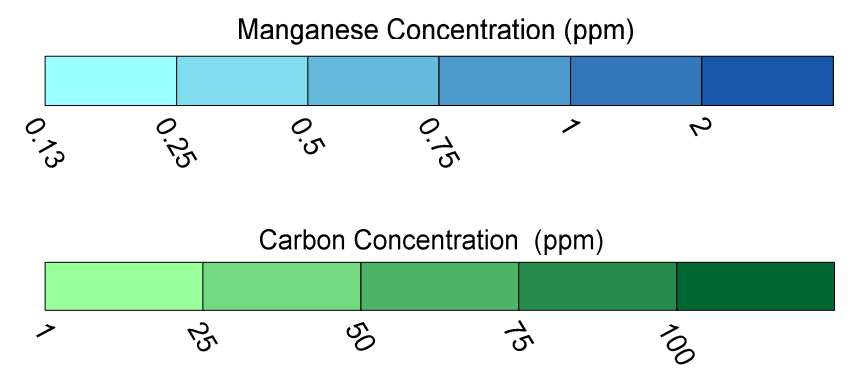
FIGURE
B-44



LOW TOC = 50 ppm

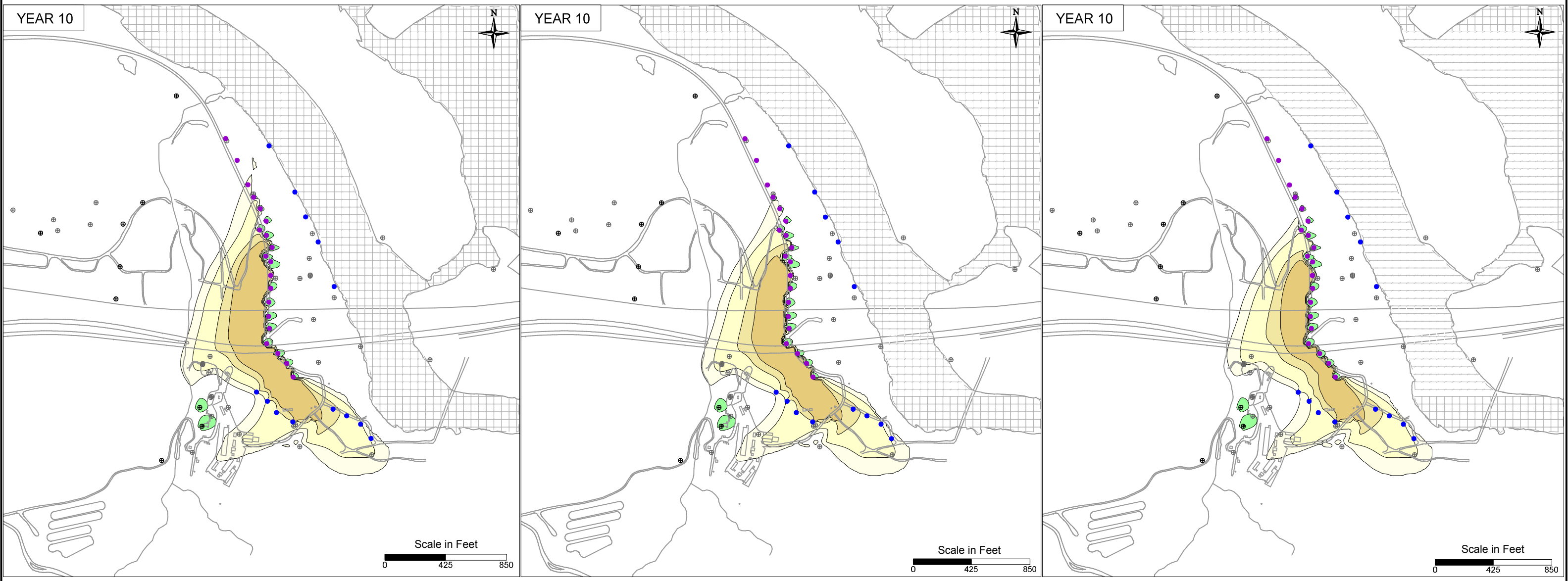
BASE TOC = 100 ppm

HIGH TOC = 150 ppm



- LEGEND**
- IRZ WELLS
 - ⊕ UPGRADIENT INJECTION WELLS
 - EXTRACTION WELLS
 - ⊕ MONITORING WELLS

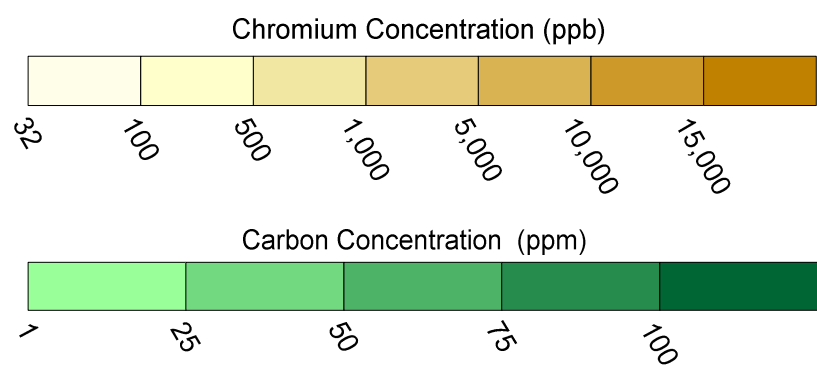
PG&E TOPOCK COMPRESSOR STATION NEEDLES, CALIFORNIA MODELING APPENDIX	
TOC CONCENTRATION SENSITIVITY: SIMULATED MANGANESE TRANSPORT RESULTS IN MODEL LAYER 2	
	FIGURE B-45



Low Riverbank Extraction Rates = 0 gpm

Base Riverbank Extraction Rates = 150 gpm

High Riverbank Extraction Rates = 300 gpm



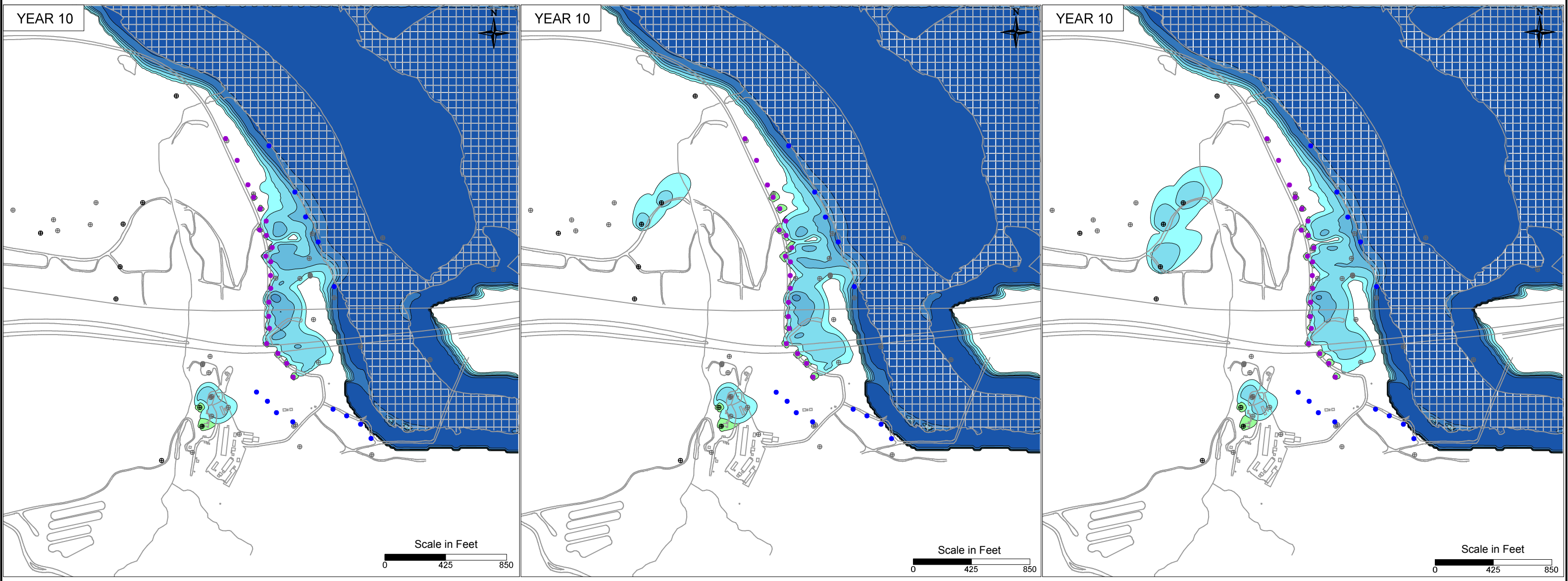
- LEGEND**
- IRZ WELLS
 - ⊕ UPGRADIENT INJECTION WELLS
 - EXTRACTION WELLS
 - ⊕ MONITORING WELLS

PG&E
 TOPOCK COMPRESSOR STATION
 NEEDLES, CALIFORNIA
 MODELING APPENDIX

RIVERBANK EXTRACTION RATE SENSITIVITY:
 SIMULATED HEXAVALENT CHROMIUM
 TRANSPORT RESULTS IN MODEL LAYER 2



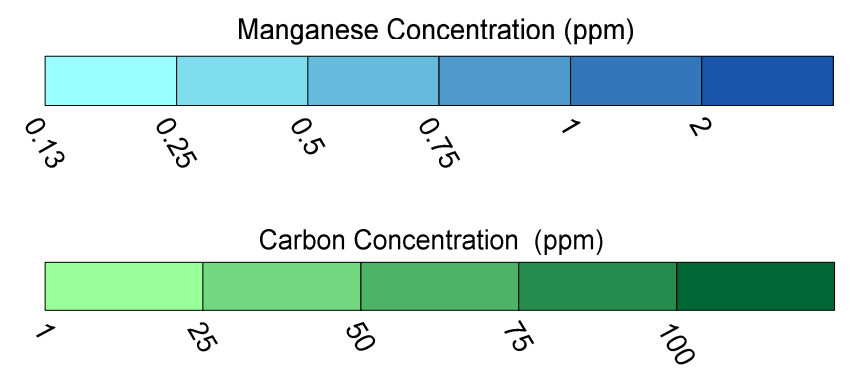
FIGURE
B-46



Low Riverbank Extraction Rates = 0 gpm

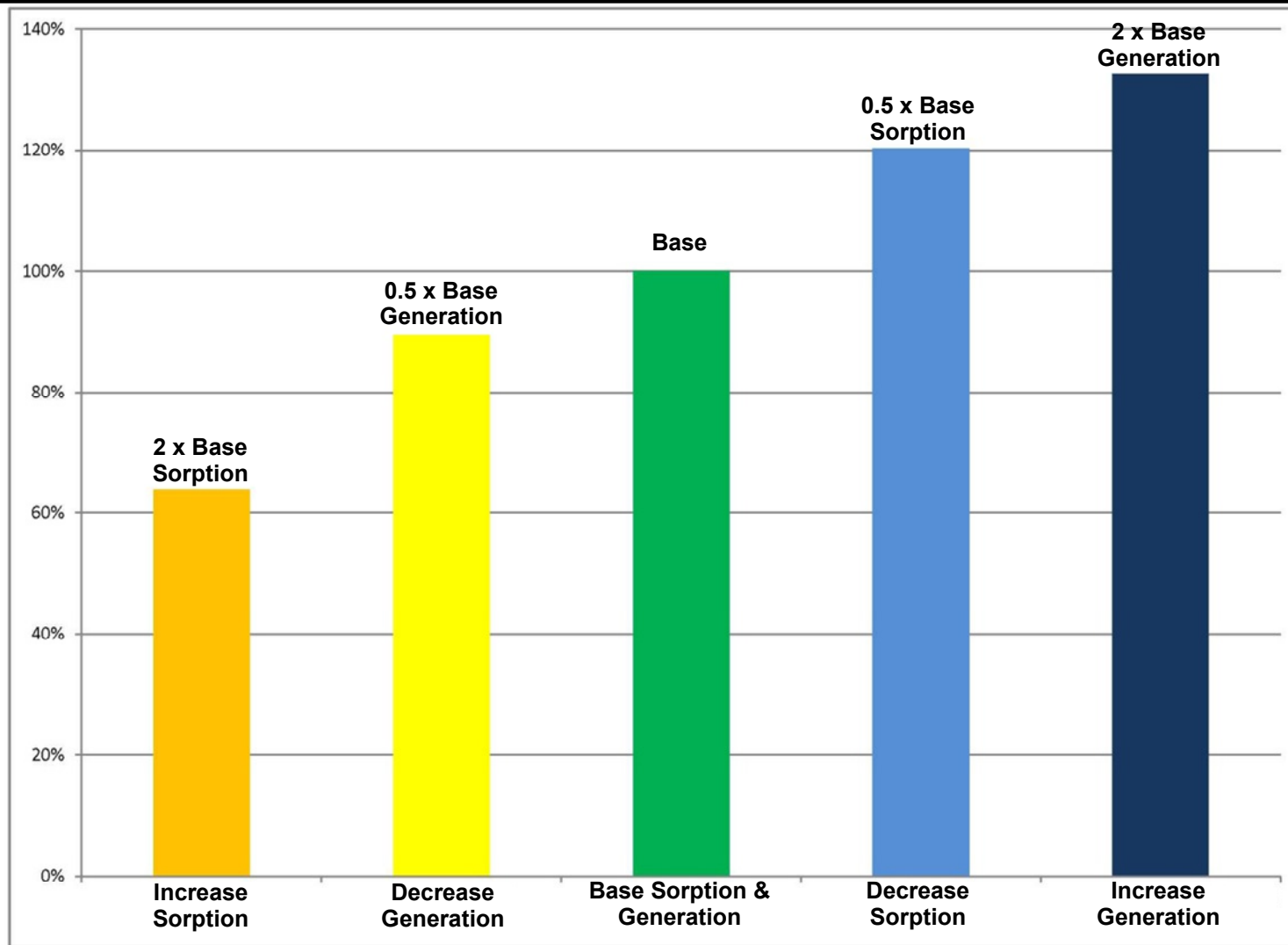
Base Riverbank Extraction Rates = 150 gpm

High Riverbank Extraction Rates = 300 gpm



- LEGEND**
- IRZ WELLS
 - ⊕ UPGRADIENT INJECTION WELLS
 - EXTRACTION WELLS
 - ⊕ MONITORING WELLS

PG&E TOPOCK COMPRESSOR STATION NEEDLES, CALIFORNIA MODELING APPENDIX	
RIVERBANK EXTRACTION RATE SENSITIVITY: SIMULATED MANGANESE TRANSPORT RESULTS IN MODEL LAYER 2	
	FIGURE B-47



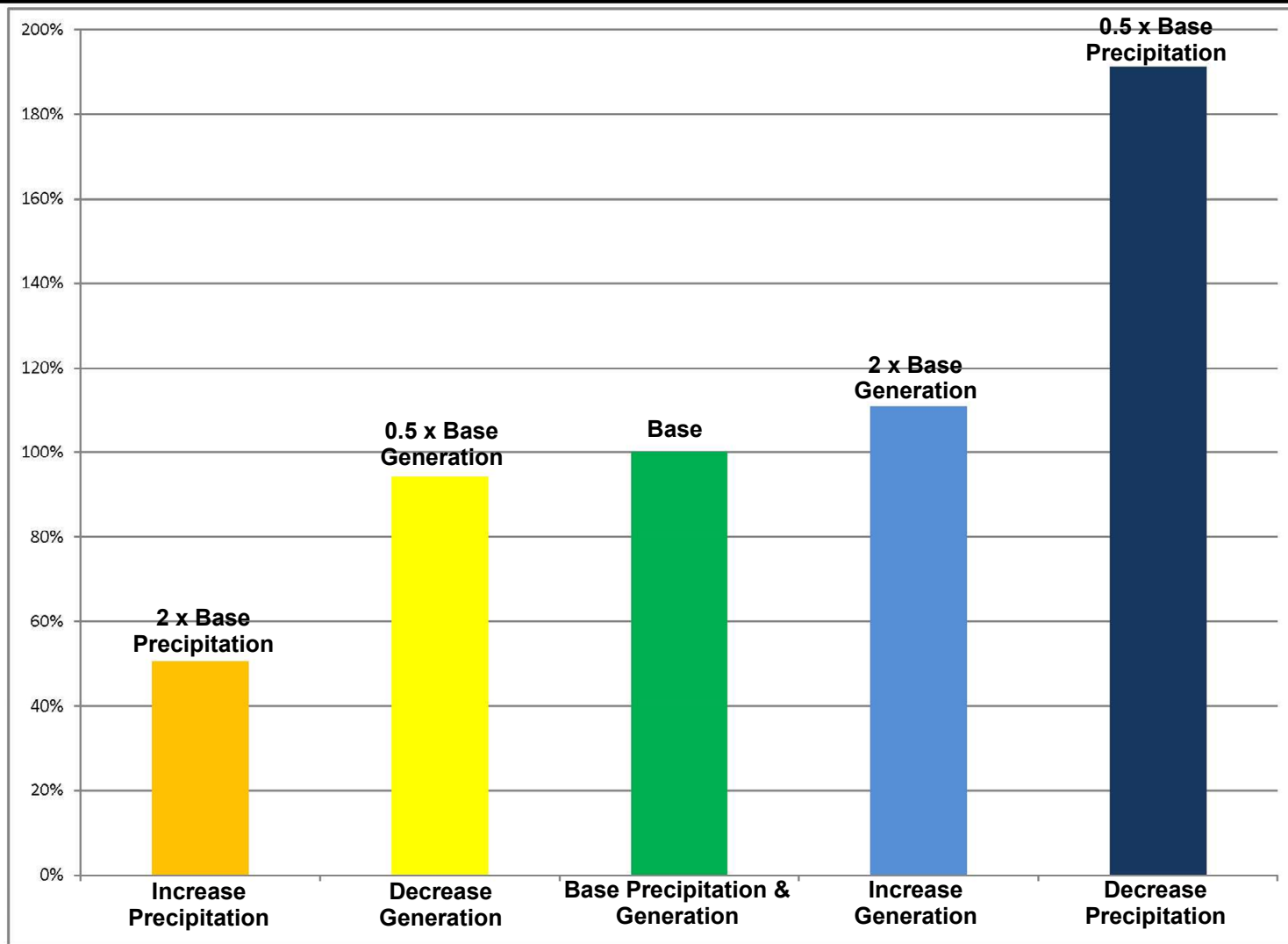
Relative Change in Dissolved Manganese Mass After 10 Years of Simulated Transport

PG&E
 TOPOCK COMPRESSOR STATION
 NEEDLES, CALIFORNIA
 MODELING APPENDIX

SENSITIVITY OF MANGANESE
 GENERATION AND SORPTION AFTER
 10 YEARS OF SIMULATED TRANSPORT

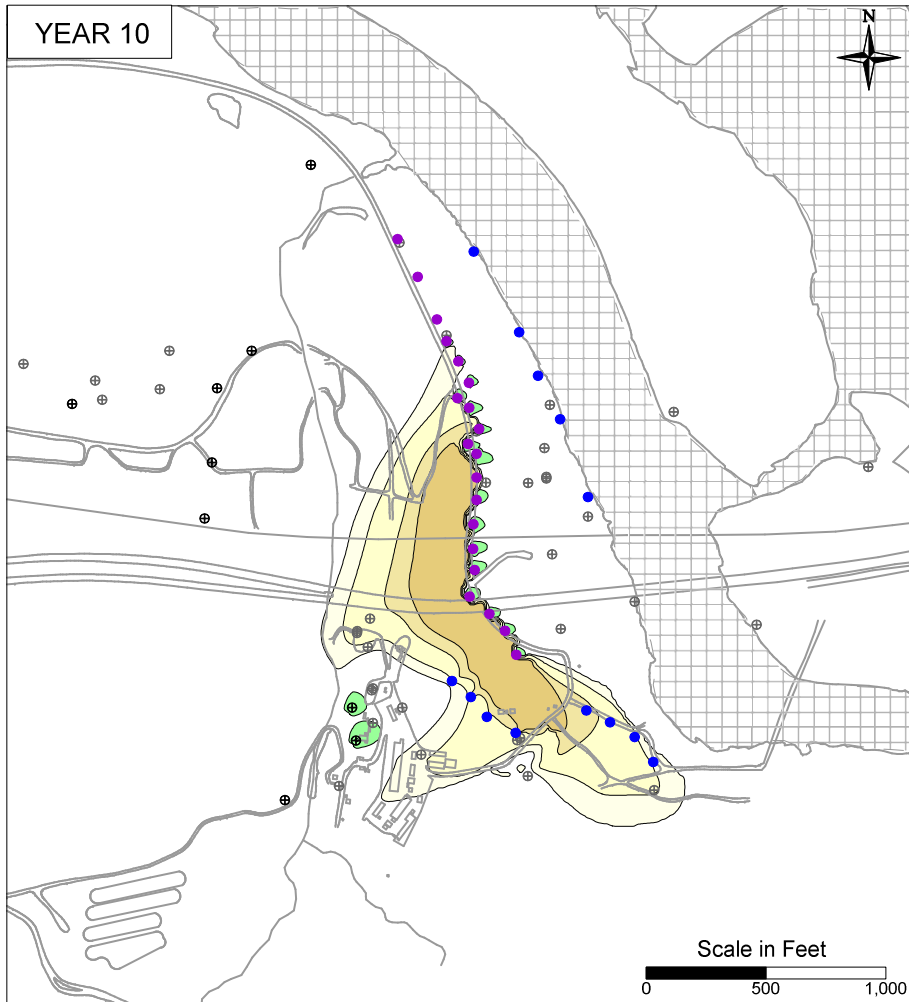


FIGURE
 B-48

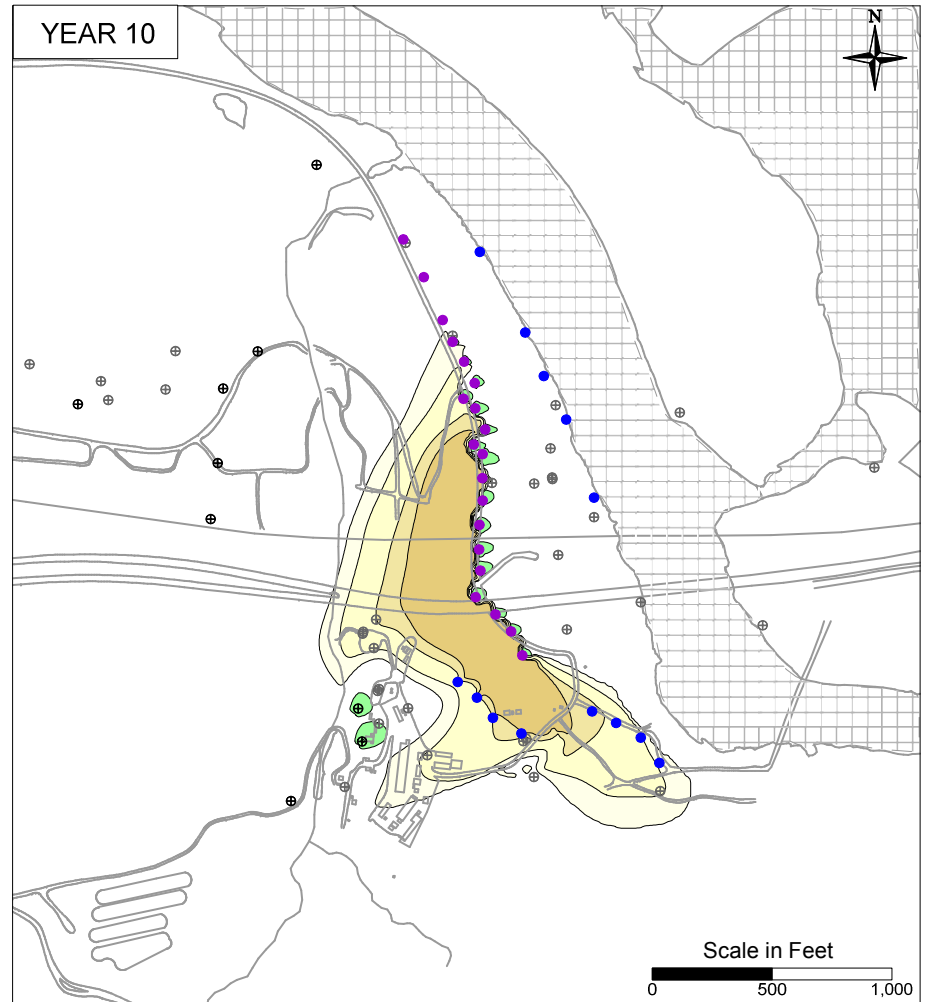


Relative Change in Dissolved Arsenic Mass After 10 Years of Simulated Transport

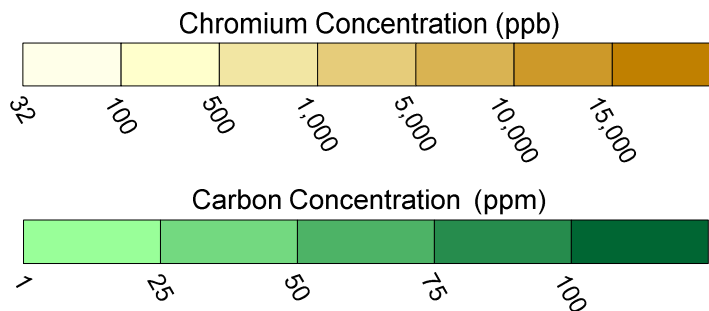
PG&E TOPOCK COMPRESSOR STATION NEEDLES, CALIFORNIA MODELING APPENDIX	
SENSITIVITY OF ARSENIC GENERATION AND PRECIPITATION AFTER 10 YEARS OF SIMULATED TRANSPORT	
	FIGURE B-49



Base Sorption: $K_d = 0.05$ mL/kg



Increased Sorption: $K_d = 0.10$ mL/kg



LEGEND

- IRZ WELLS
- ⊕ UPGRADIENT INJECTION WELLS
- EXTRACTION WELLS
- ⊕ MONITORING WELLS

PG&E TOPOCK COMPRESSOR STATION NEEDLES, CALIFORNIA MODELING APPENDIX	
SORPTION SENSITIVITY: SIMULATED HEXAVALENT CHROMIUM TRANSPORT RESULTS IN MODEL LAYER 2	
	FIGURE B-50

